BRNO UNIVERSITY OF TECHNOLOGY

VYSOKÉ UČENÍ TECHNICKÉ V BRNĚ

FACULTY OF ELECTRICAL ENGINEERING AND COMMUNICATION

FAKULTA ELEKTROTECHNIKY
A KOMUNIKAČNÍCH TECHNOLOGIÍ

DEPARTMENT OF ELECTRICAL POWER ENGINEERING

ÚSTAV ELEKTROENERGETIKY

DISTANCE PROTECTION DESIGN USING DIGITAL INPUT DATA

DISTANČNÍ OCHRANA VYUŽÍVAJÍCÍ DIGITÁLNÍ VSTUPNÍ DATA

DOCTORAL THESIS
DIZERTAČNÍ PRÁCE

AUTHOR   Kinan Wannous
AUTOR PRÁCE

SUPERVISOR   doc. Ing. Petr Toman, Ph.D.
ŠKOLITEL

BRNO 2020

Bibliographic citations:

WANNOUS, Kinan. Distance Protection Design Using Digital Input Data. Brno, 2020. Dostupné také z: https://www.vutbr.cz/studenti/zav-prace/detail/127828. Doctoral Thesis. Vysoké učení technické v Brně, Fakulta elektrotechniky a komunikačních technologií, Department of Electrical Power Engineering. Supervisor Petr Toman.

BRNO UNIVERSITY OF TECHNOLOGY

Abstract

Faculty of Electrical Engineering and Communication

Doctor of Philosophy

Distance Protection Design Using Digital Input Data

by Ing. Kinan Wannous

IEC 61850-9-2 specifies that the transmission of sampled measured values (SMVs) over an Ethernet network, using sampled values generated by merging units of IEDs or individual merging units, instrument transformers [3].

The implementation of IEC 61850-9-2 depends on the dataset specifications such as time synchronization, sample counts, and interval time.

The dissertation is focused on protection algorithms and analyses the impact of IEC 61850-9-2LE on physical protections with (analog-digital) input data of voltage and current. With the increased interaction between physical devices and communication components, the test proposes a communication analysis for a substation with the conventional method (analog input) and digital method based on the IEC 61850 standard. The thesis analyses the merging unit's functions for relays using IEC 61850-9-2LE. The proposed method defines the sampled measured values source and analysis of the traffic.

Further, the thesis deals with the programming of protection function algorithms in Matlab. The model evaluated the harmonics impact on digital relays and the impact of current transformer saturation on distance protection.

In the end, the thesis deals with the assessment of the benefits of IEC 61850-9-2LE using a neural network.

The last chapter focuses on a real-time application that subscribes the data stream coming from a substation near the protection laboratory in Brno University of Technology. IEC 61850-9-2 LE SMVs are used to transmit the traffic to a university laboratory with 16 km of fiber optic cable. The application built using Matlab and can read the traffic from the ethernet port, the traffic decoded and convert from ASCII to the decimal numbers then draw the current and voltage values. The application developed without using any need for additional hardware, the requirements are the ethernet port RJ45 from the station and pc that is running Matlab. The benefits and features of the application, easy to use, ability to implement all the distance protection functions, calculation of the RMS values of the voltage and current, harmonic distortion, the harmonic components with FTT analysis, distance protection characteristics and fault impedance calculation. All calculations implemented in real-time, moreover, in this chapter include sensitivity analysis of the Matlab model in previous chapters. Distance protection functions discussed in this thesis used the offline model of Matlab or captured with Comtrade format files.

Keywords:

Contents

List of Figures

List of Tables

List of Abbreviations

1PPS	One Pulse Per Second
ABB	Asea Brown Boveri
AC	Alternating Current
ACSI	Abstract Communication Services Interface
ACT	Application Configuration Tool
ADBS	Amplitude Dead Band Supervision
ADC	AnalogueTo Digital Converter
ADM	Analog Digital Conversion Module
ANSI	American National Standards Institute
APDU	ApplicationProtocolData Unit
AR	Autp Reclosing
ARP	Address Resolution Protocol
ASCII	American Standard Code For Information Interchange
ASCT	Auxiliary Summation Current Transformer
ASD	Adaptive Signal Detection
ASDU	Application Service Data Unit
ASN.1	Abstract Syntax Notation One
AWG	American Wire Gauge Standard
BBP	Busbar Protection
BFP	Breaker Failure Protection
BIM	Binary Input Module
BOM	Binary Output Module
BS	British Standard
BSR	Binary Signal transfer function Receiver Blocks
BST	Binary Signal transfer function, Transmit Blocks
CAN	Controller Area Network
CB	Circuit Breaker
CBM	Combined Backplane Module
CID	Configured IED Description
COMTRADE	Common Format Transient Data Exchange
CPIM	Cyber Physical Interface Matrix
CR	Carrier Receive
CRC	Cyclic Redundancy Check
CS	Carrier Send
CT	Current Transformer
CVT	Capacitive Voltage Transformer
DAR	Delayed Auto Reclosing
DARPA	Defense Advanced Research Projects Agency
DBDL	Dead BusDead Line
DBLL	Dead Bus Live Line
DC	Direct Current
DES	Distributed Energy Sources
DFT	Discrete Fourier Transform

DNP	Distributed Network Protocol
DPQR	Disturbance Power Quality Recorder
DR	Disturbance Recorder
DRAM	Dynamic Random Access Memory
DRH	Disturbance Report Handler
DSP	Digital Signal Processor
DTT	Direct Transfer Trip
FFT	Fast Fourier Transform
GE	General Electric
GOOSE	Generic Object Oriented Substation Event
GSSE	Generic Substation State Event
HMI	Human Machine Interface
HSR	High Availability Seamless Redundancy
HVDC	High Voltage Direct Current
ICT	Information And Communication Technology
IDMT	InverseDefinite Minimum Time
IEC	International Electrotechnical Commission
IED	Intelligent Electronic Device
IEEE	Institute Electrical and Electronic Engineers
IP	Internet Protocol
IPv4	Internet Protocol Version 4
LD	Logical Device
LED	LightEmitting Diode
LD	Logical Nodes
MAC	Media Access Control
MMS	Manufacturing Message Specification
MU	Merging Unit
OSI	Open Systems Interconnection
PC	Personal Computer
PES	Power Engineering Society
PRP	Parallel Redundancy Protocol
PTP	Precision Time Protocol
PV	Photovoltaic Sources
RMS	Root Mean Square
RTDS	Real Time Digital Simulator
SAS	Substation Automation System
SCADA	Supervisory System
SCL	Substation Configuration Language
SCSM	Secific Communication Service Mapping
SIPSUR	Sistema Integrado De Protección para Subestaciones Rurales
SLG	Single Phase Ground
SV	Sampled Values
SVCB	Sampled Values Control Block
THD	Total Harmonic Distortion
UDP	User Datagram Protocol
XML	Xtendable Markup Language

List of Symbols

m	Angular frequency
C_0	Zero sequence capacitance usually equal to phase to earth capacitance
E	Phase voltage before fault
E_{L1}	Phase voltage of Line 1 (phase A)
I_0	Zero sequence current
I_A	Current of phase A
I_B	Current of phase B
I_C	Current of phase C
I_e	Earth fault current without fault resistance
I_{ef}	Earth fault current with some fault resistance
R_0	Zero sequence resistance also known as leakage resistance
R_f	Fault resistance
R_L	Resistance connected parallel to the compensated coils
Z_0	Zero sequence impedance
Z_1	Positive sequence impedance
Z_2	Negative sequence impedance
δE	Drop of Global Efficiency
σ_{hj}	Geodesic path between node h and j
λ	Eigenvalues
A	Adjacency Matrix
a_{jh}	Adjacency matrix entry
$b(l)$	Node Betweenness Centrality
$b(e)$	Edge Betweenness Centrality
$\mathcal{D}$	Diagonal matrix of degrees
b_{global}	Global Betweenness Centrality
b_c	ICT Betweenness Centrality
b_e	Electric Betweenness Centrality
D	Distances matrix
d_{hj}	Distance between h and j
E	Efficiency
E_c	Efficiency for ICT nodes
E_e	Efficiency for Electrical nodes
e_m	mth edge in E
$\mathcal{H}$	Hermitian Matrix
K_h	Node Degree
k_{eh}	Electrical node degree
k_{ch}	ICT node degree
$\mathcal{L}$	Laplacian matrix
m	Number of edges in the Graph
n	Number of nodes in the Graph
$P(k)$	Degree distribution
$P(k_{in})$	In-degree distribution

$P(k_{out})$	Out-degree distribution
$\mathcal{V}$	Set of vertices
$\mathcal{V}_c$	Set of ICT vertices
$\mathcal{V}_e$	Set of Electric vertices
v_n	nth vertex in $\mathcal{V}$
$\mathcal{W}$	Weights matrix
x	Eigenvectors matrix

Chapter 1

INTRODUCTION

The numerical relay is a focal concept of the power system automation for protecting the equipment and limiting the damage. The Thesis explains the signal processing of power quality disturbances using MATLAB 2016, MathWorks, Natick, MA, USA) Simulink, especially the power quality impact on the measurements of the power system quantities; the test simulates the function of protection in power systems in terms of calculating the current and voltage values of short circuits and their faults. Power system automation has several levels to integrate between the power substations and the substation supervisory system (SCADA). The IEC 61850 standard helps digitize substations as part of equipment to device communication that is needed for protection, control, monitoring and measurement functions. The most recent part of the IEC 61850 communication protocol is the IEC 61850-9-2 part for the transmission of sampled values SV. This standard applies to electronic current transformers voltage with digital output, merging units –MUs –and an intelligent electronic device such as protection devices, field controllers and energy meters. The IEC 61850 standard unites the structure, requirements, and communication specifications that can be implemented during sharing of data among IEDs, the first announcement of the cooperation and creates a platform between the substation automation system (SAS) and the substations (IEC 61850 2003) [69]. The challenges to implementing the IEC 61850 are processing a huge amount of real time data and replacing some parts of substations to create a better environment to implement IEC 61850. The use of IEC 61850 as the basis for smart grids includes the use of merging units (MUs) and deployment of relays based on microprocessors. IEC 61850 standard defines communication protocol for intelligent electronic devices at electrical substations. It describes in IEC 61850-9-2 sampled values and how to digitalize measurements. Transferring data in digital format is used for the protection and monitoring application. The challenge nowadays is sharing the current and voltage measurements in substations and uses it for monitoring and protection application. Due to the fact that current and voltage transformers are able to convert the analog signals to digital format. The IEC 61850 standard for substation authorizes the combination of all control, protection and monitoring functions by one protocol, nowadays, all manufacturers realize the importance and the need to merge the communications of all IEDs in a substation, numerous IEDs can control commands at high speed and share data. This coordinated control can partly eliminate the need for wiring in a substation. Many utilities have already established systems of interconnected IEDs, which make IEDs measurements available to use for centralized substation and control, whilst, the majority of data in IEDs is left uncollected due to the traditional techniques were designed to support SCADA. IEC 61850 was created to be an internationally standardized method of communications and integration with goals of supporting systems built from multivendor IEDs networked together

2

to perform protection, monitoring, automation, metering, and control [68]. A micro-processor provides the ability to process large amount of information and to make the tripping decision trip, another important application of permanent power quality monitoring is a distribution power quality recorder (DPQR) in the digital relay that can be used to define the measurements of events which occurred in the power system such as internal/external fault diagnosis, fault measurements, zero current sequences and disturbance recording. The hierarchy structure of power system automation contains electrical protection, control, measurement, monitoring and data communications. The power system automation is a system that is integrated into the various components connected to the power network. The numerical relay is a focal concept of the power system automation to protect the equipment and limit the damage. The system's components have better communication with each other; the information is exchanged via dozens of communication protocols; the concept can be characterized by only one sensor obtaining and collecting information from the network instead of a sensor per each component in the power system. The power system automation has several levels to integrate into the power substations and the substation supervisory system (SCADA). They include Sampled Values (SV) and Generic Object Oriented Substation Event (GOOSE) protocols which are mapped directly to the Data Link layer for reduced protocol overhead hence increased performance; and Generic Substation State Event (GSSE) protocol which features its own custom protocol mapping [75]. IEC 61850-9-2, process bus is defined as standard:

- IEC 61850-9-2 standard for communication networks and systems in substations, part 9-2: "Specific Communication Service Mapping (SCSM) - Sampled values over ISO/IEC 8802-3" [71].

- Implementation Guideline for digital Interface to instrument transformers using IEC 61850-9-2 to facilitate implementation and enable interoperability, the UCA International Users Group created a guideline that defines an application profile of IEC 61850-9-2, which Commonly referred to as IEC 61850-9-2LE for "light edition" [69].

Chapter 2

THE STATE OF THE ART

2.1 QUADRILATERAL RELAY ALGORITHM AND PROTEC-TION

Since quadrilateral characteristics are discontinuous, its characteristics cannot be generated by electromechanical relays devices. The ability to detect significant resistance associated with the restriction is important. The ability to closely enclose the desired trip area results in a more secure application. Quadrilateral elements with plain reactance reach lines can introduce reach error problems for resistive earth faults where the angle of total fault current differs from the angle of the current measured by the relay. This is the case where the local and remote source voltage vectors are phase shifted with respect to each other due to pre fault power flow. Polygonal impedance characteristics are highly flexible in terms of fault impedance coverage for both phase and earth faults [66].

The algorithm of distance relay generally requires current and voltage input signals, namely, harmonic magnitude and phase of three voltages and currents signals each, zero sequence magnitude and phase current to obtain phase quantities. In this work, all the signals are obtained and taken samples of signals namely three phase to ground voltages and three phase currents [12]. Modern distance relays offer quadrilateral characteristic, whose resistive and reactive reach can be set independently. Therefore, it provides better resistive coverage than any mho type characteristic for short lines. This is especially true for earth fault impedance measurement, where the arc resistances and fault resistance to earth contribute to the highest values of fault resistance [66].
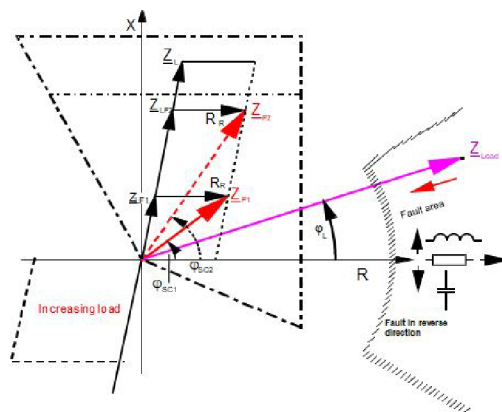
FIGURE 2.1: Quadrilateral characteristic [66]

RELAY CHARACTERISTICS AND IMPEDANCE DIAGRAM

Since utilities need to keep all the settings of the relays from different types and various manufacturers in a database, they need to overcome these differences. Things get further complicated when the distance relays settings need to be coordinated with other relays in front or behind them or when the distance characteristics have to be tested to evaluate the relay performance or to analyze its operation. In these cases, knowing the settings is not sufficient, further knowledge of the behavior of relay performance may be required as well [26]. Quadrilateral relay is usually set to three zones to protect and cover the transmission line. Three zones quadrilateral characteristics used to protect the transmission line are shown in figure 2.1 and figure 2.2.

An important feature of distance protection is its inherent remote backup functionality. The overreaching zones operate with set time delays that are coordinated with remote protection devices. For this purpose, a grading time of the back up stages is required to ensure that selectivity is maintained during normal protection operation while time delay backup protection operates in the case that a breaker fails to operate during a fault.
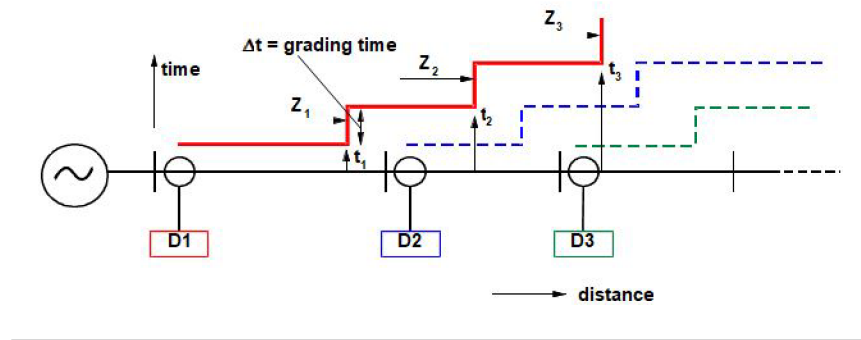
FIGURE 2.2: Graded distance zones

This characteristic is provided by modern distance relays, and their resistive and reactive reach can be adjusted independently. Its resistive coverage is better than for any mho type characteristic for short lines. The impedance characteristic of most digital and numerical distance protections with this characteristic can be set with respect to the impedance of the load or the arc. The quadrilateral characteristic is the most appropriate for the earth fault impedance measurement, where the arc resistances and fault resistance to earth increase the values of fault resistance.

2.1.1 TESTING OF MULTIFUNCTIONAL DISTANCE PROTECTION DEVICES

The functions in the distance relay have a hierarchy that needs to be considered for the testing of the device. First of all, the secondary currents and voltages, which are applied to the distance protection relay, are filtered and processed in the analog input module and they provide instantaneous sampled values to the internal digital data bus of the IED. These sampled values, which can be logged when an abnormal system condition, are detected or used to calculate various measurements (e.g. current and voltage phasors or superimposed components) and they can be used by different protection functions [22] and as shown in figure 2.3.

The outputs of the measurement elements become the inputs to a protection or other
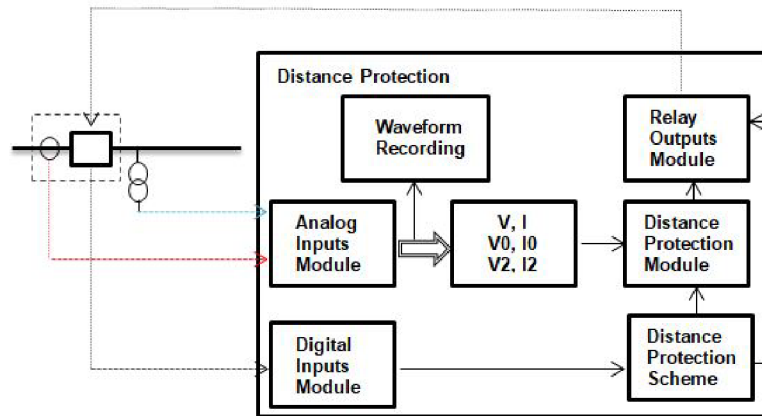
FIGURE 2.3: Developed Distance Protection

functional elements of the device. Each basic protection element operates based on specific measured value i.e. phase or sequence current, voltage, and frequency. Measurements of active, reactive and apparent power or power factor are often available from the relays when they are required in the substation automation system [40] and as shown in figure 2.4.
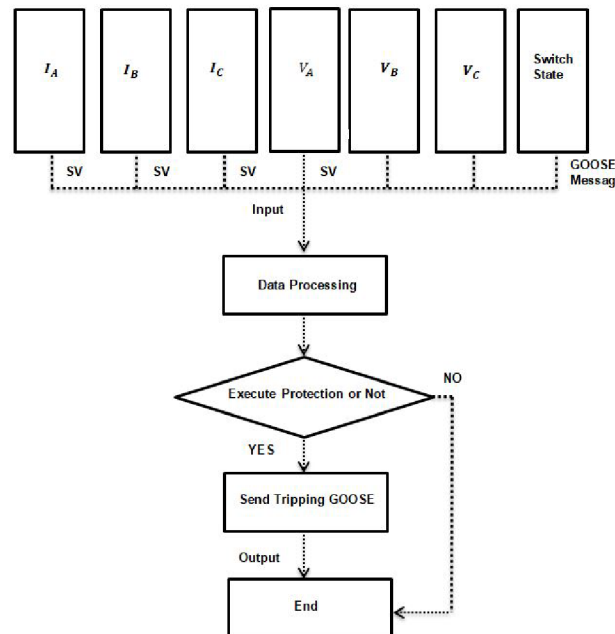
FIGURE 2.4: Communication of Relay Protection

2.1.2 DISTANCE TO FAULT LOCATION

Any transmission line of electrical energy is characterized by its resistance and reactance per unit length, in other words, its total impedance is proportional to its length distance. When a fault occurs, the distance to fault location is computed by the fault

locators which are integrated with the distance relays. These fault locators execute the measurement when the current passes by zero. This property helps them to eliminate not only the influence of the fault resistance but also one of the line resistance. The instantaneous voltage does not depend on line and fault resistances but only on the line inductance as shown by the equations (2.1) and (2.2)

$$u(t) = (R_L + R_F) \cdot i(t) + L_L \frac{d_i}{d_t} \tag{2.1}$$

For (t)= 0 then we have

$$u(t) = L_L \frac{d_i}{d_t} \tag{2.2}$$

FAULT RESISTANCE

When a phase to phase or phase to earth fault occurs in the line, accompanied by the production of the arc, there will be generated in the line a new impedance R_F with a resistive character which is in series with the line impedance. R_F is known as fault resistance or arc resistance. In case the system is supplied from one end (single ended infeed), the distance protection located on the source side will correctly measure the fault distance because, according to the equation (2.6), the fault resistance R_F affects only the real part of impedance while the reactance depends on the distance measurement, remains the same as discussed previously. In case the line is supplied from both ends (double ended infeed) and the fault with arc occurs between the two sources (see figure 2.5), then there will be voltage drop caused by the short circuit current from the other side infeed through the fault resistance which has the same effect as an additional source and increases the measured fault resistance. According to the equations (2.3), (2.4), (2.12) and (2.5).

$$\overline{U}_A = \overline{I}_A \cdot \overline{Z}_L + (\overline{I}_A + \overline{I}_B) \cdot R_F \tag{2.3}$$

$$\overline{U}_A = \overline{I}_A \cdot (\overline{Z}_L + R_F) + \overline{I}_B \cdot R_F \tag{2.4}$$

$$\overline{Z}_A = \frac{\overline{U}_A}{\overline{I}_A} = \overline{Z}_L + R_F + \frac{\overline{I}_B}{\overline{I}_A} \cdot R_F \tag{2.5}$$

$$\overline{Z}_A = \overline{Z}_L + R_F \cdot (1 + \frac{\overline{I}_B}{\overline{I}_A}) \tag{2.6}$$
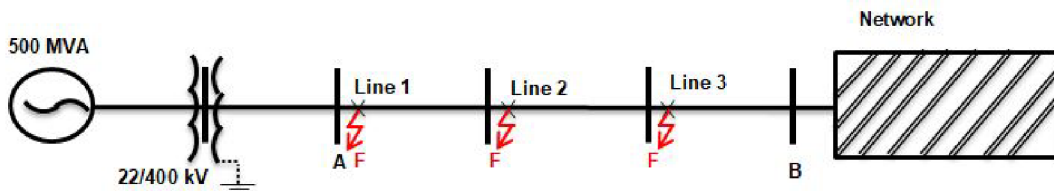
FIGURE 2.5: One line diagram of power system model

TABLE 2.1: IEC 61850-9-2 standard

Area	IEC 61850-9-2 standard	Guideline IEC 61850-9-2 LE
Sampling rate	Free parameter	80 samples for protection and measurement applications 256 samples for power quality
Content of dataset	Configurable	3 phases current + neutral current values and quality 3 phases voltage + neutral voltage values and quality
Time synchronization	Not defined	Optical pulse per second (1PPS)

2.2 IEC 61850-9-2 STANDARD

2.2.1 SAMPLED VALUES (SVs)

- Enables sharing of values and measurements among IEDs.

- Transmission of sampled analog (especially *U/I*) and digital values from primary technology over the Ethernet network.

- Data are sent in continuous data stream and packet (data link layer).

- Interface electronic device that enables digital communication over an Ethernet network using Sampled Measured Values.

- Providing time-coherent SMV with multiple analog values and digitizes them according to IEC 61850-9-2.

- IED = Merging Unit in UGD.
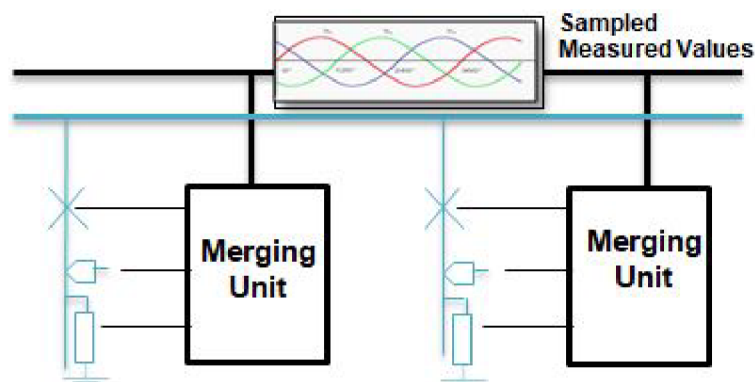
FIGURE 2.6: sampled values (SVs) [81]

Merging units are connected to the secondary sides of the current and voltage transformers and publish the voltage and current values as sampled values (SV) Ethernet packets as shown in figure 2.6. Digitalized analog data is transferred by Fiber Optic cables to receiving protection relays (IEDs) via IEC 61850 process bus, a packet of data includes sampled values, GOOSE messages and precision time protocol. IEDs are connected to process bus by Ethernet switches. IEC 61850 standard uses Ethernet

TABLE 2.2: DataSet members

Sampled values	Quality attribute
I1 sampled value	I1 quality attribute
I2 sampled value	I2 quality attribute
I3 sampled value	I3 quality attribute
I0 sampled value	I0 quality attribute
U1 sampled value	U1 quality attribute
U2 sampled value	U2 quality attribute
U3 sampled value	U3 quality attribute
U0 sampled value	U0 quality attribute

TABLE 2.3: Calculation Of communication bandwidth

Maximum amount of SMV	Single and PRP redundant	HSR redundant
50 Hz system	9	4
60 Hz system	8	4
Two SMV publishers	SMV=12.3 Mb/s	SMV=12.3 Mb/s
	GOOSE+MMS=87.7 Mb/s	GOOSE+MMS=37.7 Mb/s

as the physical communication layer, the sampled values are transferred via available communication bandwidth of Ethernet. The transmission speed is 100 Mbit per second (100Mb/s) and light edition of this standard for MV applications determines two specific sampling rates:

- 80 samples per period for protection applications, samples can be transferred using Ethernet.

- 256 samples per period for metering applications.

Sampled Measured Value message is duplicated within T depending on sample rate (SmpRate) and number of ASDUs (samples) per message (NoASDU) [81] as shown in figure 2.7.

$$T = \frac{1}{SmpRate \times NoASDU} \tag{2.7}$$

Sampling rate for 80 samples per cycle:

$$f_1 = 80 \times 50Hz = 4kHz => T = \frac{1}{4kHz} = 250\mu s \tag{2.8}$$

$$f_2 = 80 \times 60Hz = 4.8kHz => T = \frac{1}{4.8kHz} = 208\mu s \tag{2.9}$$

Data volume broadcasted by one IED:
Each IED SMV frame includes 160B=1280b

$$50Hz \times 80 \times 1280b = 5.12Mb/s \tag{2.10}$$

According to the network traffic standard is recommended to keep 50 Mb/s reserved for MMS telegram between IEDs, SCADA system and GOOSE messages and 50 Mb/s ethernet capacity is used for SMV data sharing.

This part describes the experimental measurement provided on the test setup in the laboratory of protection relays at the Brno University of Technology. PCM600
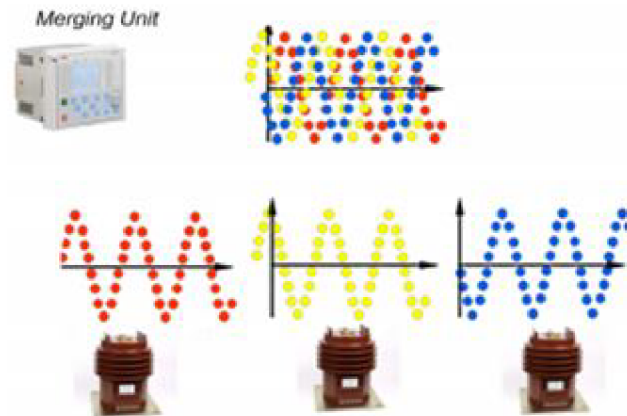
FIGURE 2.7: Merging unit and SMVs [81]
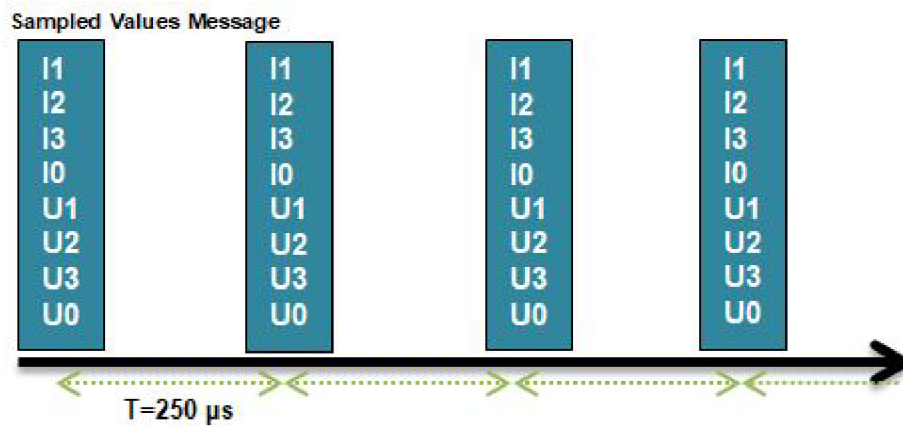
FIGURE 2.8: IEC 61850-9-2, Process bus Data Exchange SmpRate = 4kHz

is a tool providing control and configure ABB IEDs, it is an adapted tool with IEC 61850 standard, which enables data exchange and provides efficient functionality for application configuration. PCM600 offers data transfer between IEDs. The settings in PCM600 offer a view and modify IED parameters. These parameters can be exported and imported in XRIO format or other formats [70]. Configuring Process bus to share voltage information between two IEDs (REF615 outgoing feeder and REF615 incoming feeder) is summarized in the following steps:

- In this test, the process bus communication enables voltage sharing between IEDs as (SMV- Sampled Measured Values). Digital values of current and voltage transfer over an Ethernet network as shown in figure 2.8.

- SMVSENDER function block should be added to enable and active sending sampled values according to IEC 61850 standard as shown in figure 2.11. The communication channel is established and REF615 sender starts sending the voltage as sampled values (80 samples per cycle).

- In PCM600, a new project is created for two feeder relays REF615 (incoming

and outgoing). IEC 61850 Configuration Tool offers Client Server Communication and matrix of available IEDs which are connected to the switch. One protection relay should be selected to be Sender protection relay. The SMVAENDER function block provides share the sampled values from sender protection relay as process bus sender.
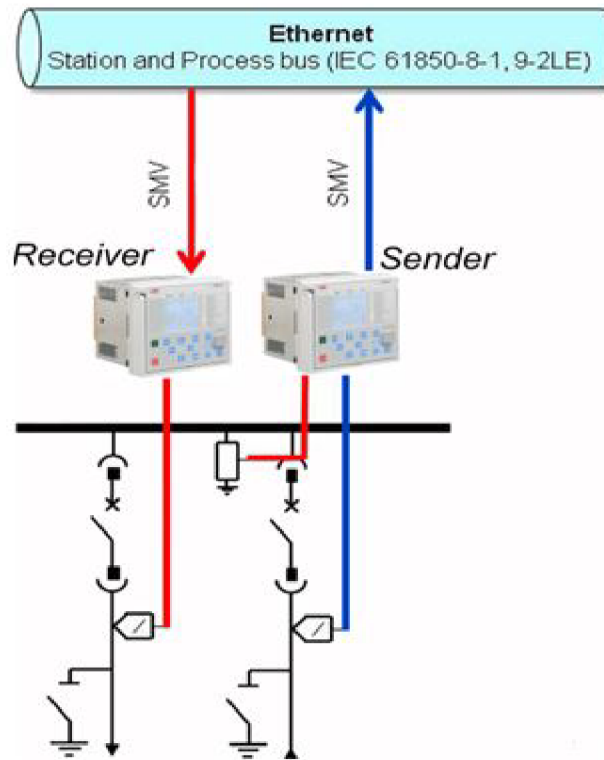
FIGURE 2.9: REF615 Outgoing feeder – REF615 incoming feeder

TABLE 2.4: Settings for sampled values communication

Protection Relays	IP Address	Subnet	Technical Key
REF615	172.16.2.2	255.255.0.0	ABBJ1K02A1
REF615	172.16.2.1	255.255.0.0	ABBJ1K04A1

In the REF615 receiver protection relay, IEC 61850 Configuration Tool is used to establish the communication between two IEDs. As shown in figure 2.10 and figure 2.11 Process Bus communication and Control Block Attributes. Sampled Value Control Block (SvCB) attributes:

- APPID – unique SvID in network
  Reserved value range is from 0x4000 to 0x7FFF
  Default value is 0x400 based on UCA 9-2LE

- MAC address
  The unique Multicast address per SvCB is recommended.
  The multicast address range is from 01-0C-CD-04-00-00 to 01-0C-CD-04-01-FF.
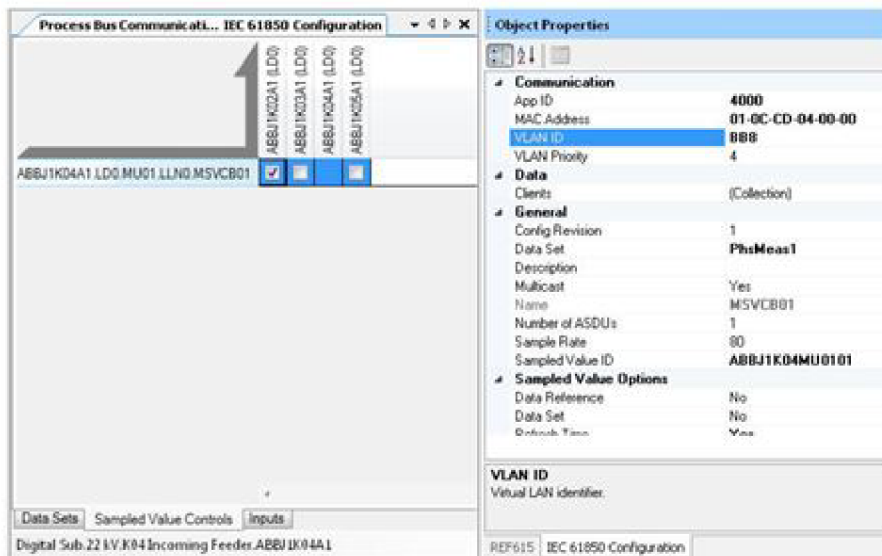
FIGURE 2.10: Process Bus and Control Block Attributes
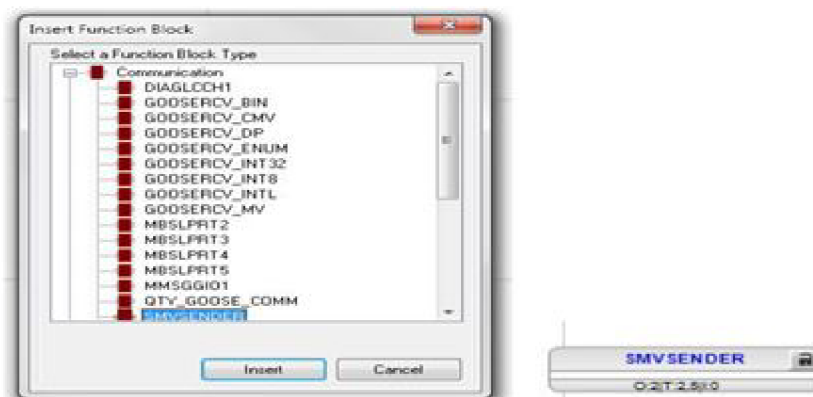
FIGURE 2.11: SMVSENDER function block in PCM600 Application Configuration

- SV Control block name
  This block is created automatically, technical key.

- DataSet definition
  When SMVSENDER function block is added the DataSet generated automatically.

- VLAN ID
  Value range according to IEC 61850-90-4) is from 0xBB8 (3000) to 0xDB7 (3511). The default value is 0x000.

- VLAN priority
  The default value is 4 as per IEC 61850-9-2 (value range 0 . . . 7).

2.2.2   TEST SETUP WITH OMICRON

Omicron CMC 256 is a tester device that can test IEDs functionality and offers the IEC 61850 communications (GOOSE messages and sampled values). Three phase voltage and current then transfer these signals to relay protection over ethernet network [70], additionally, 3x FTP cables terminated with the RJ45 connector can be used and tCMLIB REF6xx is an interface adapter for connecting ABB protection relays with sensor inputs (e.g. REF615 or REF601) .
Analogue signal:

-

$$3 \times I \ (150mV \ for \ 50Hz \ system) \tag{2.11}$$

-

$$3 \times U \ (2V for \ 20kV \ system) \tag{2.12}$$

IEC 61850 testing tools enables different test set to verify the IEC 61850 and communication. SVScout provides the visibility to measure and monitor the sampled values for the substation engineer, additionally, the SVScout software provides merging unit testing by comparing two SV streams, more precisely, SVScout makes sampled values visible and shows detailed values of the primary voltages and currents. One important feature of SVScout is the ability to make a comparison between different SV streams, it includes the RMS values and phase angles which displayed in a phasor diagram and a measurement table. CMC256 provides some interfaces to test of process bus IEC 61850-9-2. It simulates current and voltage sensors by using Rogowski coils for current measurements and a voltage divider for voltage measurements. The output of the sensor is connected to the ethernet ports in the IED device, the IED provides interface that showing the measurements of power, power factor, voltages, and currents. Moreover, this IED shares the voltage measurements with the receiver IED that is connected to switch and ethernet. the communication between two IEDs according to the standard is based on MAC addresses (media access control address), it means the source IED have to know the MAC address of the destination IED, otherwise, the data packets could be lost in the network and the measurement cannot reach the final destination, the mac address of any device is unique and every IED has his own MAC address. Some tools and software provide the possibility to show and analyze the data packet which is sent over the network, Wireshark software offers the option to show the packet content and information about the source, destination, values of voltage and current in the Hexadecimal system [74]. SVScout sampled values are the platform that can compare the output of merging units and establish recording the waves as Comtrade format, however, estimated delay time of sending and receiving SMV has been measured as shown in figure 2.12. There are a few parameters can define the delay time of SMV:

- The number of hops in networks.

- Internal application delay of protection.

- Store and forward latency.

- Queue latency: queue latency calculated when the port has started to send a full sized frame (1500 bytes) before SMV frame and the switch has been configured to prioritize SMV.

- Theoretical max delay.
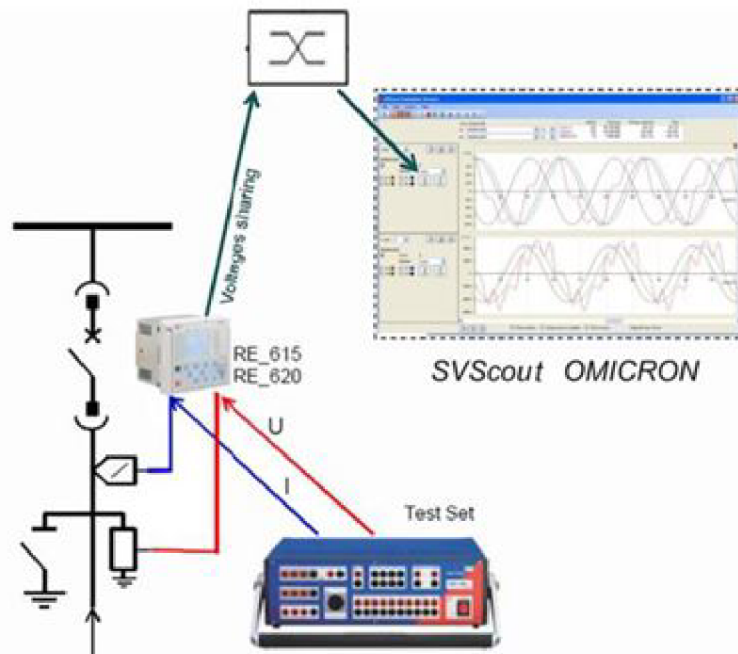
FIGURE 2.12: CMC256 connected to publisher relay / Testing of Process bus

- Recommended max delay setting.

As mentioned previously, there are several parameters to be considered in order to calculate the time of delay for the sampled values, where the protection delay is about 1.25 to 6.25 ms depending on the delay characteristics of the sampled values [75]. Wireshark software tends to focus on network traffic flow rather than judging packet content. It monitors the network traffic with the available protocols in the networks as well as the sampled values contain details of source and destination, it shows each packet of measurement separately in ASCII [73].

2.3 SUMMARY

This chapter describes the standard IEC 61850 which is a communication protocol for electrical devices used in substations. This uses the sampled values and GOOSE protocols which are mapped directly to the data link layer for reduced protocol overhead. In this chapter, IEC 61850 standard is discussed including parameters for sampled rate of analogue values, configurable for content of dataset.
sampled values are important in electrical parameters they are beneficial in such a way that they enable sharing of values, transmit sampled analogue and digital values, sending of data in data link layers, interference and providing time coherent SMV. The sampling rates are defined in this chapter as the transmission speed is 100 Mb/s so 80 samples per period for protection application.
Testing of multifunctional distance protection devices is also discussed in this chapter. The measurement of active, reactive and apparent power or power factor are often available from the relays when they are required in the substation automation

system. Another technique is explained here which is quadrilateral relay algorithm and protection. It includes the calculation of bandwidth. The algorithm of distance relay required input signals which are harmonic magnitude, phase of three voltage and current signals each, zero sequence magnitude and phase current to measure phase quantities.

Relay characteristics and impedance diagram play an important role in measuring the values of electrical parameters. Distance relay has a feature of inherent remote back up functionality. Its resistive coverage is better than any mho type characteristic for short lines. The quadrilateral characteristic is the most appropriate for the earth fault impedance measurement while the polygonal impedance characteristics are highly flexible in terms of fault impedance coverage for both phase and earth faults. Omicron is a testing device used for the testing of IEDs functionality and offers the IEC 61850 communication. The delay time of SMV can be defined by the number of hops in a network, internal application delay of protection, store and forward latency, theoretical maximum delay, recommended max delay setting and a new term named queue latency. The queue latency is defined as when the port has started to send a full sized frame before SMV frame and switch has been configured to prioritize SMV. Another precaution is important to reduce error which is network packet analysis to make safe the packet traffic.

Chapter 3

THE AIMS OF THE DISSERTATION

The objectives of the dissertation are as follows:

- Defining the protection function algorithms.

- Creating a Simulink model for distance relay protection which can define the fault type, fault impedance and total harmonic distortion.

- Evaluation of harmonic impact on the digital relays and comparing the protection model with a physical digital relay.

- Testing the merging units of the digital relay and Omicron device in the laboratory and compare the functions and timing analysis. By using neural net pattern recognition, we could find the relation between the inputs (number of samples/ms—interval time between the packets) and the source of the data.

- Developing real time application that subscribes the data stream coming from a station near protection laboratory in Brno University of Technology. IEC 61850-9-2 LE SMs are used to transmit the traffic to university laboratory with 16 km of fiber optic cable . The application built using MATLAB and can read the traffic from the ethernet port, the traffic decoded and convert from ASCII to the decimal numbers then draw the current and voltage values. The application developed without using any need for additional hardware.

Chapter 4

THE IMPACT OF CURRENT TRANSFORMER SATURATION ON THE DISTANCE PROTECTION

The distance protection relay calculates the voltage and current at the relay location and evaluates the ratio between these quantities. Distance relays are widely used on transmission and even distribution systems. Current transformers (CT) are the very important part of the power system protection. The main purpose of a CT is to transform the primary current in a high voltage power system to single level that can be handled by delicate electronic device. This chapter deals with the influence of CT saturation on distance digital relay. Saturation of the CT is evaluated for fault close to the relay location.

4.1 THE EXCITATION CURVE OF CTS

The electrical power system has many elements which are important to ensure security and protection of the system. The current transformer is a device which is connected to the power system and is used to produce low current that is possible to use in protection devices. The current transformer has two parts (primary and secondary). The primary side has few coil turns and the secondary side has a large coil turns. This structure is used to obtain low current on the secondary side; the current which is produced in secondary side is used for several functions in power system such as metering and protection, therefore, the output current of the current transformer becomes the input for the protection device, however, the ratio between the primary winding and the secondary winding have caused the current saturation during faults which occurs in the transmission line. In this case, the relay which is connected to the current transformer cannot respond or trip in right way [47]. The current transformer is used for different functions as was mentioned above (metering and protection), however, the level of accuracy depends on the operation type. There is a relationship between the accuracy of the CT and rated current and the good accuracy is important for metering [77].

4.1.1 CHARACTERISTICS OF CURRENT TRANSFORMER

The current transformer primary winding is connected in series with the device in which the current is to be measured. Since current transformer is fundamentally

18

a transformer, it transmits the current from the primary to the secondary side, inversely proportional to the turns so as (4.1):

$$I_p = n \times I_s \qquad (4.1)$$

where n is the ratio of turns between the secondary and primary winding.
The equation (4.1) explains the normal transformer with a different number of windings between the primary and secondary side. Figure 4.1 explains the equivalent circuit for a current transformer. Reactance X_m explains the magnetizing current; the secondary current which is generated in secondary side is divided into internal current and magnetizing current. Current I_s represents the internal winding current.
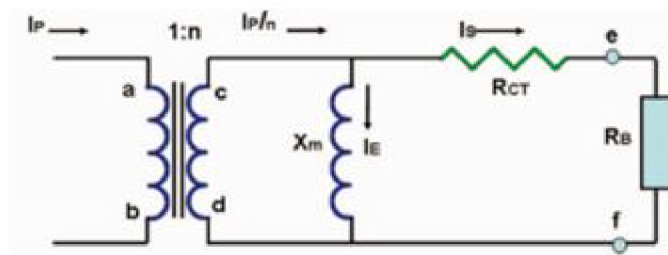
FIGURE 4.1: Equivalent circuit for a current transformer [52]

4.1.2 SATURATION TEST

The current transformer can be tested as connected the secondary side to the voltage source then measured the current which produced on the secondary side, taking into consideration that the primary side remains open without load during the test. The voltage increased gradually with measuring the current until reach to the saturation point which is started when the voltage increased 10 % and the secondary current increased 50%. After this point, any small increase in voltage has resulted in large increases in current that supposed to mean the saturation started [45]. Thane test starts with decreased the voltage value gradually and writing the current value for all voltage values until the voltage value becomes at the end is equal zero to make sure that core. Demagnetization after that we can draw the magnetic curve [46] [55].

4.1.3 AC SATURATION

The alternative current had resulted in producing the alternative magnetic flux. The flux is proportional to the secondary current, consequently, when the current increased, the flux increased too as shown in figure 4.2. The saturation has appeared when the current increased to the high value (faults), then the flux increased to the high value which the iron core not able to afford this flux [49] [52]. This equation explains the relationship between the different parameters which create the current saturation curve and the specific domain that is allowed for the current transformer to work without saturation , however, there are details about the ratio between inductance and resistance which is major parameter to define the saturation curve, in
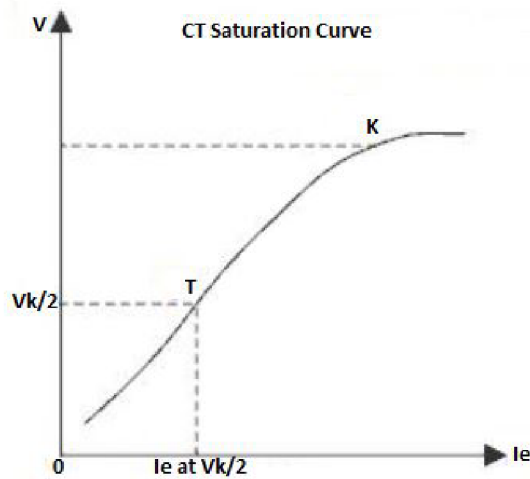
FIGURE 4.2: Secondary excitation curve

TABLE 4.1: Excitation curve values [55]

V_e(volt)	I_e (amper)	Z_e(ohm)
3	0.001	3000
7.5	0.002	3750
12.53	0.003	4167
18	0.004	4500
60	0.01	6000
150	0.02	7500
200	0.025	8065
300	0.05	6000
400	0.2	2000
447	1	447
486	10	49

general, the current transformer has maximum fault current which can be applied in protection without saturation after this maximum value the current saturation appears [50] [51].

$$B_s \cdot N \cdot A \cdot \omega = \frac{X}{R} \cdot I_f \cdot Z_B \qquad (4.2)$$

Moving to the equation to explain how we can avoid the current saturation in the current transformer by observing the ratio between the major parameters If fault current, the ratio of reactance and resistance and current transformer burden. In equation (4.3) we assumed that the voltage is 20 times between primary and secondary:

$$20 \geq (\frac{X}{R} + 1) \cdot I_f \cdot Z_B \qquad (4.3)$$

where I_f is the fault current in current transformer; Z_B is the burden impedance and X/R is the ratio of reactance and resistance.
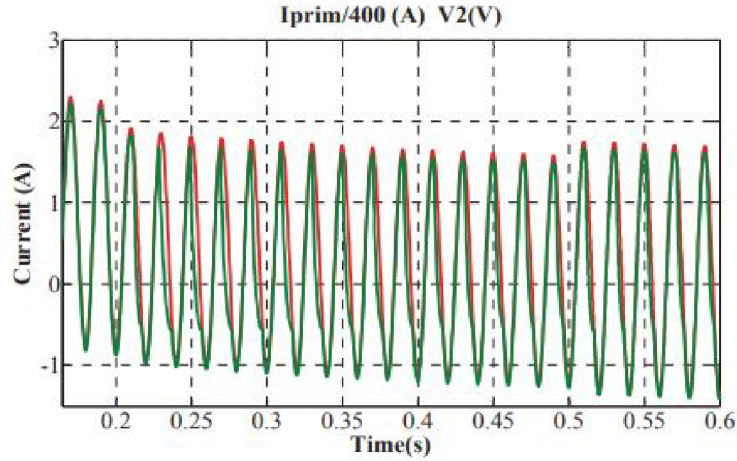
FIGURE 4.3: Secondary current of transformer with CT saturation

4.2 POWER SYSTEM AND CT TRANSFORMER BY SIMULINK

The model consists of two sources, 100 km transmission line and load, current transformer block which includes the influence of current saturation on power system and distance protection [56].

This chapter explains the impact of CT saturation on the distance protection. As we mentioned above the power system simulation contains first of all the source then the CT block. Inside this block there is current transformer also the saturation parameters for this specific system. After the CT block the current signal is moved to the distance protection block which uses this signal with many functions starting from the filter, sampled values and discrete fourier transformer [56]. The current waveform as shown in figure 4.3 illustrates fault current and healthy phase currents. The fault was started from 0.2s and at 0.5s the phase A current comes back to steady state.

DISTANCE PROTECTION BLOCK

The distance protection is designed to detect the faults which occur in the transmission line. The distance relay divides the transmission line impedance to the zones, every zone covers part of the line [60]. The algorithm is used in the distance protection as shown in eq (4.4). This algorithm calculates the impedance of single phase fault, however, the saturation impact on the protection algorithm had resulted on calculation of the fault impedance [57].
Figure 4.3 explains the secondary current under the impact of the current saturation. Current waveform is used in protection block with signal processing.
Single phase fault can be calculated as:

$$\overline{Z}_{slg} = \frac{\overline{V}_A}{\overline{I}_A + 3 \cdot k \cdot \overline{I}_0} \tag{4.4}$$

where
V_A and I_A are voltage and current phase respectively.
I_0 is zero sequence current.
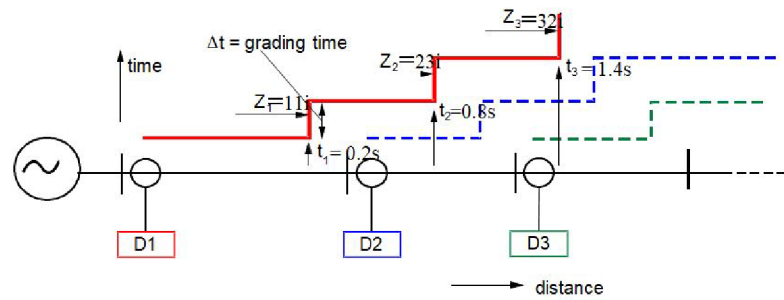
FIGURE 4.4: Grading time of relay zones

k is a residual compensation factor.

This chapter presents the way to simulate the influence of CT saturation on a distance protection relay by using the MATLAB/Simulink for the quadrilateral type distance protection relay. On another hand, there could be study of the effects of CT saturation on a distance relay characteristic. The setting for zone 1 and zone 2 are based on line length. The distance protection is designed to divide the high voltage transmission line to the zones, each zone contains part of the high voltage transmission line, and the zone 1 is set to 80 percent of the first part of line. The setting of the distance protection considers the line impedance which is the major parameter to design this protection. The setting of Zone 2, Zone 3 etc. Depends on the length of other parts of the line. In the simulated example Zone 2 is set to 120 percent of the first part of line. Zone 3 is set to cover 240 percent of the first part of the line. The distance protection block which is created in MATLAB/Simulink includes some functions of the signal processing such as mentioned above [60] as shown in figure 4.5.

The simulation results are presented for fault in phase A. Time development of impedance measured and calculated by relay is in figure 4.6 and figure 4.7. The results for the remaining faults can also be determined using the formula (4.4). It presents how the distance protection has detected the fault with current saturation.

Figure 4.6 and figure 4.7 show the three zones of the designed distance protection which cover different parts of transmission line under study. The figure 4.6 explains where the fault occurs without impact of current saturation (from the Simulink without CT block). The result fault impedance is 9 ohms. It means the fault occurred in the first zone. The figure 4.7 shows the fault impedance under the impact of current saturation (as mentioned above that the first block is simulated the current transformer). Current saturation had resulted in an error in the calculated fault impedance, Moreover; there is an error of the algorithm which is used to calculate the fault impedance. Due to this error, the distance protection is not working as it should. Discrete Fourier Transform (DFT) is used to obtain magnitude and phase components in the time domain of input signal. The Fourier block can programed to calculate the magnitude and phase of the fundamental, the DC component and any harmonic component of the input signal. As shown in figure 4.8 green line it's the impedance without saturation and black one the impedance with saturation.
The Fourier block is used to extract the fundamental frequency components from the distorted fault signals by eliminating decaying DC components. Figure 4.9 shows the magnitude waveform obtained for current signal with/out saturation. The brown

line is the current without saturation and the black one with saturation.

The distance protection could be impacted by the saturation of current transformer; especially tripping time could delay, because the algorithm which is used for calculation of the fault impedance in the protection relay. This algorithm is using both current and voltage signals. The saturation effect in current has result in a failure of the calculation. This error could lead to the problems in functions of the protection. So the distance element is under reach and has slower operation time and CT saturation increases the measured impedance in the distance element.

4.2.1 SYSTEM MODEL

The model consists of a synchronous machine (generator) 500 MVA operating at 20 kV line to line rating voltage, 500 MVA transformer connected D/Y, primary 20 kV, secondary 400 kV, three phase 400 kV, 50 Hz power system and 150 km transmission line are splatted to three 50 km lines connected between three buses as shown in figure 4.5.
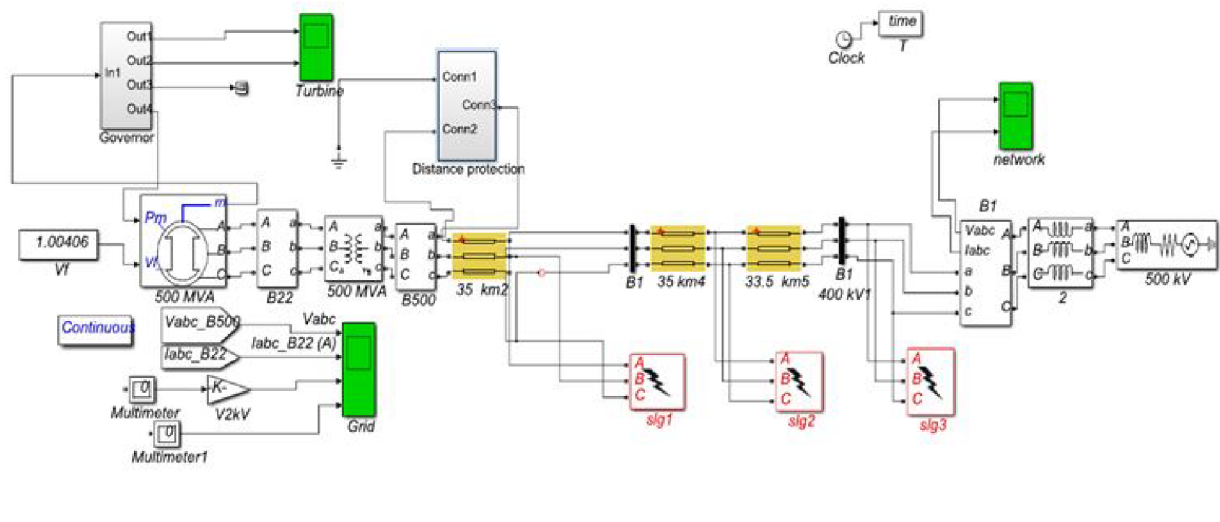
FIGURE 4.5: The power system model in Matlab simulation

SHORT CIRCUIT OF A SYNCHRONOUS MACHINE

For modeling the synchronous machine there is used the block from SimPower Systems library. This model has two input ports for Simulink interface blocks P_m, V_f, one output port m for Simulink interface blocks and three ports A, B, C for interface with modeled power system [61].

Under steady state short circuit conditions, the armature reaction of *a* synchronous generator produces a demagnetizing flux. In terms of a circuit, this effect is modeled as a reactance in series with the induced electromagnetic field. This reactance, when combined with the leakage reactance of the machine, is called synchronous reactance. The index d denotes the direct axis. Since the armature reactance is small it
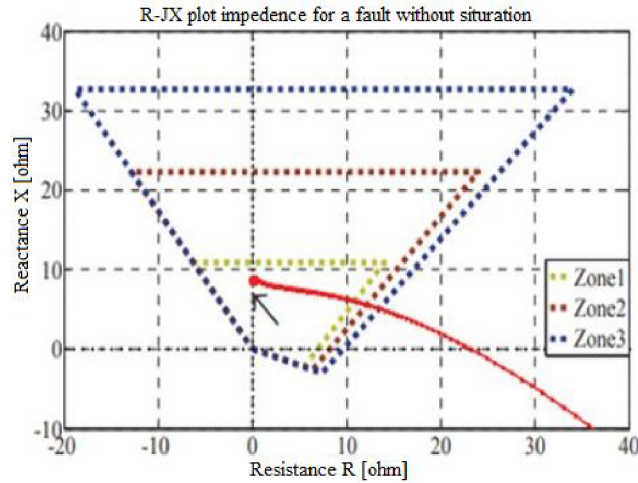
FIGURE 4.6: Secondary current of transformer without CT saturation
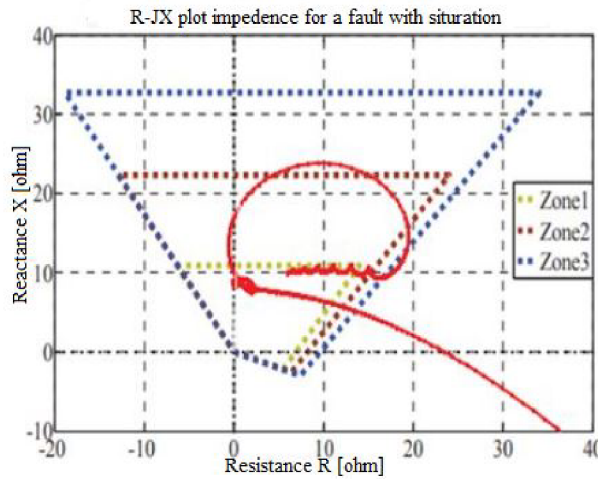
FIGURE 4.7: Secondary current of transformer with CT saturation

can be neglected. The steady state short circuit model of a synchronous machine [65][61] is shown in formula (4.5).

$$X''_d = X_1 + \frac{1}{[\frac{1}{X_a} + \frac{1}{X_f} + \frac{1}{X_{dw}}]} \qquad (4.5)$$

It is called the subtransient reactance of the machine. The reactance effective after the damper winding currents have died out, (shown in formula (4.6)).

$$X'_d = X_1 + \frac{1}{[\frac{1}{X_a} + \frac{1}{X_f}]} \qquad (4.6)$$

It is called the transient reactance. Of course, the reactance under steady state conditions is the synchronous reactance. Obviously is $X''_d < X'_d < X_d$. The machine thus offers a time varying reactance which changes from X''_d to X'_d and finally to X_d. When the fault occurs, the AC component of current jumps to a very large value, but the total current cannot change instantly since the series inductance of the machine will prevent this from happening. The transient DC component of current is just large enough such that the sum of the AC and DC components just after the

24
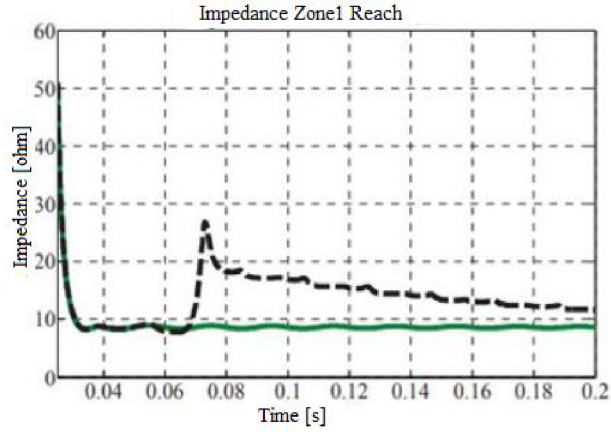
FIGURE 4.8: Impedance plot for zone 1 reach
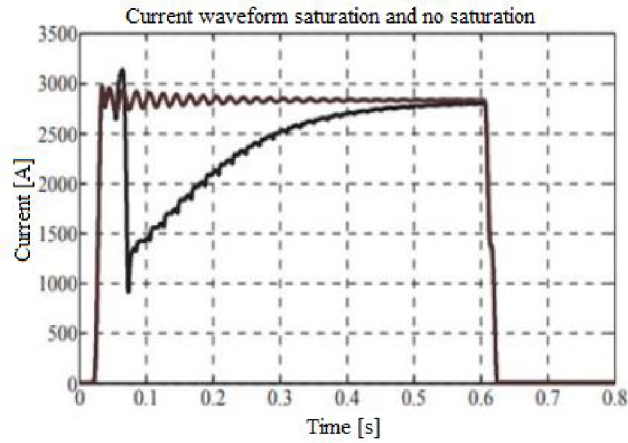
FIGURE 4.9: Current signal magnitude from FFT

fault equals the AC current just before the fault [60].

TABLE 4.2: Generator parameters

Mag	Value	Mag	Value
S_n	500MVA	X_1	0.17 pu
U_n	22kV	R_s	0.01 pu
P	500 pu	t_d'	0.87 s
X_d	2.2 pu	t_d''	0.03 s
X_d'	0.305	X_d''	0.21 pu
X_q	2.0 pu	X_q''	0.23 pu

Since the instantaneous values of current at the moment of the fault are different in each phase, the magnitude of DC components will be different in different phases. These DC components decay fairly quickly, but they initially average about (50- 60%) of the AC current flow at the moment after the fault occurs. The total initial current is therefore typically 1.5 or 1.6 times the AC component alone.

4.2.2 THREE PHASE FAULT IN QUADRILATERAL DISTANCE RELAY

Traditionally, the distance relay zones have been set according to simple rules. The nontraditional options can be grouped according to their conceptual basics: based on expert systems, mathematical optimization, adaptive protection or probabilistic methods [59, 60]. The final stage of the model is to develop the quadrilateral characteristics of the distance relay. This step helps to understand and figure out how the distance relay works. Three phase faults were set at distance 35 km, 70 km, and 110 km to check the behavior of quadrilateral characteristics distance relay of this type of near to generator fault. The most important thing to excess distance protection to clear faults immediately which can reduce the negative influence of the fault on the substation devices. Analog input module is a filter and processes the secondary currents and voltages which supplies distance protection relay then analog input module provides immediate sampled values to the internal digital bus. After that inputs of protection can be taken from outputs of the measurement elements [39]. Quadrilateral characteristics with their availabilities to be increased only in one direction (R or X) are used to overcome the problem of high resistance fault. For each stage of distance relay, the characteristics can be extended only in R direction with a fixed X setting [67].

- The criterion used for zone 1 reactive reach. The first criterion states that zone 1 only has to operate for faults on the line since this zone is instantaneous. Zone 1 should not operate for faults at the remote bus, by selectivity. Zone 1 reactive reach ($XR1$) will be set to 80% of the reactance of the protected line ($XL+$): $XR1= 80\%XL+$.

- The criterion used for zone 2 reactive reach. It will be considered that the main objective of zone 2 is to cover the sector of the line that is not covered by the zone 1. This implies that the reactive reach should be set to cover more than 100% of the protected line impedance, in order to guaranty sensitivity for internal faults.

- The criterion used for zone 3 reactive reach. It will be assumed that the main objective of zone 3 is to operate as backup protection for faults in adjacent lines, however, selectivity between zones 3 of different lines will have priority because zone 3 is the faster backup function.

4.3 SUMMARY

This chapter describes the impact of the current transformer saturation on the distance relay, the model designed in Matlab Simulink. The test includes apply fault and draw the fault locus on the quadrilateral relay characteristics. The three-phase fault set in distance 35km, 70km, 100 km, The distance protection designed to divide the high voltage transmission line to the zones, each zone contains part of the high voltage transmission line, and the zone 1 set to 80 percent of the first part of the line. The setting of the distance protection considers the line impedance which is the major parameter to design this protection.

Chapter 5

EVALUATION OF HARMONICS IMPACT ON DIGITAL RELAYS

This chapter presents the concept of the impact of harmonic distortion on a digital protection relay. The aim is to verify and determine the reasons of a maltrip or failure to trip the protection relays, the suggested solution of the harmonic distortion is explained by a mathematical model in the MATLAB Simulink programming environment. The digital relays have been tested under harmonic distortions in order to verify the function of the relay's algorithm under abnormal conditions. The comparison between the protection relay algorithm under abnormal conditions and a mathematical model in the MATLAB Simulink programming environment based on injected harmonics of high values is provided. The test is separated into different levels, the first level is based on the harmonic effect of an individual harmonic and mixed harmonics. The test includes the effect of the harmonics in the location of the fault point into distance protection zones. This chapter is a new proposal in the signal processing of power quality disturbances using MATLAB Simulink and the power quality impact on the measurements of the power system quantities, the test simulates the function of protection in power systems in terms of calculating the current and voltage values of short circuits and their faults. The chapter includes several tests: frequency variations and decomposition of voltage waveforms with Fourier transforms (model) and commercial relay, the effect of the power factor on the location of fault points, the relation between the tripping time and the total harmonic distortion (THD) levels in a commercial relay, and a comparison of the THD capture between the commercial relay and the model.

5.1 INTRODUCTION

In electrical engineering, the protective relay is a relay device designed to trip a circuit breaker when a fault is detected and has the ability to measure the power system quantities through the internal logic of a microprocessor. Digital relays have become more efficient and functional, especially for each of the following processes: the digital relay features accurate methods to calculate the voltage, current measurements, and other electrical quantities, and has become a communication standard for electrical Substation Automation Systems (SAS). Digital relays include multiprotection functions such as distance protection, overcurrent protection, under voltage protection, etc. In addition, there are many measurements that can be done using the microprocessor, such as internal/external fault diagnosis, fault measurements, zero current sequences, and disturbance recording. Additional functions of the digital relays, such as monitoring, metering, setting groups, fault recorder communication,

and reports, have no direct relation to the protective elements. The hierarchy structure of power system automation comprises an electrical protection relay, control, measurement , monitoring, and data communications. Power system automation is a system that is integrated into the various components connected to the power network. The numerical relay is a focal concept of the power system automation for protecting the equipment and limiting the damage. The system's components have better communication with each other; the information is exchanged via dozens of communication protocols, this concept can be characterized by the fact that one sensor is enough to obtain and collect information through the network instead of a sensor per component in the power system. Power system automation has several levels to integrate between the power substations and the substation supervisory system (SCADA). It defines both the information model and services used for communication between the Intelligent Electronic Devices (IEDs) in a substation. Some studies presented the practical test of the harmonic influence on electromechanical and microprocessor relays, the test implemented the current signal accompanied by the total harmonic distortion on relays, these studies found that the mixed harmonics influence is minor on the protective relays, conversely, the influence of pure signal above the fundamental frequency found a significant effect on protection relays function [21-25]. The evaluation influence of the power quality on the proactive relays presented using the simulation models (Mathcad software) [26-29], these studies focused on the advantages and distances of the relay algorithm. The harmonic distortions in the power system and the associated problems caused by nonlinear loads were briefly discussed. A review related to various methodologies for detecting and measuring harmonics based on this review of a new hybrid method for detecting and measuring harmonics is introduced in these references [30-31]. Few studies explore the research associated with quantifying the cost of reliability and power quality. Various power quality disturbances are investigated and possible methods of quantifying both the effect and cost are presented [33-35], moreover, it aims at analyzing and probing the influences of harmonics to differential relays. It analyzes and compares the mathematic models which are constructed by using EMTP and the test results [36,37]. It presents the impact of the fault in the power line based on the short circuit and abnormal condition, comparing the fault tripping time on the distance relay with two simulation scenarios developed using the MATLAB environment [38]. This chapter explains the signal processing of power quality disturbances using MATLAB 2016, MathWorks, Natick, MA, USA) Simulink, especially the power quality impact on the measurements of the power system quantities; the test simulates the function of protection in power systems in terms of calculating the current and voltage values of short circuits and their faults. The model includes a number of blocks that process the signals for the current and voltage coming from the simulator side. First, the current and voltage signals are filtered through a lowpass filter which removes the high frequency components from these signals. After the passage of the signals through the filter, there is the second level that converts the analog signals into digital signals through the processing signal within four stages. The first stage is the sampling process of the original signal, taking into account the sampling frequency which is determined to be 80 samples/cycle according to IEC standard 61850 (4000 Hz per second for systems operating at 50 Hz frequency). For this block, the input signals are analog and pulse generator signals. The signal is then inserted into a quantizer that converts the sinusoidal signal into a digital signal. Meanwhile, the signal is filtered through a digital filter. The parameters of this filter are adjusted to match the previous filter. The last stage is the calculation relating to the signal itself, which includes the amplitude angle using the Fourier transformation or an

arms calculation. The model characteristics are calculated from the parameters of the component with the intention to protect the relay, such as the transmission line, the transformer, and the generator, etc.

5.2 IMPACT OF HARMONICS ON PROTECTION RELAYS

The main reasons to study power quality as follows:

- Intelligent electrical devices (IED) have become more accurate in power quality measurements and less tolerant with higher frequency components than the nominal frequency of these devices. The major risk of harmonics in power systems is maloperation of the protective relays and the thermoelectric effect accompanied by these harmonics.

The reason to study the impact of harmonics on protective relays is the existence of harmonics in current and voltage signals which can cause a maltrip of the relay when no fault happens or the system fails to trip when there is a fault in the power system, especially when a harmonic can be noticed during a faulty performance. The relay algorithm is an important factor to define the harmonic impact. There is a difference between the higher values of relay tripping thresholds and the lower values of normal operation. A large difference will cause a higher risk of failure to trip and maloperation. The power systems quantities are converted to the digital form that provides easy implementation of digital processing signal (DPS) and analysis the power quality. Usually, the harmonic can be determined by the load characteristics; moreover, the harmonic in the current has a more intense impact than the harmonic in the voltage. In the power system, the harmonics might reduce the power quality and cause a number of problems, such as overloads in distribution systems because of an increase in the rms current value, and harmonics can also cause a shorter lifespan of generators, transformers, motors, and other power system components. On the other hand, the sensitive loads can be affected by harmonic distortion.

5.2.1 HARMONIC PHENOMENA

The total harmonic distortion (THD) can be defined as a percentage of the rms of the fundamental component.

$$THD_i = \sqrt[2]{\frac{\sum_{k=1}^{\infty} I_{h,rms}^2}{I_{rms}^2}} \times 100 \tag{5.1}$$

Where $I_{(h,rms)}$ is the amplitude of the harmonic component of order h (i.e., the h_{th} harmonic) and I_{rms} are the values of all the harmonics that can be represented as:

$$I_{rms} = \sqrt[2]{\sum_{k=1}^{\infty} I_{h,rms}^2} \tag{5.2}$$

This subsequently leads to the formula:

$$I_{rms} = I_1 \times \sqrt[2]{1 + THD_i^2} \tag{5.3}$$

The total power factor:

$$PF = \frac{P}{V_1, rms \times I_1, rms \times \sqrt[2]{1 + (\frac{THD_i}{100})^2}} \qquad (5.4)$$

The percentage voltage total harmonic distortion is:

$$THD_v = \sqrt[2]{\frac{\sum_{k=1}^{\infty} V_{h,rms}^2}{V_{rms}^2}} \times 100 \qquad (5.5)$$

where $V_{(h,rms)}$ is the amplitude of the harmonic component of order h (i.e., the h_{th} and V_{rms} are the values of all the harmonics that can be represented as:

$$V_{rms} = \sqrt[2]{\sum_{k=1}^{\infty} V_{h,rms}^2} \qquad (5.6)$$

The council of European energy regulators uses the term quality of service in electricity supply which considers three dimensions [27]:

- Commercial quality: related to the relationship between the network company and the customer.

- Voltage quality is defined by enumeration. It includes the following disturbances: the voltage magnitude, frequency and voltage variation.

- Continuity of supply concerns long and short interruptions.

The IEC (International Electrotechnical Commission) is an organization for standardization comprising all national electrotechnical committees.
There are three European standards defining the limitation of harmonic currents injected to the power system. They define the limits of the harmonic component of the input current which may be produced by the equipment:

- IEC 61000-3-2:2014 Electromagnetic compatibility (EMC) - Part 3-2: - Limits for harmonic current emissions (equipment input current $\leq$ 16 A per phase). This standard is applicable to the electrical equipment which required an input current up to 16 A.

- IEC 61000-4-7: Testing and measurement techniques – General guide on harmonics and interharmonics measurements and instrumentation, for power supply systems and equipment connected thereto. The new requirement launched for measuring harmonic should get 10 cycles of the fundamental current. Furthermore, no gap and no overlapping between the successive measuring windows are allowed.

- IEEE 519: The standard provides limitations for a harmonic distortion (a limitation on the harmonic voltage distortion provided by the distributor to the customers, a limitation on the harmonic current distortion superimposed to the system by a customer).

- Individual Voltage Distortion limits for the bus voltage level 69 kV and below should be not exceed by 3% and the total voltage distortion THD should be not exceed by 5%. Moreover, according to IEEE 519, there are more conditions with regard to the effects of harmonics on protective relays (electromechanical, static and digital relays).

- It is important to bear in mind that the impact of the power quality on the protection relays can cause incorrect trips and relay maloperation, while an incorrect tripping time occurrence depends on the power frequency variations and harmonic distortion [24].

5.3 DESCRIPTION OF MATHEMATICAL MODEL

The model is a suggested method of processing the voltage and current signals similar to the process that takes place in relays, precisely for the frequency variations and the number of samples per cycle. To ensure the validity of the test for this model, a comparison was made between the output of the model and the output of the physical relay located in the laboratory. The simulator generated signals for the voltage and current of a single phase fault (a short circuit) with the accompanying of these signals. These signals have been sent to the physical relay and have been recorded and changed the format to Comtrade (Common Format for Transient Data Exchange for power systems); after that the signals have been sent to the model; as shown in figure 5.1.
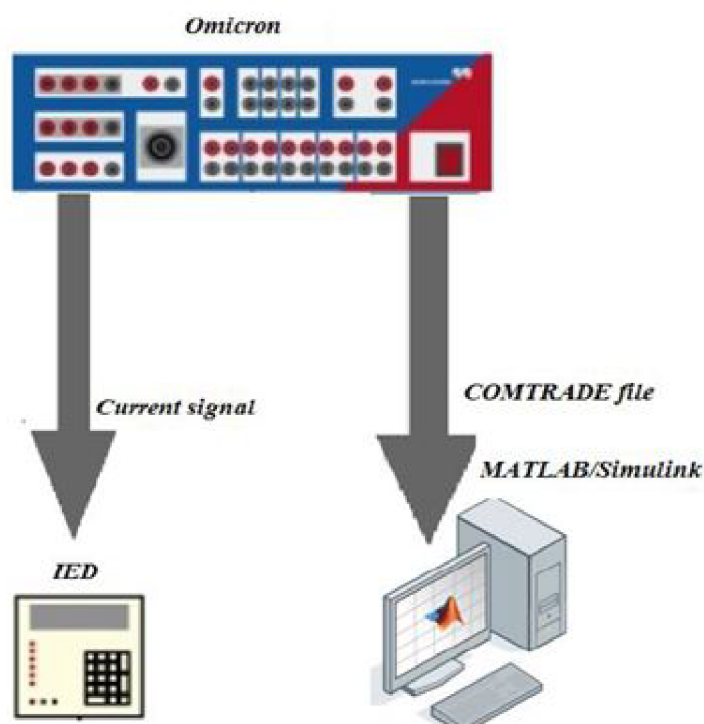
FIGURE 5.1: The test structure

Comtrade is a file format for status data related to a transient power system and storing signals. In addition to blocks that simulate these physical elements, the model also contains a display and calculation blocks for graphic representation of the results of simulated scenarios. The model presents the simulation and modeling of communication based digital relay using MATLAB, the model tested under abnormal conditions (short circuit) and under various fault types, the parameters of the derived model is based on the physical relay as shown in figure 5.6 which

presents the characteristic zones of distance relay designed in the MATLAB environment. The behavior of the model can be monitored and compared with the real protection relay by using the enerlyzer in omicron which can able to record voltage and current signals. The model reads the recorded signals by using Comtrade reader and the model offers the analysis of signals as shown in figure 5.2.
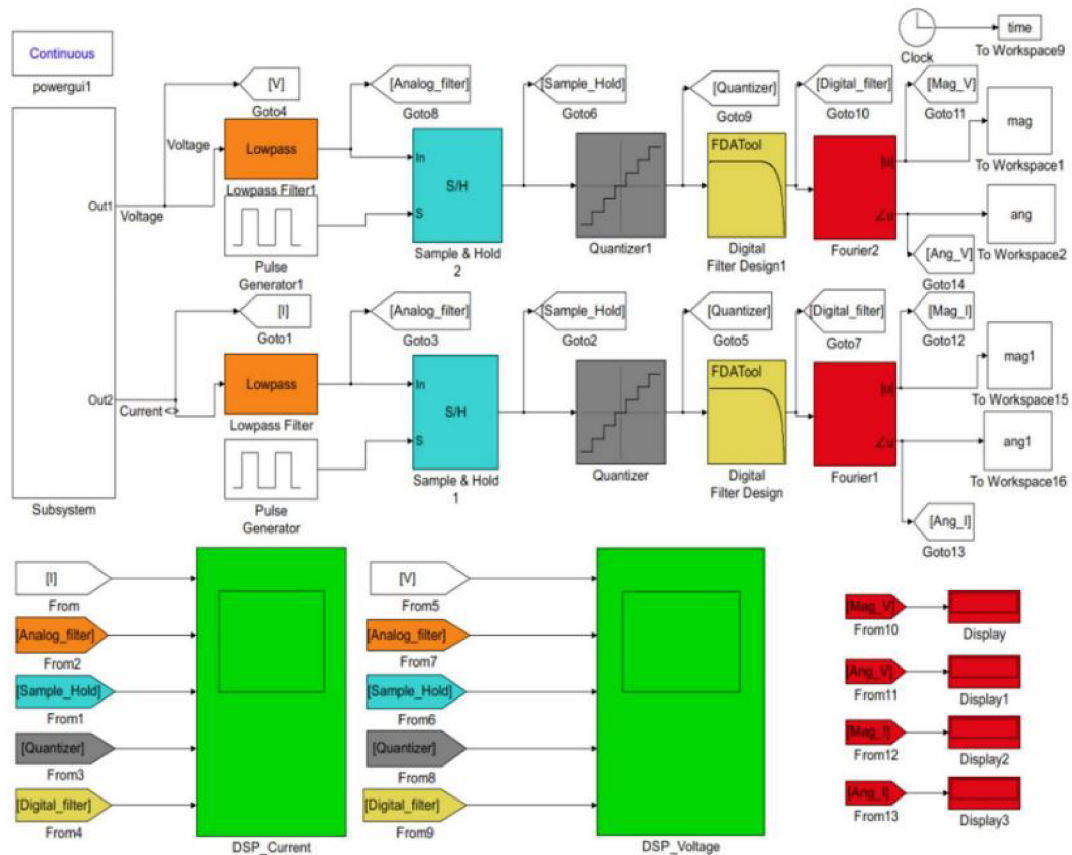
FIGURE 5.2: Model for current/voltage signal processing (DSP)

The model was made in the MATLAB Simulink programming environment (figure 5.2) using elements of the SimPower Systems library. The first step is to get the current and voltage signals from the current and voltage transformer sides and apply some functions to them. The digital processing signal is the process of modifying a signal to improve the performance of the relay, to eliminate the high frequency components, and to avoid the phenomenon of the aliasing from a fault signal; low pass antialiasing analog filters with suitable cutoff frequency are used. Holding and sampling the signal is the second block of the signal process which converts the analog signal to the sample. The quantizer converts the smooth signal into a stair step output. Fast fourier transform (FFT) is a faster version of the discrete fourier transform (DFT) which is used to find the fundamental frequency and higher frequencies contained in the input signal [26,27].

5.3.1 THE LOW PASS FILTER BLOCK

The low pass filter block can filter every channel of the input signal separately using the given design specification as shown table 5.1. A detailed description and

the possibilities of determining equivalent parameters are thoroughly discussed in [29,39].

TABLE 5.1: Parameters of low pass filter block

Parameter	Value
Passband edge frequency (Hz)	6000
Stopband edge frequency (Hz)	12000
Maximum passband ripple (dB)	0.1
Minimum stopband attenuation (dB)	80
Input sample rate (Hz)	28000*
	*Sampling frequency (3kHz,9kHz,28kHz)

The output signal from the Finite Impulse Response (FIR) filter can be described by Equation (1):

$$y[n] = b_0 x[n] + b_1 x[n-1] + ... + b_N x[n-N] = \sum_{i=0}^{N} b_i x[n-i] \qquad (5.7)$$

Where:
x[n] is the input signal,
y[n] is the output signal,
N is the filter order, an Nth order filter has (*N+1*) terms on the right hand side,
b_i is the value of the impulse response at the i_{th} instant for $0 \leq i \leq N$ of an Nth order FIR filter.

5.3.2   SAMPLE AND HOLD

The sample and hold block gets the input signal when it receives a trigger event at the trigger port. The block holds the output signal until the next triggering event occurs.

- When the trigger input rises from a negative value to a positive value, the block starts to acquire the input signal.

- When the trigger input drops from a positive value to a negative value, the block starts to acquire the input signal.

5.3.3   PULSE GENERATOR

The pulse generator block is the trigger input of the sample and hold block. It generates square wave pulses at regular intervals. The block waveform parameters (amplitude, pulse width, period, and phase delay) determine the shape of the output waveform.

5.3.4   FOURIER BLOCK

The fourier block offers the calculation the amplitude and phase of the input signal (current and voltage), total harmonic distortion. The block offers analysis of the signal components as a percentage of the fundamental signal.

- Recall that a signal *f(t)* can be expressed by a Fourier series of the form:

$$f(t) = \frac{a_0}{2} + \sum_{n=1}^{\infty} a_n cos(nwt) + b_n sin(nwt) \tag{5.8}$$

- where n represents the rank of the harmonics. ($n = 1$ corresponds to the fundamental component). The magnitude and phase of the selected harmonic component are calculated by these equations:

$$| H_n | = \sqrt[2]{a_n^2 + b_n^2} \tag{5.9}$$

where

$$a_n = \frac{2}{T} \int_{t-T}^{t} f(t) cos(nwt) dt \tag{5.10}$$

$$b_n = \frac{2}{T} \int_{t-T}^{t} f(t) sin(nwt) dt \tag{5.11}$$

$$T = \frac{1}{f_1} \tag{5.12}$$

f_1: Fundamental frequency.

5.3.5 PHASE LOCKED LOOP (PLL) SYSTEM

This block is used to synchronize a variable frequency sinusoidal signal. Meanwhile, this model is used to determine the frequency and the fundamental component of the signal phase angle which can be used to track the frequency and phase of the sinusoidal signal by using an internal frequency oscillator. The control system changes the internal frequency to keep the phase difference set to 0, as shown in figure 5.3. The model discusses two cases of Power Frequency variations when the power fre-
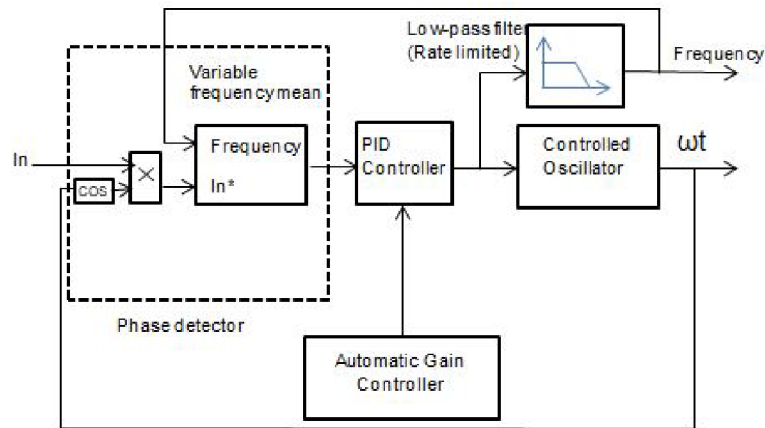
FIGURE 5.3: Phase locked loop (PLL) system

quency gradually increases from 50 Hz to 52 Hz and returns to the normal frequency after a period of time; see figure 5.4. The model compares the conventional way of calculating the frequency variation and the proposed way using a closed circuit. The proposed method is to track the frequency and amplitude of the input wave by using the frequency oscillator. In figure 5.5, in contrast, the frequency decreases by 2 Hz gradually to 48 Hz.
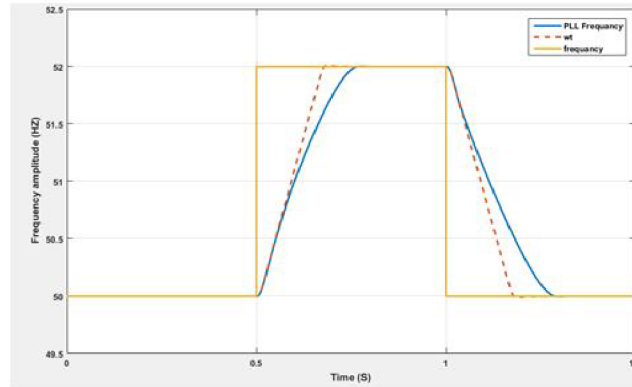
FIGURE 5.4: Frequency variation measurements between 50 and 52 Hz
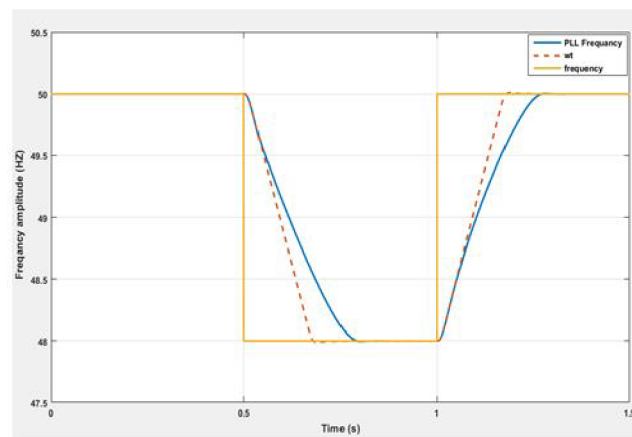
FIGURE 5.5: Frequency variation measurements between 48 and 50Hz

5.4   RELAY REPORT AND SIMULINK RESULT

Fault points were used in the tests, and a single phase with the ground (SLG) was chosen; the fault points were included in the harmonic components. The points were located near the border of zone 1 and zone 2. The characteristic zones of the distance relay and the chosen points can be seen in figure 5.6. As it is known, most digital relays use quadrilateral characteristics due to the many advantages which those characteristics can provide. The configuration and settings of the relay should be done in the first place; after that, exporting of these settings to CMC 256 is important to evaluate the relay functions. CMC 256 provides different platforms to test the relay with its zones setting, transmission line parameters, and time delay. Moreover, an advanced distance test displays the amplitude and phase of the three phase currents and voltages determined by the fault type and the fault location [31]. The distance relay is a universal short circuit protection. Its mode of operation is based on the measurement and evaluation of the short circuit impedance which, in the classic case, is proportional to the distance to the fault. Its tripping time is approximately one to two cycles (20 to 40 ms at 50 Hz) in the first zone for faults within the first 80 percent to 90 percent of the length. In the second zone, the tripping time depends on the settings which are usually 300–500 ms [40]. The parameters of the derived model are based on the physical relay, as shown in figure 5.6, which presents the characteristic zones of distance relay designed in the MATLAB environment.
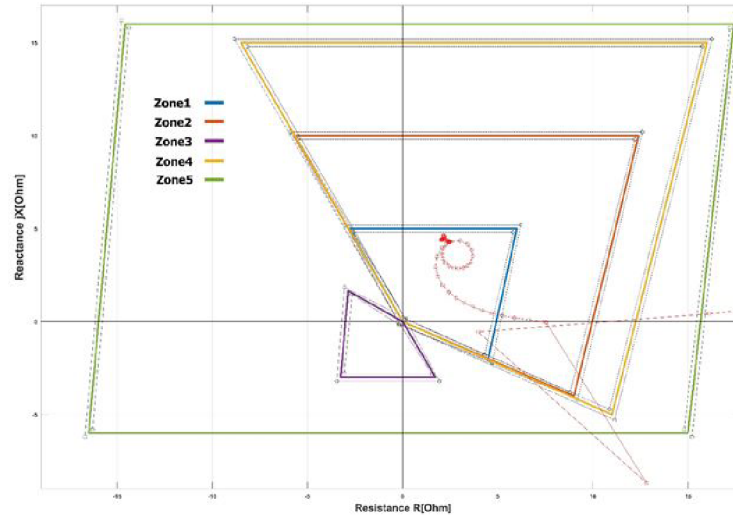
FIGURE 5.6: Characteristic zones of distance relay and fault points

THE TESTING CONDITIONS

A harmonics test allows for creating a voltage and current signals with three states: presignal refers to the signal with the fundamental frequency and presignal time can be determined according to the test conditions, signal refers to the signal accompanied by the harmonic components, post signal refers to the signal with the fundamental frequency as shown in table 5.2. Harmonic can be added to the voltage and current signals individually or mixed. The test offers the file export as Comtrade format and playback. The distorted voltage and the current waveform can be composed

TABLE 5.2: Harmonic testing conditions Omicron

Voltage	Current	Signal Definition	Trigger Condition	Harmonic Input
V_A	I_A	Presignal time	Active high	% of fundamental
V_B	I_B	signal	Active low	Absolute
V_C	I_C	Postsignal		
		Measured trip time		

of harmonic components, however, the distorted waveform can be decomposed into a fundamental sinusoidal waveform at nominal and harmonic frequencies. The decomposition of distorted waveforms can be done by Fourier transform, as shown in figure 5.7. An evaluation of the relay function and harmonics impact can be done in this test. The test is divided into different levels. The first level is based on the harmonic effect of mixed harmonics and individual harmonics. Both are used to test the protection operation and the Simulink model, considering that protection is IED and MATLAB is a Simulink model. Figure 5.7 shows three mixed harmonics (2nd, 4th, 6th) of the fundamental signal. The discrete Fourier transform is used to calculate the THD in the MATLAB model. The DFT Spectrum of a one cycle (20 ms) voltage signal was taken, applying the DFT to the first 20 ms of sampled signal results in the line spectrum at discrete frequencies 50, 100, 150 Hz, etc. Figure 5.7 shows the magnitude values of the harmonics by using equation (5.8). The figure shows that the

50 Hz component dominates; it is already visible from the original signal. The voltage signal contains significant components at even harmonics of 100, 200, and 300 Hz. Figure 5.8 shows decomposed voltage waveform with harmonic distortions of three harmonics (3rd, 5th, 7th) using the Fourier transform/ MATLAB window. The harmonic analysis was tested and measured using a MATLAB model. The test was
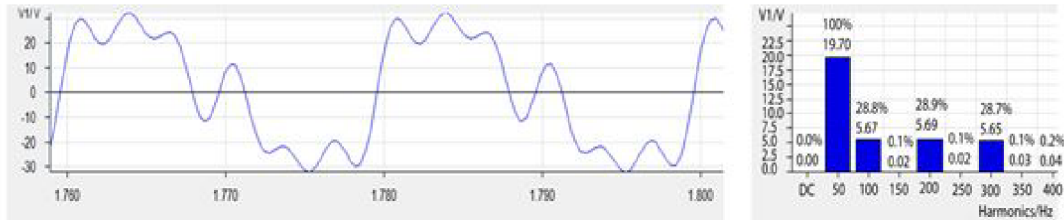
FIGURE 5.7: Decomposed voltage waveform with Fourier transforms/ MATLAB window
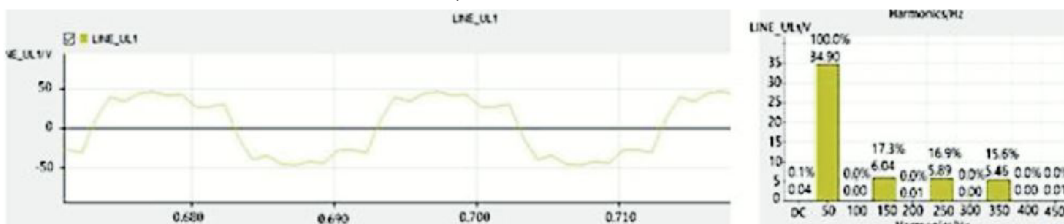
FIGURE 5.8: Decomposed voltage waveform with Fourier transforms/ MATLAB window

conducted at five different fault points and a total harmonic distortion was added to each of these tests. The total harmonic distortion on the current wave added at two points (the arrow direction up) is called an overreach, and the total harmonic distortion was added to the voltage wave at three points, as shown in figure 5.9. The total harmonic distortion was added as a percentage of the fundamental signal as follows: 10%, 20%, 30%, 40%, and 50%, and was colored in the following colors, respectively (violet, blue, yellow, red, and green). Overreach and underreach of pro-
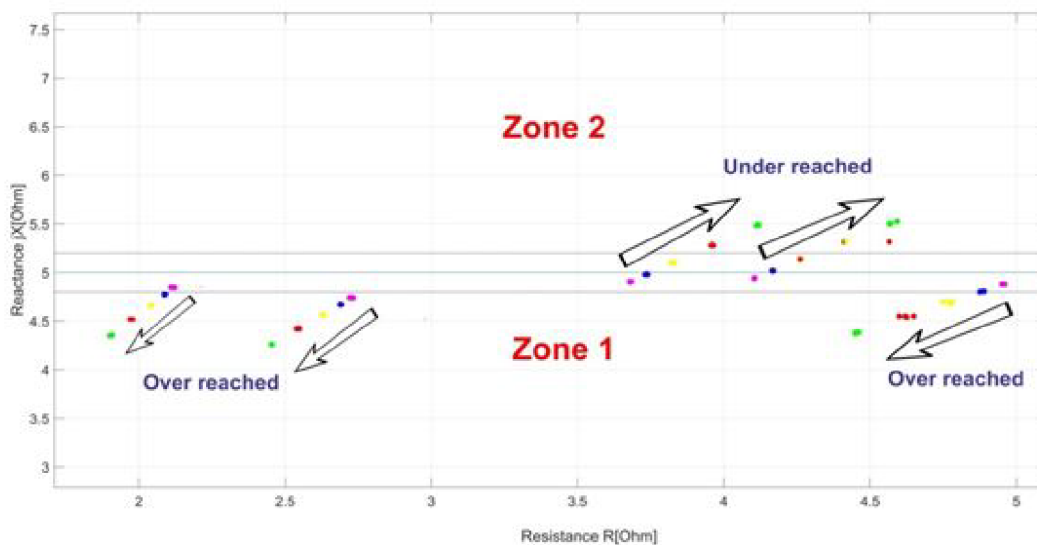
FIGURE 5.9: Quadrilateral characteristic and measured fault impedance locus

tection relays are common problems in power systems; they cause a maloperation of

the protection relays and it is impossible to detect the fault in the correct zone. The overreach of the point of the fault can cause the protection relay to send a maltrip signal, which means that the relay instead of a trip in a delayed time zone 2 will send the tripping signal in zone 1, which is not desired. A harmonic distortion can change the power factor which leads to a change in the measured impedance lower than the actual value. The overreach can be noticed from a distorted voltage waveform, as shown in figure 5.9, due to the lagging power factor. Conversely, an underreach of the point of fault can cause the change of protection relay and the decision to send a maltrip signal; it means that the relay instead of a trip at a delayed time zone 1 will send a tripping signal at zone 2, which is not desired, as shown in figure 5.9.
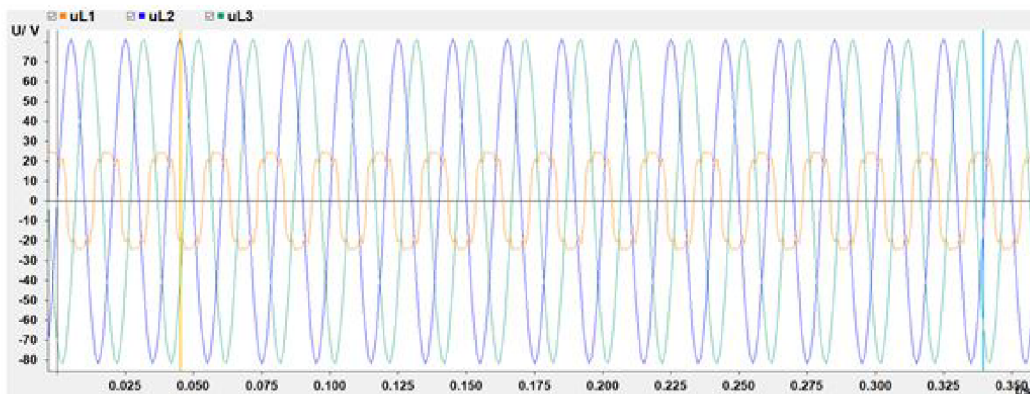
FIGURE 5.10: Voltage waveforms during single phase fault (IED)

A harmonic distortion can change the power factor, which leads to a change in the measured impedance higher than the actual value. The underreach can be noticed from a distorted voltage waveform, as shown in figure 5.9, due to the leading power factor. The overreach of the distance relays should be avoided mostly in the first zone. The test can illustrate harmonic distortion. A single phase fault operation of a distance digital relay was applied and, as a result, the relay made a maloperation decision. The analysis has been summarized from the integral disturbance recorder in the relay that has an area of memory. The relay can store all events in a disturbance recorder. Figure 5.10 shows a single phase to earth fault on the transmission line in a power system with a high harmonic content. It is assumed that three harmonics (3rd, 5th, and 7th) exist. The distance protection relay shows the instantaneous value of the three phase voltage with a high harmonic content once a single phase with earth occurs.

5.5   DISTANCE RELAY: TRIPPING TIME VS. THD LEVEL

Based on previous reports [41,42], the total harmonic distortion was measured at 30 different grids in the Czech Republic at different intervals. The measurements and evaluation of the harmonic level were made by the E. ON Distribution in the Czech Republic, operated by the company E. ON Czech Republic. More than 1000 MW of distributed energy sources (DES) are connected to this network, mainly from photovoltaic (PV) sources. According to the total harmonics of the measured points in grids, the distance relay was tested. Its mode of operation is based on the measurement and evaluation of the short circuit impedance which in the classic case is proportional to the distance to the fault. This test explains how a different magnitude

of the total harmonic distortion can influence the relay's operation and the tripping time of most digital protection relays used. A fault was located at zone 1 near the border zone 1–2 border (as shown in figure 5.11: the tripping time for fault without distortion was 23 ms (average of 10 measurements); the tests were performed with zone 1 tripping time set to 0 ms and zone 2 tripping time set to 1000 ms. It is possible to see how the harmonic distortion can affect the distance relay's accuracy and assessment of where the fault took place. During harmonic distortion, a portion of the current is missing so an excessively large impedance is measured. In our measurements on the distance protection, the zone reach is reduced. It is acceptable for near faults because the distance to the zone limit is long [33,36]. For faults close to the zone limit, an underreach is not permitted; the relay will trip in the second zone with a time delay [31].

Figure 5.11 shows the relation between the tripping time and the THD of the volt-
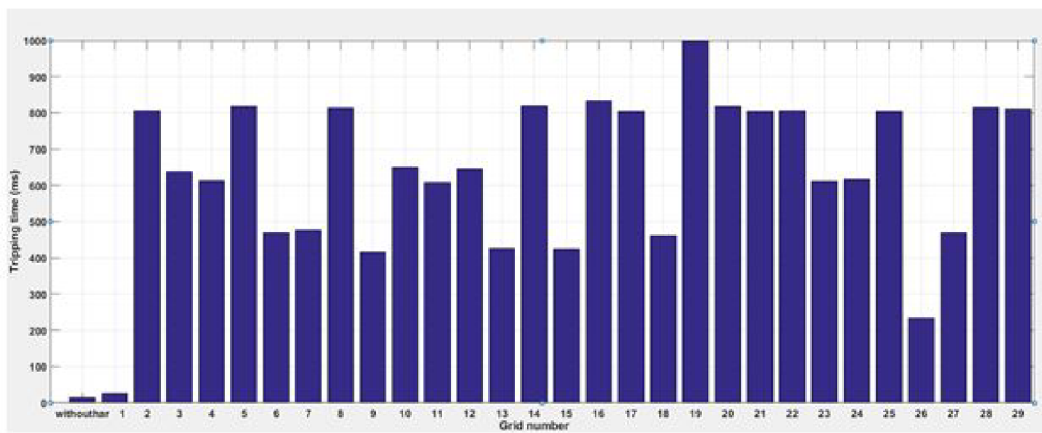
FIGURE 5.11: Distance relay: tripping time (seconds) vs THD level of grids

age. In this test, the THD does not exceed 4.5 percent. Note that the tripping time for the distance protection varies according to the added harmonic value.

Figure 5.12 presents the harmonic influence on the tripping time of the physical distance relay, where the current and voltage signals contain harmonics at a high level. The test was repeated five times and the average tripping time is presented. The type of fault is a single phase with the ground and tripping time without added harmonics of 1 s. The rms current and rms voltage should be constant during the test. For example, when the voltage and current signals contain the second harmonic, the tripping time of the distance protection is not constant, and the tripping time starts to change from 1 s to 1.6 s, meaning that the relay algorithm calculated the impedance in the third zone when the harmonic level was 10–40 percent of the current and voltage signals. Moreover, when the harmonic level was 50 percent of the current and voltage signals, the tripping time is changed to 3 s and the distance protection decision wrongly calculated the fault in zone 4.
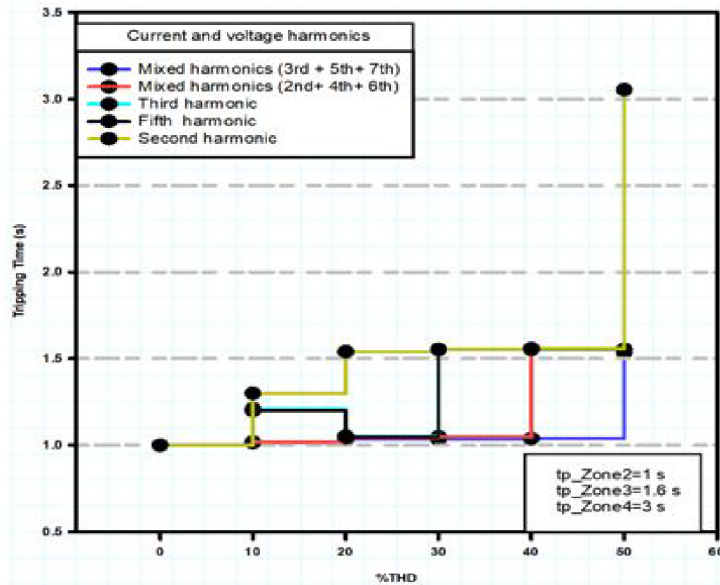
FIGURE 5.12: Distance relay: tripping time (seconds) vs %THD level

5.6 COMPARISON OF TOTAL HARMONIC MEASUREMENT BETWEEN PHYSICAL RELAY AND MODEL

The test involves a calculation of performance indicators concerning the level of harmonics through a commercial relay. This chapter contains a large number of measurements. The interval in the relay is 10 cycles in a 50 Hz system according to IEC 61000-4-30 and the model. The harmonics were added as the percentage of the current and voltage signals.

5.6.1 THE TESTING CONDITIONS

To achieve a comparison between the THD in the commercial relay and the model, EnerLyzer is used to control the measuring features of the CMC test sets. It runs as a standalone test module. It has four modes of operation: a multimeter mode, a transient recording mode, a harmonic analysis mode, and a trend recording mode. It calculates the harmonic analysis of all configured inputs (up to 64 harmonics) and displays it in a bar graph and in a tabular format.

5.6.2 TOTAL HARMONIC DISTORTION DETECTION IN PHYSICAL RELAY AND MATLAB MODEL

Through the test, the results show that the commercial relay of the harmonic capture ratio is lower than the original harmonic value. The total harmonic distortion is 10%, 20%, 30%, 40%, and 50% of the current signal according to the relay report. Figure 5.13 shows the harmonic measurements in a commercial relay. The second, third, and fourth harmonics were added as well as the three harmonics combined (2nd, 4th, 6th) and were added to the 3rd, 5th, and 7th harmonics. We can conclude that the commercial relay measures the THD with a difference of up to 35%, especially when there are three harmonics combined in the input signal, as shown in figure 5.13. The digital relays start function when abnormal conditions occurred as faults.

TABLE 5.3: The error of calculation THD for commercial relay

THD	10%	20%	30%	40%	50%
2^{nd}harmonic	2.04	3.62	3.45	3.62	3.52
3^{rd}harmonic	7.526	9.89	10.29	10.19	10.13
4^{th}harmonic	9.89	20.48	20.48	14.28	20.48
2nd+ 4th+6^{th}harmonics	17.56	21.95	21.95	21.58	21.65
3rd+ 5th+7^{th}harmonics	21.95	35.13	34.53	34.22	34.77

Abnormal events are accompanied by harmonics which are combined with the current and voltage signals.

Figure 5.13 shows the measurement of THD in a commercial relay. A harmonic mea-
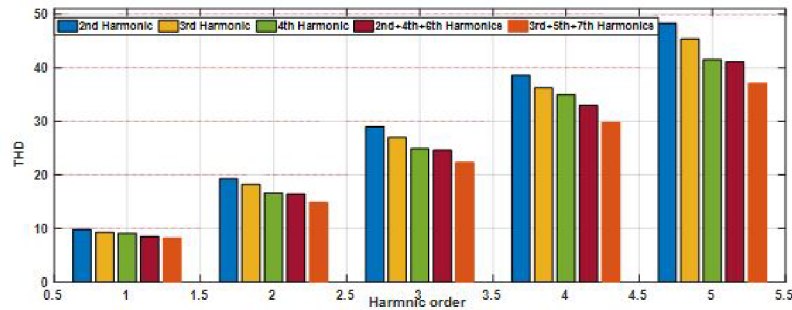
FIGURE 5.13: Commercial relay measurement of THD

surement evaluates the error of calculation, and the calculation method described above applies to the steady state fault conditions. The measurements of the third harmonic showed that the error of calculation in the commercial relay increased according to the harmonic percentage of the signal. The error of the calculation of the third harmonic is ca. 7% when the percentage of harmonic is 0–10%. After that, the error of the calculation of the third harmonic is stabilized to 10% when the percentage of harmonic is 10–50%. The highest error of the calculation of the THD can be found in mixed harmonics, as shown in Table 5.3 and Table 5.4.

The THD for mixed 3rd, 5th, and 7th harmonics is ca. 10–20% when the harmonic content is 0–10%. After that, the error of the calculation of THD for mixed 3rd, 5th, and 7th harmonics are stabilized to 33% when the percentage of harmonic is 10–50%.

Figure 5.14 shows the measurement of THD in the model. The harmonic measurements evaluate the error of calculation. The measurements of the third harmonic show that the error of the calculation in the model is increasing according to the harmonic percentage of the signal and the error of the calculation of the third harmonic is ca. 1% when the harmonic percentage is 0–10%. After that, the error of the calculation of the third harmonic is stabilized to 2% when the harmonic percentage is 10–50%. The highest error in the calculation of THD can be found in mixed harmonics, as shown in figure 5.14 and in table 5.4; the THD for the 3rd + 5th + 7th harmonics is around 1–2% when the harmonic percentage is 0–10%. After that, the error in the calculation of the THD for the 3rd + 5th + 7th harmonics is stabilized to 3% when the harmonic percentage is 10–50%.

Because the model implements the voltage and current signals, it is able to measure higher THD than the physical relay, as shown in figure 5.14. The model captures
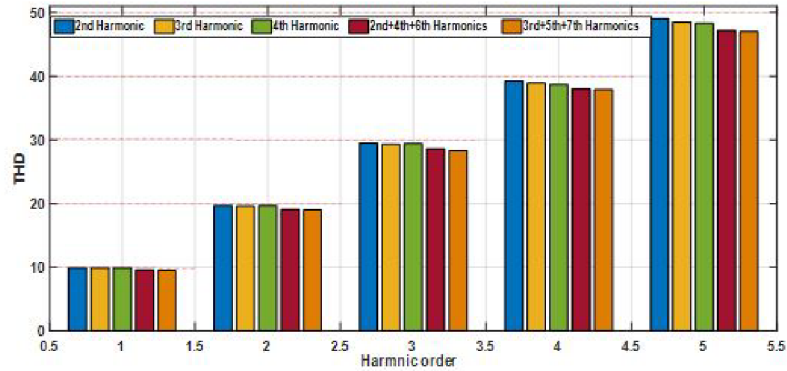
FIGURE 5.14: Model measurements of THD

TABLE 5.4: The error of calculation THD for MATLAB model

THD	10%	20%	30%	40%	50%
2nd harmonic	1	1.52	1.69	2.04	2.04
3rd harmonic	2.045	2.38	2.74	2.827	3.092
4th harmonic	1.01	1.522	2.739	3.359	3.519
2nd+ 4th+6th harmonics	4.16	4.712	4.89	5.26	5.932
3rd+ 5th+7th harmonics	5.266	5.263	6	6.1	6.38

harmonics with the accuracy of 90–95%. In the case of the individual harmonics, however, the physical relay captures with accuracy of 80–85%, as shown in figure 15.13. Similarly, mixed harmonics are inserted in the physical relay accompanied by the fault current and voltage signals. The physical relay captures mixed harmonics with accuracy of 65–70%, however, the model captures mixed harmonics with accuracy of 85–90%, as shown in figure 5.13 and figure 5.14.

The model provides a filter to reduce the harmonic distortion; this filter is built up from passive RLC components. Their values are computed using the specified nominal reactive power, tuning frequency, and quality factor. The filter has been implemented to mitigate the total harmonic distortion of the current and voltage. In case of an abnormal condition (a short circuit), the simulation implements a fault (a single phase with the ground) from 0.1 to 0.15 s. Conversely, the steady state has been implemented during the period from (0 to 0.1) s and (0.15 to 0.2) s. During the implementation of the simulation, the delay to start the calculation at the very beginning takes 0.02 s or 1 cycle. The steady state of the model takes place under normal operation and the calculation of voltage total harmonic distortion (V_{THD}) and current total harmonic distortion (I_{THD}) are implemented. Abnormal operation begins at 0.1 s and lasts for 0.05 s (2.5 cycles), which is accompanied by increasing the fault current and decreasing the voltage.

Figure 5.15 shows the computed total harmonic distortion (THD) of the current signal.

The THD is defined as the rms value of the total harmonic content of the signal divided by the rms value of its fundamental signal. For example, for currents, the THD is defined as:
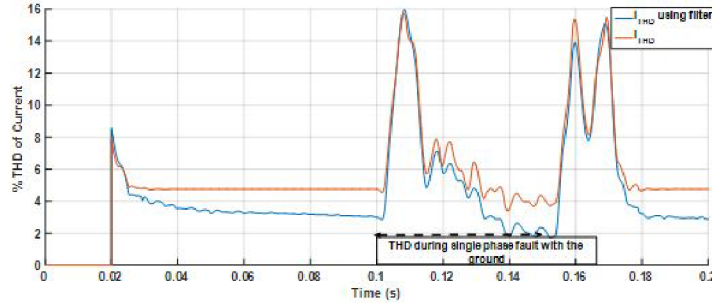
FIGURE 5.15: Compare %THD of current calculation using THD filter and without THD filter
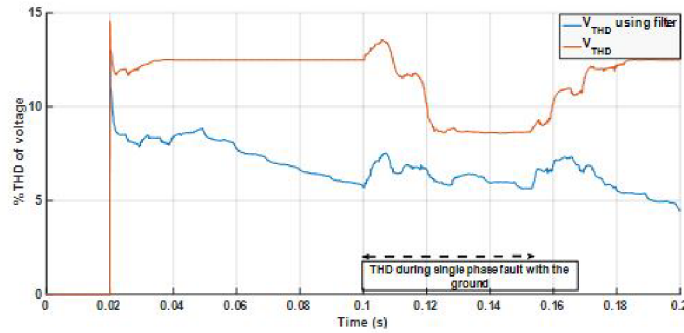
FIGURE 5.16: Compare %THD of voltage calculation using THD filter and without THD filter

$$THD = \frac{I_H}{I_F} \qquad (5.13)$$

$$I_H = \sqrt[2]{I_2^2 + I_3^2 + ... + I_n^2} \qquad (5.14)$$

I_n: rms value of the harmonic n
I_F: rms value of the fundamental current

In figure 5.15, when the simulation performs a normal condition, the I_{THD} has decreased accordingly by 1% to 2% when the filter has been implemented, during the short circuit the I_{THD} has decreased accordingly by 0.4% to 1.7%. In figure 5.18, when the simulation was run under normal conditions, the V_{THD} decreased accordingly by 5% to 7%. When a filter was implemented during the short circuit, the V_{THD} decreased accordingly by 2% to 5%.

5.7 SUMMARY

This chapter explains part of the digital signal processing in a power system. Moreover, the chapter provides different methods to compare the relay algorithm which can be used in a power system based on the impact of harmonics once they are injected in high values. The implementation of the test requires analyzing the occurrence of events in the power system. Each event contained in the input signals can be imported to MATLAB via a Comtrade reader which reads the selected event. Digital relays are limited because they can only respond to changes in the magnitude

of the fundamental current or voltage. Regarding overcurrent relays, a low level of harmonic distortion may not affect their operation, however, concerning distance relays, while the relay's ability to find faults away from zone's limit may still be reliable, when it comes to faults located near the limit of the zone, there is a possibility for the distance relay to be misguided as to the location of the fault.

Protective relays implement different techniques to measure the current and voltage. The microprocessor relays use a digital filter to take out the fundamental component. Filtering techniques were developed to accommodate a wide variety of harmonic influences. Antialiasing provides the ability to remove the frequencies higher than the Nyquist frequency; filter techniques should be implemented to reduce the harmonic level from the power system measurements. The THD filter implemented in this chapter can mitigate the THD of the current and voltage. The calculations of the THD during abnormal and normal conditions showed that the voltage harmonics were reduced by 2–5% and the current harmonics were reduced by 0.4–1.7%.

Chapter 6

ANALYSIS OF IEC 61850-9-2LE MEASURED VALUES USING A NEURAL NETWORK

Process bus communication has an important role to digitalize substations. The IEC 61850-9-2 standard specifies the requirements to transmit digital data over Ethernet networks. The chapter analyses the impact of IEC 61850-9-2LE on physical protections with (analog-digital) input data of voltage and current. With the increased interaction between physical devices and communication components, the test proposes a communication analysis for a substation with the conventional method (analog input) and digital method based on the IEC 61850 standard. The use of IEC 61850 as the basis for smart grids includes the use of merging units (MUs) and deployment of relays based on microprocessors. The chapter analyses the merging unit's functions for relays using IEC 61850-9-2LE. The proposed method defines the sampled values source and analysis of the traffic. By using neural net pattern recognition that solves the pattern recognition problem, a relation between the inputs (number of samples/ms—interval time between the packets) and the source of the data is found. The benefit of this approach is to reduce the time to test the merging unit by getting the feedback from the merging unit and using the neural network to get the data structure of the publisher IED. Tests examine the GOOSE message and performance using the IEC standard based on a network traffic perspective.

6.1 INTRODUCTION

Substations in energy systems use intelligent electronic devices (IEDs) that can share data in realtime, in order to use and share these data quickly and efficiently among the substation devices [1]. Sharing data must be standardized as a communication standard. The IEC 61850 standard unites the structure, requirements, and communication specifications that can be implemented during sharing of data among IEDs, the first announcement of the cooperation and creates a platform between the substation automation system (SAS) and the substations (IEC 61850 2003) [2]. IEC 61850-9-2 specifies that the transmission of sampled values (SVs) over an Ethernet network is located in the second layer (Ethernet layer) in an OSI system, using sampled values generated by merging units of IEDs or instrument transformers [3]. The implementation of IEC 61850-9-2 depends on the dataset specifications such as (time synchronization, sample counts, and interval time). Four currents and voltages are included into the IEC 68150-9-2 packets. Some studies have presented practical implementations of IEC 61850 that included a large number of IEDs; these studies explored the challenges coming from this technical evolution and used equipment

from multiple vendors to achieve interoperability. The references cited below discuss the requirements of interoperable distributed functions and distinguish the differences between MV and HV substations regarding IEC 61850 implementation [4,5]. Reference [6] proposes solutions to integrate IEC 61850 communication with the meters and their communication interfaces. This work implemented a complete smart grid realized on the basis of IEC standards. As further discussed in this work, the number of integrated units that can be used for monitoring and control purposes in the power system is quite small, and that means that there is also need for developed techniques for data handling to achieve realize smart distribution [7]. Research work has been presented in [8] analyzing the various communications options for scalable deployment of smart grid services. As stated in [8], the authors used the software defined utility (SDU) concept to obtain automated management of the smart grid. Reference [9] focused on the communications capabilities in traditional protections with the ability to use other technologies like WiFi and 3G for signal communication in real time. Several research articles [10,11] have proposed methods to develop self healing functionality in smart grids using IEC 61850. Reference [12] proposed a laboratory test bed for comparing the performance of digital, hybrid and traditional substations. The experiment focused on the hard in the loop test with traditional current and voltage operated protection relays and with sampled values according to IEC 61850-9-2LE. The comparison found that the relay protection function performance is very similar to that of classical substations, with the advantage of the data transmission in digital form. Reference [13] focused on the configuration of IEC 61850 GOOSE service for easy implementation with electric protection systems; the authors proposed an algorithm to achieve full implementation of the IEC 61850 instead of the hard wired network connection. Reference [14] focused on the reliability analysis of the cyber physical interface matrix (CPIM) methodology. The test calculated the impact of the physical device failure and the communication devices failures. This chapter contains the following sections:

- Section 2: Time synchronization over a process bus. This section contains the test structure with the devices used during the test. It contains the GPS parameters and initial test of the signal which generated from the GPS.

- Section 3: The IEC 61850 sampled values testing. This section contains the sampled values test with the OMICRON device and the test structure and sampled values directions.

- Section 4: The timing analysis of sampled values streams. This section contains the result of the measurement of the OMICRON merging unit and physical relays. (CMC publisher, IED publisher 2x IED subscriber) when time synchronization is applied.

- Section 5: Generic Object Oriented Substation Events (GOOSE). A GOOSE trip signal is sent from the publisher IED to the subscriber IED. This test found that when the GOOSE message is sent to the receiver IED (tripping signal), the signal is duplicated four times with a size of 147 bytes per packet, the average interval time between the packets was practically constant from the first to the fourth packets (278 μs) and the average interval between the fourth and the fifth packet was 102 ms.

- Section 6: Machine learning. By machine learning, we found a link between two parameters (number of samples/ms – interval time) and used to determine the publisher. The inputs and the target provided to the network and the

algorithm breaks up the data for test sets (training 70%—validation 15%—testing 15%), the best validation was in epoch 23.

6.2   IMPACT OF IEC 61850 ON SUBSTATION OPERATIONS

The main goals to implement IEC 61850 standard [15] are as follows:

- Increase the power quality, reducing the copper wires that are plugged into the IEDs and acheiving faster response to short circuit faults.

- The IEC 61850 standard provides the interoperability between IEDs from various manufacturers and offers a friendly configuration that can be implemented at a site without external support.

- Reducing the cost of operation and maintenance in the substations.

- This standard provides secure and fast data transmission among IEDs and substation devices.

- The IEC 61850 functionality is flexible and easy to implement by using the tools properly.

The challenges to implementing the IEC 61850 [15] are processing a huge amount of real time data and replacing some parts of substations to create a better environment to implement IEC 61850. The IEC 61850 structure includes 14 parts, as shown in figure 6.1. The IEC 61850 standard offers a data model that can replace the physical devices by the logical devices. In this way IEC 61850 is able to virtualize to all devices in the power system. Each logical device (LD) has logical nodes (LNs) that provides the functions of the devices. These functions are called "distributed functions" in SAS, and the three main rules to implement the distributed functions are:

- The IEC 61850 configuration should follow the performance requirements.

- The communication interface between IEDs and the system should follow the IEC 61850 standards communication fundamentals.

- Establish the communications between devices by mean transfer data between IEDs and the power system among the SAS.

The structure of the data model in the IEC 61850 standard is virtual (data object, logical device, logical node), although, it represents real data that are used by the energy system (monitoring, protection and automation systems) [11]. IEC 61850 offers various features that cover all aspects of the substations measurements, as follows [11]:

- Data characterization such as sampling frequency, sampling counts, and time synchronization.

- Communication specification that can be summarized as a generic object oriented substation event (GOOSE), manufacturing message specification (MMS), SMV, and Ethernet communication.

- The data structures and data object services.

According to the specification of the IEC 61850 can be summarized as follows:

- Definition and determine how to access the structure for the data's abstract communication services interface (ACSI) and the configuration of the communication solution and compatible protocols.

- Standardizing the output data from IEDs and categories the sharing of data between GOOSE and SMV orders.

- The IEDs and network communications are implemented using eXtendable Markup Language (XML).
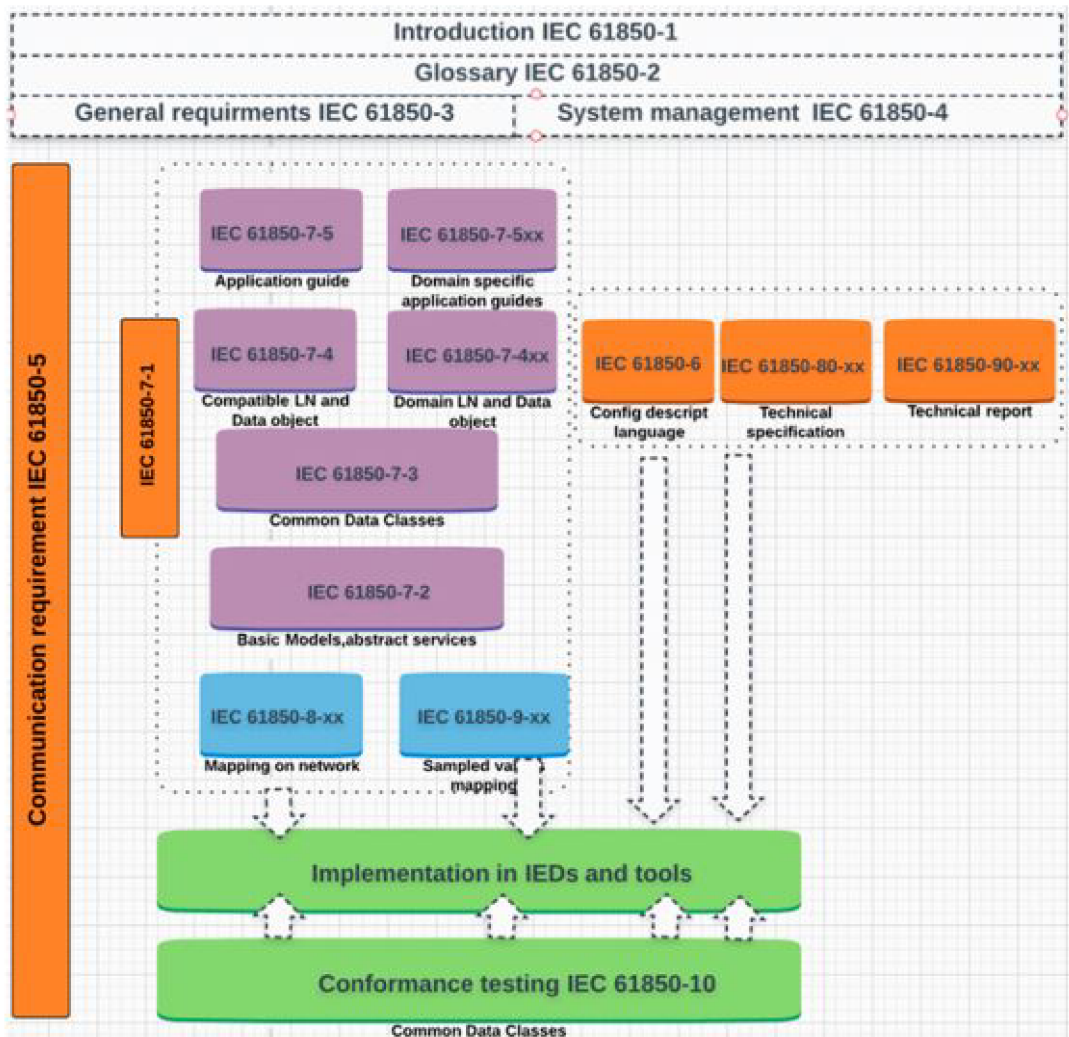
FIGURE 6.1: IEC 61850 structure

6.3   THE IEC 61850 INFORMATION SYSTEM

Logical nodes (LNs) are the most important part of the IEC 61850 hierarchical model. This model is designed to provide the way for implementation the interoperability among IEDs within the power system, the model represents the actual devices in the power system as logical devices LDs) that are plugged into logical nodes. The physical devices contain distributed functions that are responsible for exchanging data; each LN is linked with a function in the physical device [4]. The data model

explains the hierarchy of IEC 61850, the definition of the logical device and server is specified by the administrator. Depending on the data model structure, the data of substation operations can be assigned to one of these logical nodes, for instance, the measurements function group begins with "M" and the protection function group begins with "P". In figure 6.2 from left to right, the device name is the first part and the logic node (LN) is the second part, the attribute that represents a function is the third part, "st" represents the status attributes, "Pos" represents the position of the circuit breaker and "Val" represents the value of the status.
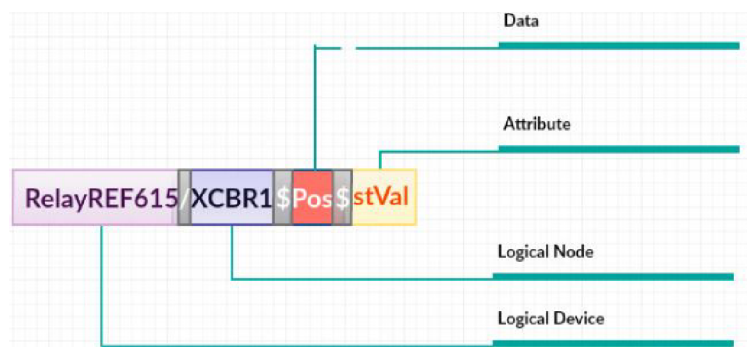
FIGURE 6.2: IEC 61850 Object Name Structure

6.4 TIME SYNCHRONIZATION OVER A PROCESS BUS

Time synchronization is an important element in sampled value applications due to the problems that can be caused in case the time synchronization is lost due to phase shifts, maloperation or wrong tripping. In the laboratory during implementation the SMV IEDs configuration, the time synchronization can be done by the IEDs-publisher. In this way the IED-subscriber will follow and get the same phase error limit. In case of using several merging units connected together and sharing data among the power system, the time source according to IEC 61869 is required. This time source will be a global area clock, however, a local area clock cannot match the time in the global area clock. There are various methods that can be implemented to achieve the time synchronization in the whole testing system and between the merging units such as master slave architecture for clock distribution (IEEE 1588) precision time protocol (PTP). IEEE 1588 is used to achieve the time synchronization because the IEDs are adaptable to this method and offered high accuracy time synchronization. According to IEC 61869, the GPS or time source is sharing the time over the process bus side by side with sampled values. The configuration of the time synchronization of IEDs is shown in figure 6.3. In IEDs, time synchronization is enabled by using synch source (IEEE 1588—slave), IED-subscriber (figure 6.3) shows a synch accuracy of 23 ns. More precisely, the sampled values and PTP are using the same.

More precisely, the sampled values and PTP are using the same network cable, however, a cut in the Ethernet cable can cause SMV and PTP transfer failure. The relation between sampled values and time synchronization is called SmpSynch. This attribute is an indicator of time source loss, moreover, SmpSynch gives details about the time source (GPS) and the sampled values sources (IED-publisher). Table 6.1 provides the settings of the GPS data and the timing accuracy that are used to achieve the time synchronization in our network [4].
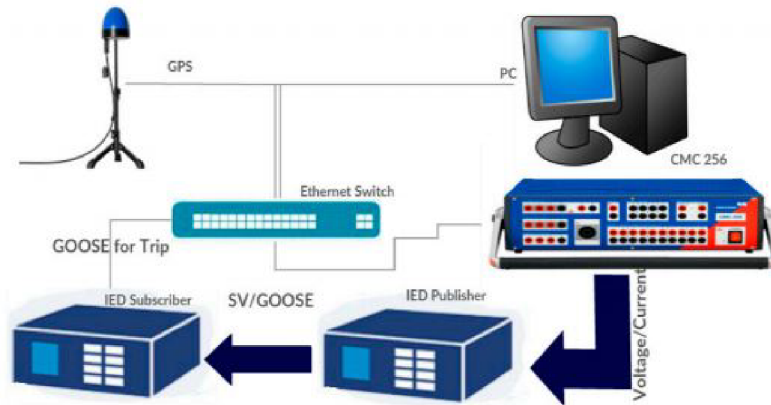
FIGURE 6.3: The full scheme of testing the IEC 61850 (SMV-GOOSE)

TABLE 6.1: GPS data sheet and timing protocols

V_e(volt)	I_e (amper)	Z_e(ohm)
3	0.001	3000
7.5	0.002	3750
12.53	0.003	4167
18	0.004	4500
60	0.01	6000
150	0.02	7500
200	0.025	8065
300	0.05	6000
400	0.2	2000
447	1	447
486	10	49

PTP CLOCK TYPES IN TIME SYNCHRONIZATION

The time synchronized is required to get more accurate measurements and implement the Peer to Peer (PTP) protocol. Grandmaster is synchronized with an external source such as a CMGPS 588 (GPS) controlled time reference. The synchronization unit is an antenna integrated GPS that works as PTP grandmaster clock according to IEEE 1588. Ordinary clock reads can be performed from IEDs or CMC 256 plus. This test requires an advanced Ethernet switch (Hirschmann). Table 6.2 lists the GPS status and the timing protocol that was implemented during the experiments (the synch interval between two synchronized messages is 1 s, and announcing the time-out and losing the time synchronization takes 3 s.

The GPS sends three messages to synchronize the devices (announce message, synch message and follow up message) and it duplicates them each second, in order to keep all IEDs synchronized as shown in figure 6.4 and figure 6.5.

6.5 THE IEC 61850 SAMPLED VALUES TESTING

The test includes three stages. The first one sends sampled values from one IED to another (publisher to subscriber). An Omicron CMC 256 plus is used to generate

TABLE 6.2: PTP time synchronization and settings

CMCGPS 588	CMCGPS 588)	Time Interval	Time Interval
GPS	Locked	Sync interval	1 s
PTP	Master	Announce interval	1 s
NTP	Synchronized	Announce receipt timeout	3 s
Satellites usable	4	Peer mean path delay	85 ns

FIGURE 6.4: The measured interval time between synchronization announcement messages
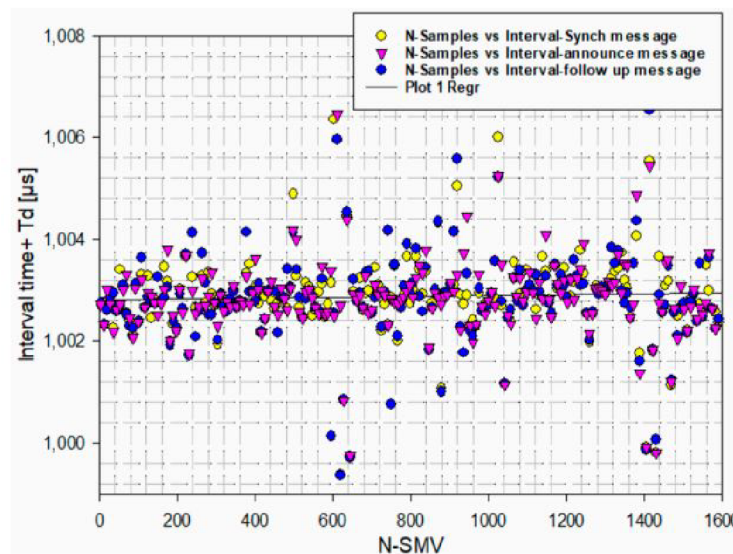
FIGURE 6.5: The measured interval time between announcement messages—follow up messages—synch messages of synchronization.

analog voltage and current signals, the signals are transferred to the CMLIB A to send it using Ethernet cables to the IED port (IED-publisher). As connection box for low level signals a CMLIB A is used for connecting the low signal outputs of a CMC for measurement or controlling purposes. The CMLIB A set (VEHZ1105) includes the CMLIB A box (VEHZ1101) and the 16 pole LEMO cable (VEHK0003) [16]. As shown in figure 6.6 and table 6.3.

52
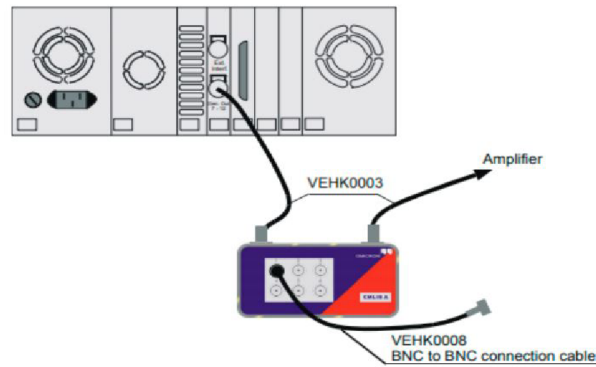
FIGURE 6.6: CMLIB A Hardware Configuration

TABLE 6.3: CMLIB A Hardware Configuration

Linear Voltage Sensor		Rogowski Current Sensor	
NominalvoltageofOMICRON	2 V	NominalvoltageofOMICRON	150 mV
OutputSystemchannels	L to L	OutputSystemchannels	L to L out 4–6
Min Frequency	0 Hz	Min Frequency	0 Hz
Max Frequency	1 kHz	Max Frequency	395 Hz

The analog signal is converted to a digital signal in the IED (A/D converter). The IED-publisher publishes the sampled value signal according to the standard IEC 61850 with 80 samples/cycle in a 50 Hz system. The subscriber IED is receiving the digital signal SMV and reacts according to the signal and the configuration of the IED. SVScout software is used to visualize sampled values and subscribes to the SMV streams from multiple merging units and shows the waveforms. An Omicron CMC 256 simulator is used to simulate the current transformer (CT) and voltage transformer (VT) signals as shown in figure 6.7 [10].

SAMPLED VALUES TEST

The sampled values test can be implemented to simulate the merging unit of the IED-publisher. The configuration of the test is required to import the substation configuration language (SCL) file of the publisher IED, moreover, the sampled values test tests the IEC 61850 9-2 LE process bus. It is able to generate up to three sampled values streams in the test set. In order to publish the sampled values it is important to set the analog voltages and currents generated at the voltage and current outputs of the test set.

SVSCOUT SOFTWARE

This is a tool for visualizing the IEC 61850 sampled values; it provides the possibility to test the digital protection that is working with IEC 61850 sampled values as shown in figure 6.8. It used to receive, view, process and save sampled values to the implementation guideline of the UCA International Users Group IEC 61869-9 standard. The data packets can be obtained from many sources at the same time and the timing analysis for those data streams could be performed.
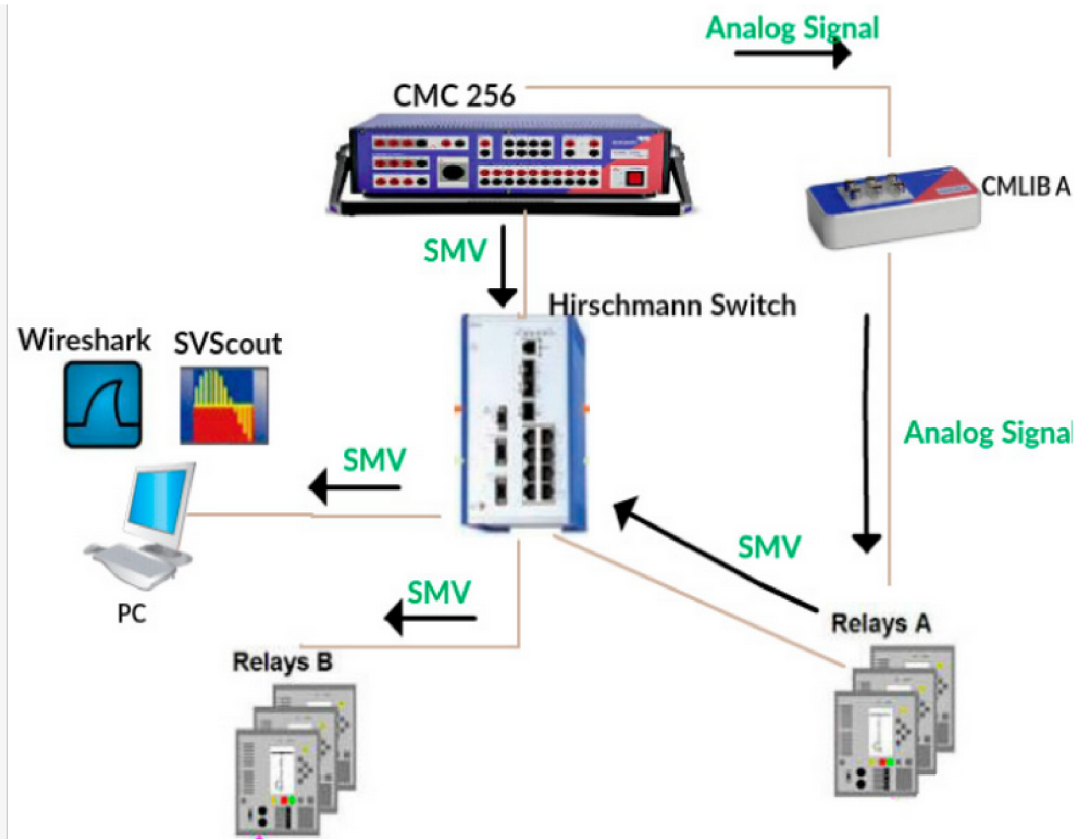
FIGURE 6.7: Experiment structure and network devices
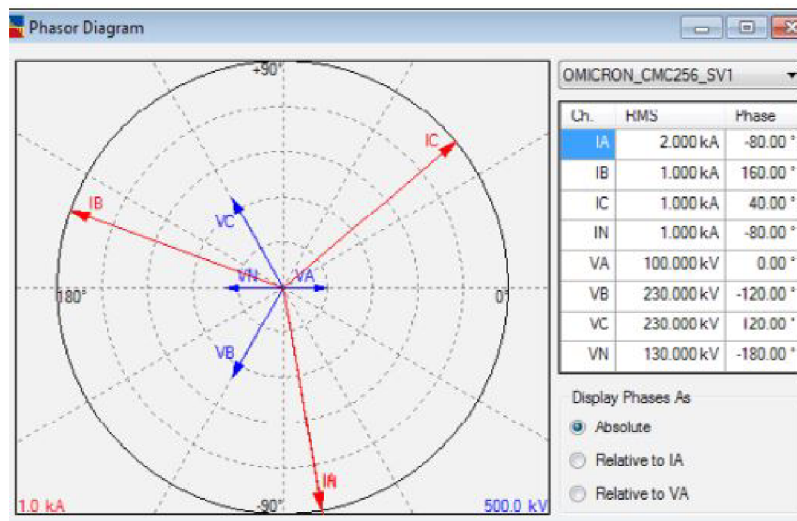
FIGURE 6.8: Omicron sampled values test configuration

6.6   THE TIMING ANALYSIS OF SAMPLED VALUES STREAMS

In order to understand the data acquisition of sampled values, the comparison of
sampled values between IED_MU and CMC_MU with no time synchronization of
the CMC 256, the measurements of the merging unit are implemented in the lab-
oratory, the CMC 256 is configured to publish the sampled values to simulate the
merging unit of the IED merging unit by importing the SCL file of the IED-publisher,

thus, the CMC Omicron provides the ability to publish the sampled values and the comparison with the IED merging unite offering a way to analyze the time as shown in figure 6.9. The interval between two packets can be calculated as T = 1/4000 = 250 ms, more than that, the delay time is accompanied by the interval as shown in table 6.4. The IED-publisher publishes the sampled values and the time synchronized as the local clock (master clock) of the publisher IED [8].

TABLE 6.4: Time display and time references

Frame Size [bytes]	Round Trip Latency [μs]
128	241
256	292
512	426
1280	645
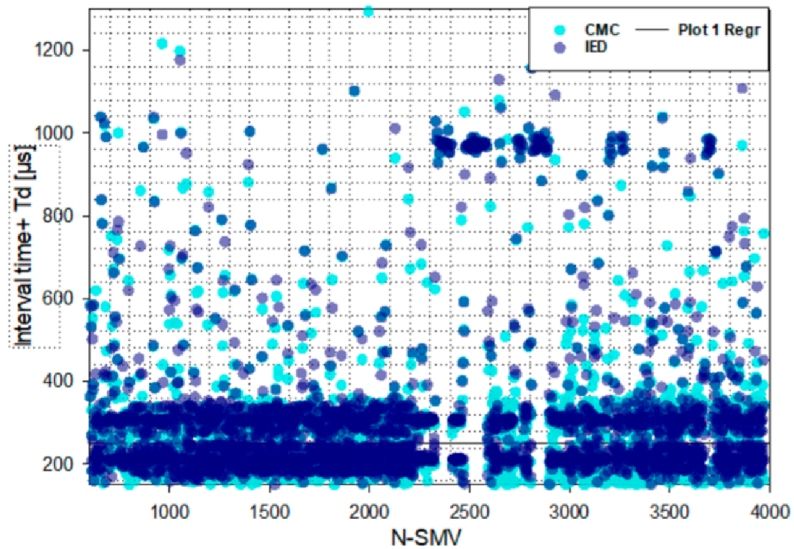
FIGURE 6.9: The interval time in microseconds between packets of CMC—Simulator, an IED

TIME DISPLAY AND TIME REFERENCES

Time display formats in Wireshark can be explained according to the following steps:

- While packets are captured, each packet is timestamped. Each capture file includes these timestamps which is important for later analysis.

- According to RFC 2544 testing methodology, RFC 2544 requires the standard frame sizes (128, 256, 512, and 1280) bytes.

Brno University of Technology performed tests to measure the roundtrip latency on the fiber optic cable (Ethernet transmission) [17], finding the following results: Figure 6.10 presents the number of packet per millisecond. The figure shows the comparison between the merging units of the IED and CMC, the number of packets is proximity around four packets for each merging units, with some high number of

packets for the IED-publisher and a low number of packets for the IED publisher. The CMC hold still the number of packets to four packets per ms. Experiments offer the possibility to make a comparison between two merging units, the physical relay merging unit and the simulated merging unit (CMC). The figure shows that regression of the samples is 230 μs in case of time synchronization applied to both merging units. The simulated merging unit shows a constant interval of time between the packets as shown in the figure, however, the merging unit of a physical IED in 4000 samples showed that the interval time is not constant, the sender IED sends packets with 126 bytes length and the subscriber IED sends packets with 122 bytes length.
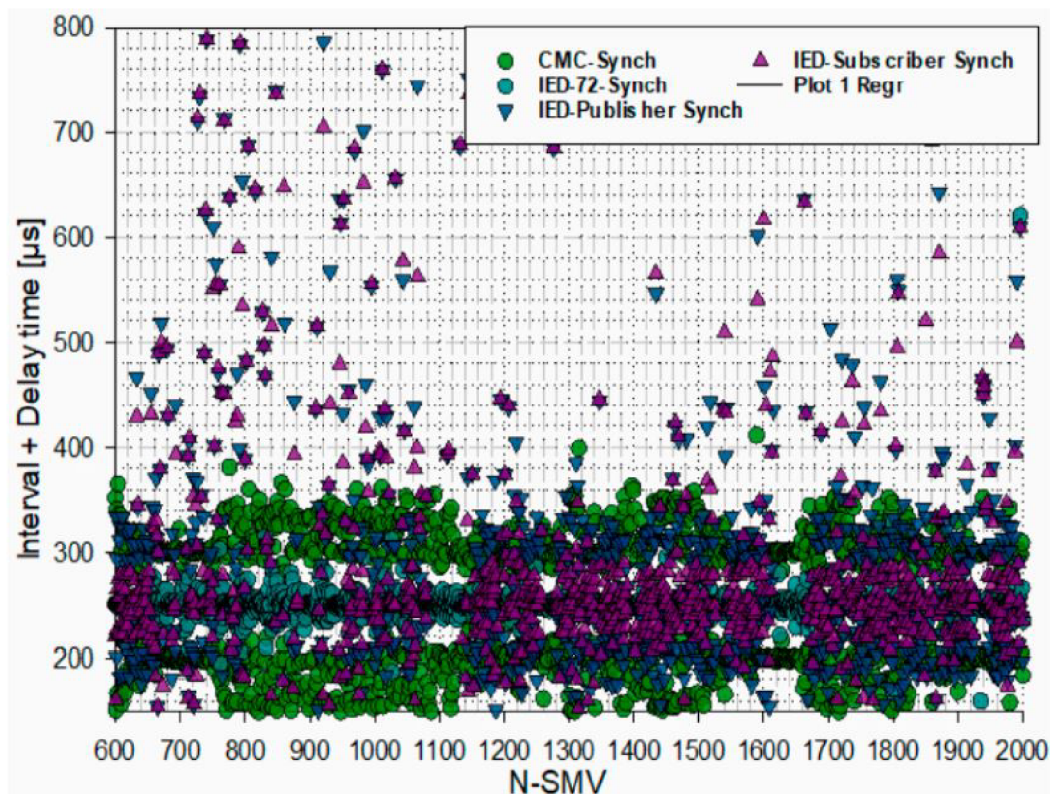
FIGURE 6.10: The calculation of time duration to publish the sampled values. The CMC publisher sends packets with interval 250 μs and IED-72 follows by sending packets to keep the system synchronized

Figure 6.11 shows the SMV packets between the publisher and subscriber of physical relays, the regression of the interval time is around 240 μs, the current and voltage signals are plugged in the IED, the publisher converted them to a digital form and sent them to the IED-subscriber [9].

In figure 6.12, CMC is the publisher of SMV that is synchronized by the global clock (GPS), IED-72 is the receiver or subscriber of the SMVs, according to the measurements the publisher is sending the packets and waits for the subscriber to send a confirmation of acceptance of the packets which explains why there are small delay times from the publisher in this case [18].

In order to make the study clear, Wireshark was used to capture the sampled values streams and packet delay time or the time between two following streams calculated in two cases, the first one when two IEDs are connected and are an IED-publisher and IED-subscriber with time synchronization. The second case is when the CMC Omicron 256 plus merging unit is connected through the Ethernet switch
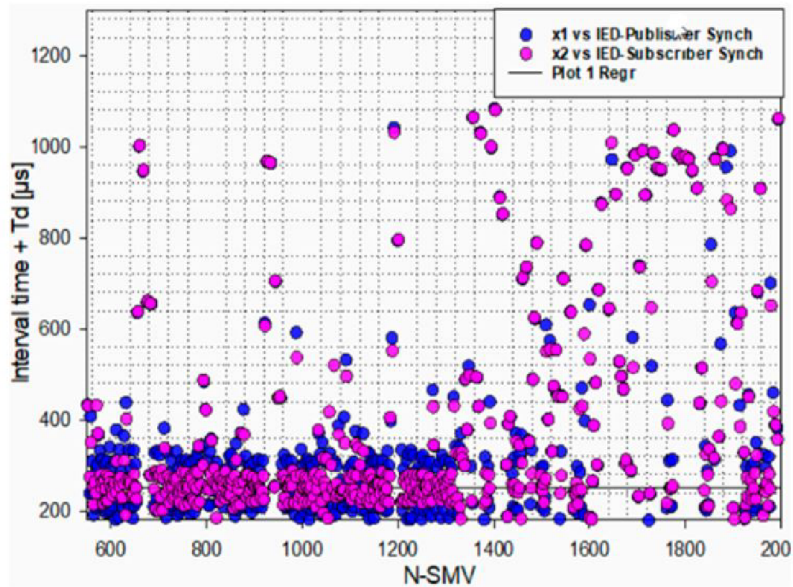
FIGURE 6.11: The interval time + delay time in μsec between publisher/subscriber IEDs.
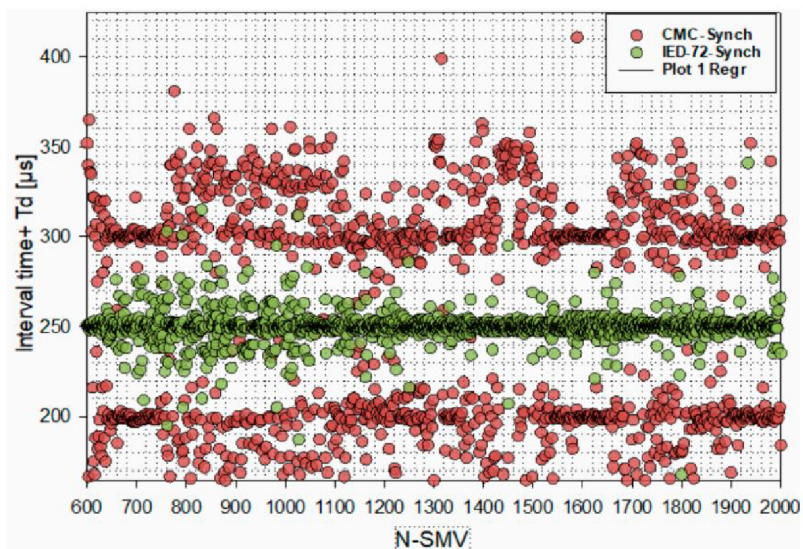
FIGURE 6.12: The interval time + delay time in μsec between publisher/subscriber (CMC and IED-72)

to the IED-subscriber. The difference between no synchronization and synchronized time is that the IEDs start to synchronize with the master grand clock (GPS). The sample count is an important parameter to determine and view the links between the synchronization time and the sampled value measurements. In order to explain and verify the sample count, the measurement is implemented with different cases, first with the SMV from merging units of IED without time synchronization, second with the SMV from IED merging units with time synchronization. The third count is the SMV from the CMC Omicron merging unit without the time synchronization; the fourth count is the SMV from the merging unit of the CMC Omicron with time synchronization. The last count is the count of the samples values of the merging unit of CMC Omicron and IED in parallel with time synchronization as shown in

TABLE 6.5: PTP time synchronization and settings

IEC 61850 -9-2	50 Hz System	60 Hz System
HSR redundant network	4	4
PRP redundant network	9	8
T	250 μs	208 μs
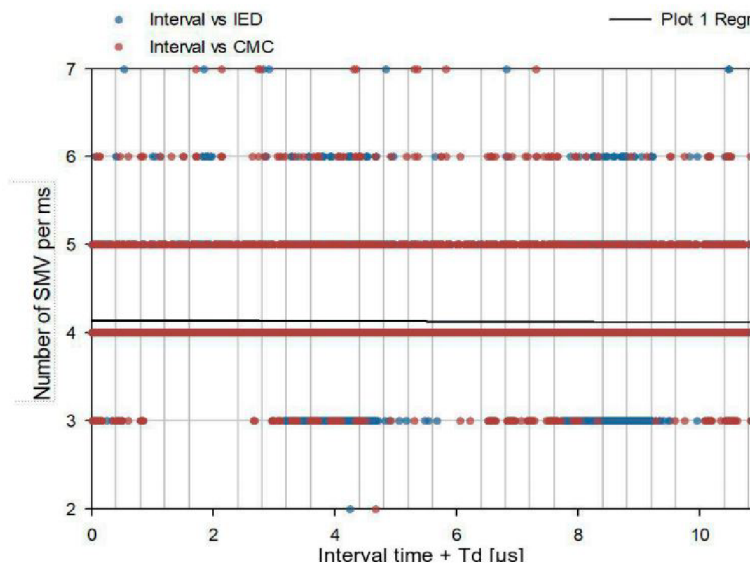
figure 6.13.

FIGURE 6.13: Number of packets per ms for IED publisher/CMC MU

The SMV packets from different sources can be analyzed by using the Wireshark software which is the tool used to capture the network traffic. SMV streams of merging units of IEDs or the CMC Omicron can be monitored and analyses can be done to measure the interval time between different packets from the merging units and eventually Wireshark offers the way to show the dropped or lost packets. Figure 6.7 offers a diagram or schematic of a test, where the Omicron CMC acts as a current and voltage source (CT transformer sensor, VT transformer sensor), two IEDs are connected and is configured to be a publisher of sampled values and the second IED is a SMV subscriber, a network capture tool (Wireshark, SVScout), CMC Omicron merging unit, eventually using GPS time synchronization as shown in Figure 3. The IEC 61850-9-2 standard determines the sampled frequency which is based on the power system frequency that according to the IEC 61850 standard is 4 kHz for a 50 Hz system, or 4.8 kHz for a 60 Hz one. For one unit stream, the interval between one packet and the following packet is between (200 μs to 250 μs). SVScout is the tool which is used in the graphical display that allows one to verify the published measured values and compare the samples from other merging units. The SVScout enabling the way to compare the streams from merging units and save the report in comtrade format. The delay of packets can be caused by many reasons: lack of numerical precision, merging unit accuracy and sample count rate [19]. The calculation of communication capacity shown in table 6.5.

Available communication capacity for two SMV publishers in a parallel redundancy protocol (PRP) network [19] is given by:

$$SMV = 12.3\ Mb/s \tag{6.1}$$

$$GOOSE + MMS = 87.7\ Mb/s \tag{6.2}$$

Available communication capacity for two SMV publishers in a high-availability seamless redundancy (HSR) network [13] is:

$$SMV = 12.3\ Mb/s \tag{6.3}$$

$$GOOSE + MMS = 37.7\ Mb/s \tag{6.4}$$

6.7 GENERIC OBJECT ORIENTED SUBSTATION EVENTS (GOOSE)

IEC 61850 GOOSE, with its fast transfer characteristics within a network environment (<3 ms as defined by the standard), is now being widely used for protection purposes in place of conventional dedicated wiring. As described, this brings great benefits to the user since the needed dedicated wiring can be reduced. The test provides the ability to implement the IEC 61850 standard (SMV, GOOSE). The sampled values and GOOSE message published and the GOOSE trip signal is sent from the publisher IED to the subscriber IED. Figure 6.14 shows the subscriber interface before sending the GOOSE message (trip signal) and figure 6.14 shows the trip signal sent and the input changed to true. In order to capture the GOOSE message that was sent from one IED to another, we use the IED Scout software that provides the sniffer for GOOSE messages and provides the interface to monitor the signal status. PCM 600 is the tool used to configure the protection relay and add digital data transfer functions. The PCM 600 provides the way to start the IEC 61850 communications through process bus communication or GOOSE.

The IED Scout tool provides the ability to map the GOOSE message and the dataset of all the IEDs in the network, in order to implement interoperability between the devices on SAS. Figure 15 shows the IEDScout tool and the dataset of the IEDs that are part of the configuration (publisher, subscriber) and the interface of this tool imports the Configured IED Description (CID) file and linked the IEDs according to the configuration as shown in figure 6.15. The GOOSE message measurements show that the same packet is duplicated five times with a length of 147 bytes per message, the interval between GOOSE messages is not constant, conversely, the interval begins to be longer than the first interval between the first and second packet of GOOSE messages, as shown in figure 6.16. The interval starts at 278 μs and the last interval ends at 102.66 milliseconds, and the same thing occurs for four different GOOSE messages. Eventually, the GOOSE messages have been removed from the network and the network protocol analyzer. The configuration of GOOSE communication is implemented in the subscriber and publisher IEDs, the GOOSE message is sent from publisher to subscriber once the voltage or current is higher than the limit [20].
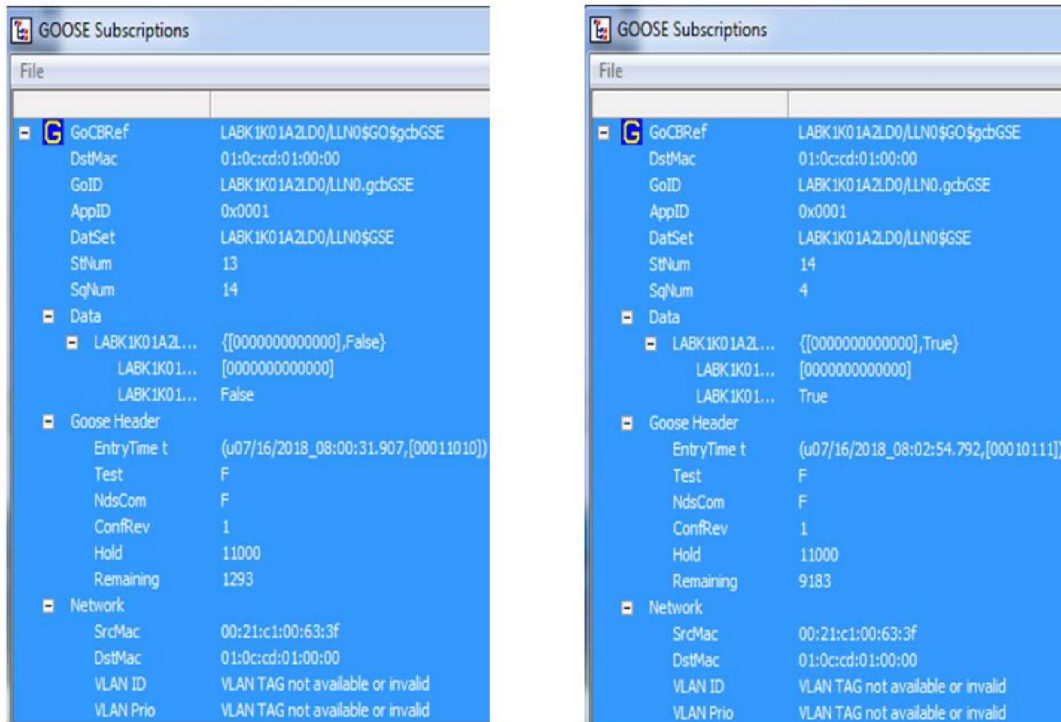
FIGURE 6.14: The full scheme of testing the IEC 61850 (SMV-GOOSE). (a) Shows the mapping of a GOOSE message with the dataset details. It shows the tripping signal is false before increasing the current and overcurrent function of IED takes action, (b) shows changing of the status to true, which means the GOOSE message (tripping signal) is sent to the subscriber.
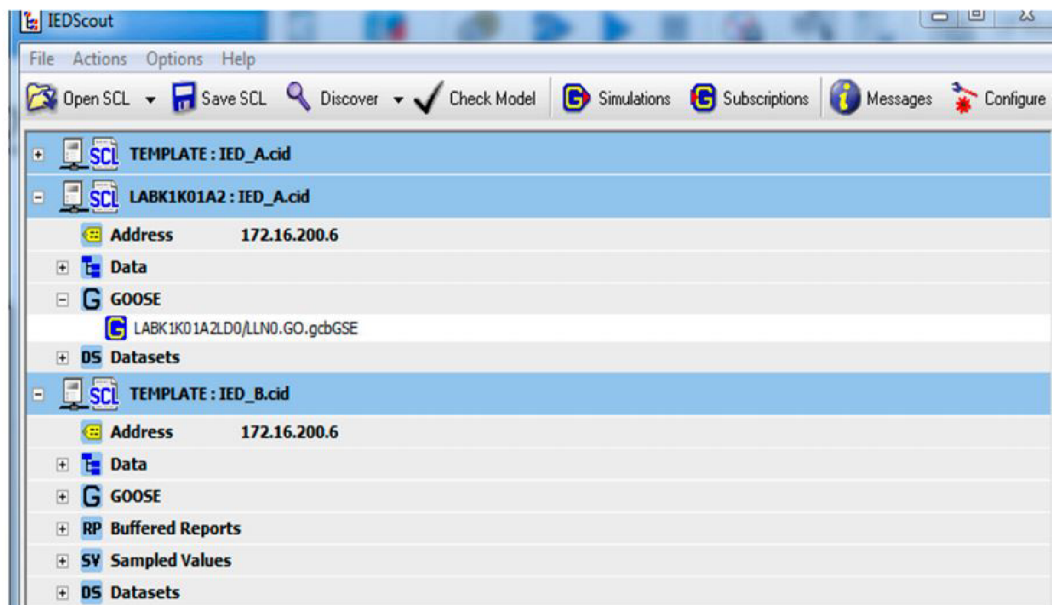
FIGURE 6.15: The structure of IED SCL and GOOSE mapping
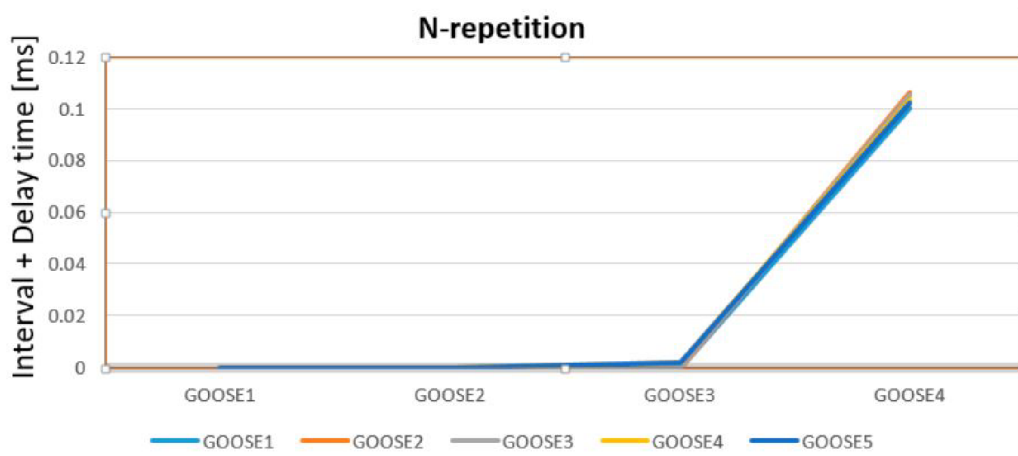
FIGURE 6.16: GOOSE Messages duplicities for five different GOOSE
messages. n-repetition

6.8 MACHINE LEARNING

Machine learning techniques are used for power quantity analysis and decision
making tasks (accurate forecasting, comparing different machine learning techniques).
The data description of the model can be summarized by the IED merging unit and
CMC merging unit. A Substation Configuration Language (SCL) file is exported
from the IED-publisher to CMC, the data set of the model contains two parameters
(interval time between packets, the number of packets per ms), the goal is to find
the link between the number of samples and interval time and determine which
merging unit is sending the SMV and help the subscriber IED to figure out the cor-
rect sender of sampled values. The parameters of both merging units are captured
by the network protocol analysis; in figure 6.17 and in table 6.6 data preparation is
added to show the link between the input parameters and the sender of sampled
values. The main goal of this test was to determine the source of the sampled values
streams.

TABLE 6.6: Data preparation and input array size

Input		Target_Output	
Parameter	IED_Publisher	CMC_ Simulated	IED_Subscriber
4000 1	(4000 1)	IED	
Number of samples per ms	4000 1	4000 1	CMC

A few points noticed during the test of sampled values:

- IED-subscriber took time to determine the publisher merging unit, and a delay
  time to recognize the publisher side. Practical implementation showed that the
  simulated merging unit of the IED could not subscribe immediately.

- The number of samples is the first input parameter for data preparation; each
  merging unit includes a number of samples per second.

- Interval time between packets used in this test is the second input parameter
  for data preparation.
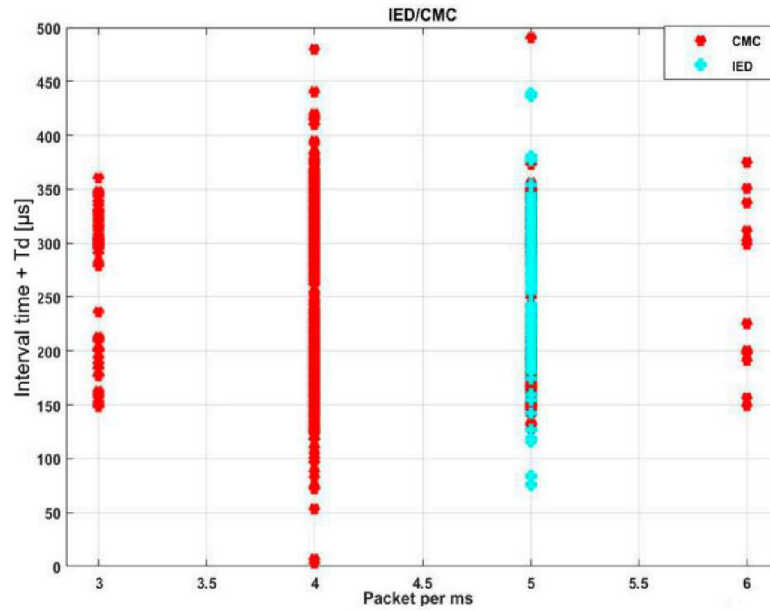
FIGURE 6.17: Data preparation of parameters

- Measurement of the merging units showed that the quick response of the merging unit subscriber is important in IEC 61850. The data link layer (layer 2) is a lower level addressing structure to be used between end systems and concerned with forwarding packets based on layer addressing scheme and the MAC address of the destination.

- The interval time and the number of samples are parameters used as inputs for this test, using relay protection merging unit and CMC merging unit data to feed the training set and test set.

- By using neural net pattern recognition, we could find the relation between the inputs (number of samples/ms—interval time between the packets) and the source of the data.

- By using this technique, technicians can save time and ensure they are testing the correct merging unit.

- According to our test the subscriber protection relay takes time to respond to the new traffic of sampled values.

The original dataset was divided into test and validation sets. With these settings, the input vectors and targets vectors are randomly divided into three sets as follows:

- The training set is 70%.

- The validation set is 15% to prove that the network stops training before overfitting.

- The testing set is 15% and is used as an independent test of network generalization [6].

A two layers feedforward network is included in the standard network that is used for pattern recognition, with a sigmoid transfer function in the hidden layer and a softmax transfer function in the output layer. MATLAB uses 10 hidden neurons as

the default set, and the number of output neurons is set to 2. Table 6.7 shows the number of samples for each merging unit and the test split of the input samples into training and test sets accordingly.

TABLE 6.7: Training set and test set

Training Set			Test Set		
Value	Count	Precent	Value	Count	Precent
CMC	2379	49.55%	CMC	1621	50.66%
IED	2422	50.4%	IED	1579	49.34%

Figure 6.18 shows the best validation performance of the network. The plot is used to obtain a plot of training record error values against the number of training epochs, eventually, the error of training decreases after more epochs and retraining, and the best performance is taken from the epoch (epoch 23) with the lowest validation error.
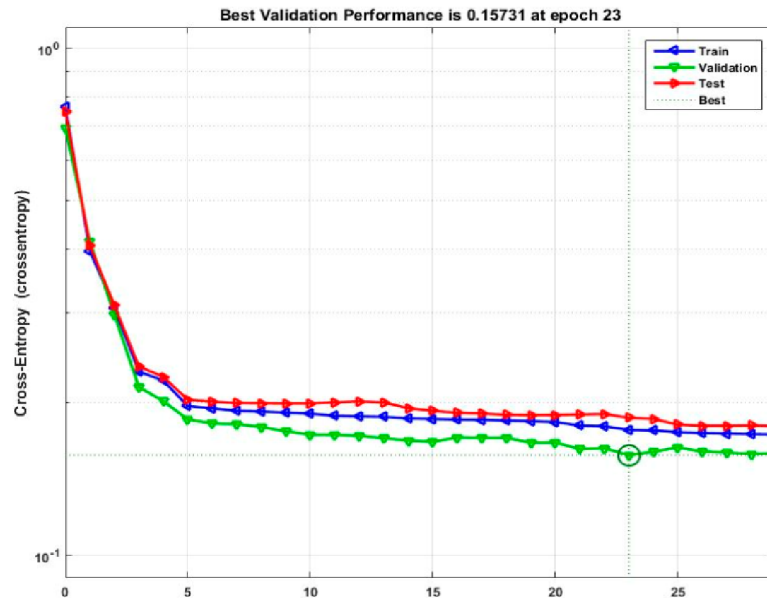
FIGURE 6.18: The best validation performance at epoch 23, validation error at the lowest point

Figure 6.19 shows the test performance of the network (input—hidden networks—output), and contains all of the information related to the training of the network. The structure keeps track of several variables during the course of training, such as the value of the performance function, and the magnitude of the gradient. The best validation indicates the iteration at which performance reached a minimum.

6.9 SUMMARY

This chapter is all about the analysis of IEC 61850-9-2LE measured value using a natural network. In the substation devices the data is being used for multiple purposes and this data can be measured through intelligent electronic devices. This chapter is divided into multiple sections including time synchronization section, sampled values section, timing analysis of sampled values streams section, GOOSE (generic
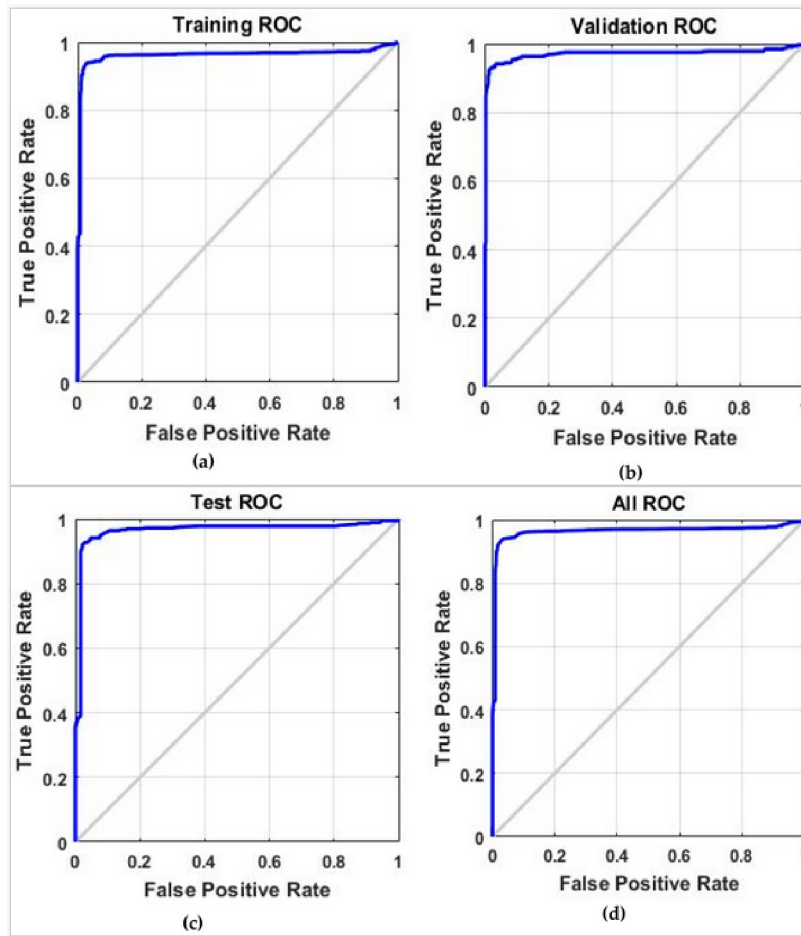
FIGURE 6.19: The receiver operation characteristic curve (a) shows the training ROC that is exploring the tradeoff between true positives and false positives, this curve is a metric used to examine the quality classifier, (b) represents the validation ROC, (c) represents the test ROC, (d) represents the All ROC

object oriented substation events) section and the last is machine learning section.

The main goals to implement IEC 61850 are to increase power quality, reduce the copper wire, providing the interoperability, reducing the cost of operation and maintenance, secure and fast data transmission and flexible functionality. To create a better environment to implement IEC some parts of the substation should be replaced as well as to make the huge amount of real time data processing easier. To implement the distribution function there are three rules to follow first of all is the IEC configuration should follow the performance requirements, the communication interface between IEDs and the system should follow the IEC 61850 standard communication fundamentals and the last one is that the establishment of communication between devices by mean transfer data between IEDs and the power system among the SAS. There are some features offered by IEC 61850 which includes the data characterization, communication specifications and the most important is the data structures and the data objects' services.

The specifications of IEC 61850 can be summarized as the definition and determine how to access the data structure, standardizing the output data categorized the sharing of data and the communication implementation of IED and network by using

eXtendable Markup Language (XML). This chapter also explains in detail the IEC 61850 information system. There are four main object structures which are Data, Attribute, Logical Nodes and Logical Devices. The time synchronization is an important element in sampled value applications due to the problem that can be caused in case of time synchronization is lost. The relation between the time synchronization and sampled values is called SmpSynch. It gives details about the time source (GPS) and the sampled values source (IED publisher).

Peer to peer (PTP) protocol is also explained in this chapter, this is actually defined as the time synchronized is required to get more accurate measurements and implement PTP protocol. The GPS sends three massages to synchronize the devices these are announce message, synch message and follow up message. The IEC 61850 includes three stages for sampled value testing. First is to send sampled measured values, second is to convert analogue into digital and the third one is to check the values in the software named SVScout. Simulation of the merging units of the IED publisher is the main task performed for sampled value testing. The software is used for the visualization of sampled values. It can receive, view, process and save sampled values.

This chapter examines the IEC 61850-9-2 standard based on the sampled measured values. It provides different methods to compare the timing analysis between the merging unit of physical protection relay (IED) that converts the current and voltage signals from the conventional transformers into a digital signal and shares it with sampling frequency (4000 samples/second) and the simulated merging unit of an Omicron 256 CMC that is used to publish SMV to the physical relay (IED-subscriber). The implementation and configuration of the test requires two IEDs are applicable to sending and receiving SMV and GOOSE messages according to standard IEC 61850. Modern IEDs are able to publish four current signals and four voltage signals and share the voltage in the power system. GPS is used to synchronize the time and keep all the devices in the same time and without phase offset. In summary, we can conclude the following from the experiments above:

- The IED-subscriber starts to send sampled measured values once the global clock is applied (GPS-time synchronization), conversely, IED-subscriber does not send or publish SMV once the internal clock is applied from the publisher IED.

- The interval time between the samples is 250 μs according to the IEC 61850 standard, and the network analysis tool shows that four MAC addresses are available, in this case (CMC-publisher, IED-publisher- 2x IED-Subscriber) with time synchronization is applied, however, the interval time is around 240 μs with the local clock of the publisher IED or CMC merging unit, and the interval time is around 230 μs with the global clock (GPS) applied.

- The number of samples per millisecond of IED-publisher: the number of packets is not constant, the range was between 3 to 5 packets/ms, while with CMC-publisher: the number of packets is almost constant at 5 packets/ms.

- GOOSE message configuration is implemented to the IEDs (sender-receiver), the GOOSE message is sent to the receiver IED (tripping signal), the signal is duplicated four times with a size of 147 bytes per packet, the average interval time between the packets was practically constant from the first to the fourth packets (278 μs) and the average interval between the fourth and the fifth packet was 102 milliseconds.

- IED-subscriber is subscribing the SMV from the IED-publisher and CMC-publisher equally, IED-subscriber is unable to recognize who is the publisher of the SMV (IED or CMC) due to the fact the CMC-publisher has the same dataset as the IED-publisher (that is, in fact, what happened when CMC-publisher was simulating the IED-publisher). Wherefore, a model is applied to predict if the IED-subscriber would recognize which merging unit is sending the sampled values based on different attributes, to implement the approach, train a classifier using different models and measure the accuracy and compare models, using the classifier for prediction. The preparation data includes two parameters (number of samples/ms - interval time between the packets) for each publisher of SMV (IED or CMC). By using neural net pattern recognition that solves the pattern recognition problem using two layer feed networks (nprtool), the inputs and the target provided to the network and the algorithm break up the data into test sets (training 70%- validation 15%- testing 15%), and the best validation was in the 23rd epoch.

- This method can be used for optimization of testing procedures in substations where IEC 61850-9-2LE are implemented. This method can be used for shorter test preparation, to lower the cost and help support research projects since it allows one to implement better platform and services as well as to integrate different communication protocols when necessary.

Chapter 7

IEC 61850 9-2 LE SAMPLED VALUES TOOL USING MATLAB SOFTWARE

This chapter focuses on a real time application that subscribes the data stream coming from a station near protection laboratory in Brno Unversity of Technology. IEC 61850-9-2 LE SMVs are used to transmit the traffic to university laboratory with 16 km of fiber optic cable. The application built using MATLAB and can read the traffic from the ethernet port, the traffic decoded and convert from ASCII to the decimal numbers then draw the current and voltage values. The application developed without using any need for additional hardware, the requirements are the ethernet port RJ45 from the station and pc that is running MATLAB. The benefits and features of the application, easy to use, ability to implement some the distance protection functions, calculation the RMS values of the voltage and current, harmonic distortion, the harmonic components with FTT analysis, distance protection characteristics and fault impedance calculation. All calculations implemented in real time, moreover, in this chapter include sensitivity analysis of MATLAB model in previous chapters. Distance protection functions which discussed in this thesis used the offline model of MATLAB or captured with Comtrade format files. In this chapter will evaluate the protection functions with real time stream from the substation, the application includes the following features:

- Instances of voltage and current measurement.

- Harmonic components.

- Fault detection and fault impdance calculations.

- Mho characteristics plot for each type of faults.

7.1 MODELING DISTRIBUTION LINE

The distribution line parameters are used in MATLAB equations for the protection functions in real time. The distribution line 22 kV goes through 9 facilities. Each stop has a power transformer as shown in figure 7.1. The length of the distribution from point 1 to point 2 is 4 km and the line parameters for the distribution line found in table 7.1.
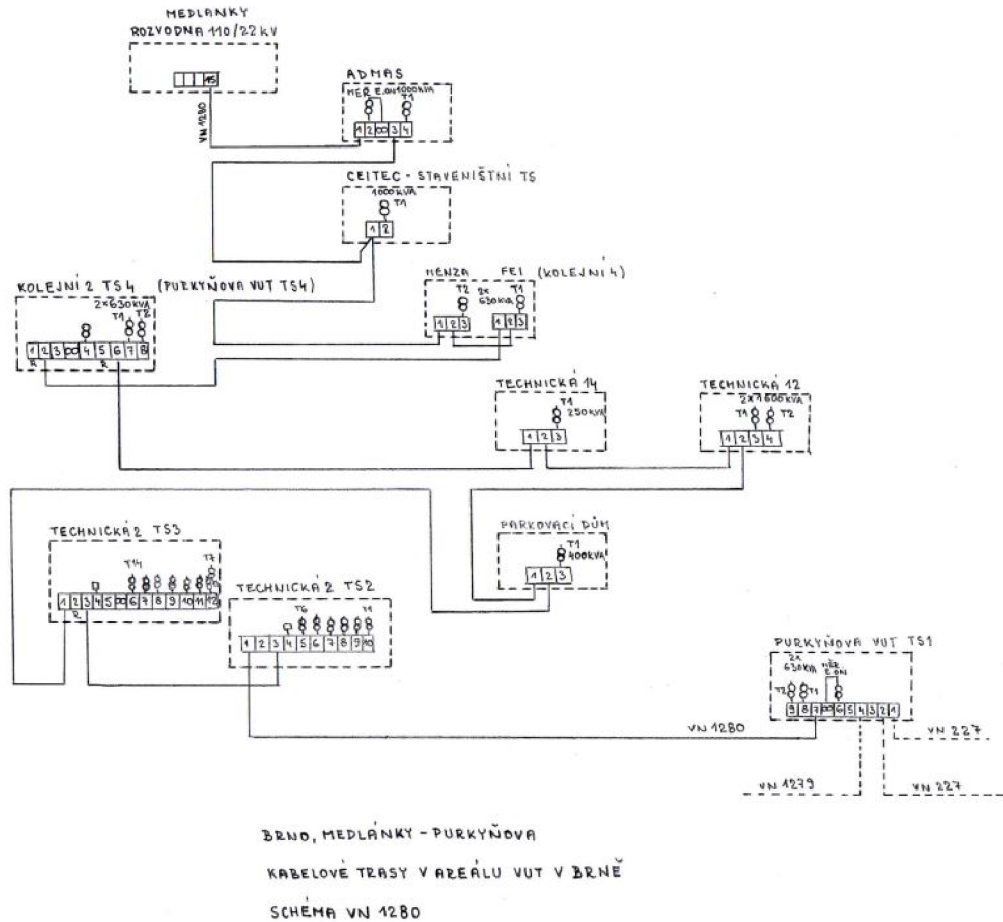
FIGURE 7.1: Modeling Distribution Line and Distance Relay

TABLE 7.1: Data preparation and input array size

No.of core(mm2)	1x240/25
Conductor shape	RM
Conductor (mm)	18.1
Thickness(mm)	5.5
Diameter (mm)	30.4

7.2 BUILDING GRAPHICAL USER INTERFACE

The final stage of the project is to develop the GUI for the finished model. After completed, this GUI will become an educational tool for the students in enhancing their understanding of distance relay characteristic. This GUI was developed using MATLAB which includes the functions harmonic distortion of the received sampled values traffic from substation using FTT, voltage and current RMS, in output session divided into fault detection (line to ground fault, a line to line fault). The tool includes the impedance calculation according to the IEC 61850 9-2 LE such as line parameters (*tx* line length, positive sequence resistance, positive sequence inductance) and impedance plots for each fault type.

7.2.1 HARMONIC DISTORTION

This tool includes the functions that we discussed in the previous chapter in this dissertation, first function harmonic distortion and harmonic components of the current and voltage signals in real time, the difference between the study in chapter 5 and this chapter is that the traffic is in real time and with a real signal from a physical substation. In this chapter, we used the equations similar to the Simulink model in chapter 5 for the harmonic components. The calculation of harmonic components used Welch's method which based on the concept of using periodogram spectrum estimates, which are the result of converting a signal from the time domain to the frequency domain. It reduces noise in the estimated power spectra in exchange for reducing the frequency resolution. Due to the noise caused by imperfect and finite data, the noise reduction from Welch's method is often desired.

$$THD_i = \sqrt[2]{\frac{\sum_{k=1}^{\infty} I_{h,rms}^2}{I_{h,rms}^2}} \times 100 \tag{7.1}$$

$$THD_v = \sqrt[2]{\frac{\sum_{k=1}^{\infty} V_{h,rms}^2}{V_{h,rms}^2}} \times 100 \tag{7.2}$$

$$I_H = \sqrt[2]{I_2^2 + I_3^2 + ... + I_n^2} \tag{7.3}$$

I_n: rms value of the harmonic n
I_F: rms value of the fundamental current

7.2.2 RELAY CHARACTERISTICS AND IMPEDANCE DIAGRAM

Line measurement of positive, negative and zero sequence parameters of distribution lines with single inductance used to calculate the fault impedance. In figure 7.2, we can get the following equation based on the voltage and current vectors shown as above.
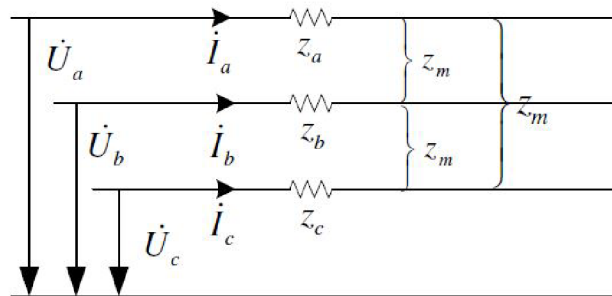

FIGURE 7.2: The equivalent circuit for single circuit lines

For single circuit:

$$\begin{pmatrix} \overline{Ua} \\ \overline{Ub} \\ \overline{Uc} \end{pmatrix} = \begin{pmatrix} \overline{Zaa} & \overline{Zab} & \overline{Zac} \\ \overline{Zab} & \overline{Zbb} & \overline{Zbc} \\ \overline{Zac} & \overline{Zbc} & \overline{Zcc} \end{pmatrix} \begin{pmatrix} \overline{Ia} \\ \overline{Ib} \\ \overline{Ic} \end{pmatrix} \tag{7.4}$$

$\overline{Z_{aa}}, \overline{Z_{bb}}, \overline{Z_{cc}}$ is the value of self impedance of three phase respectively. $\overline{Z_{ab}} = \overline{Z_{ba}}$, $\overline{Z_{ac}} = \overline{Z_{ca}}$, $\overline{Z_{bc}} = \overline{Z_{cb}}$ is the mutual impedance between a,b,c phase. (7.4) can be simplified as:

$$\overline{Uabc} = \overline{Zabc} \times \overline{Iabc} \tag{7.5}$$

7.2.3   DESCRIPTION OF THE TOOL

It is important to evaluate and test IEC 61850 standard in real time, the real time simulator is expensive and it is not available in every substation, therefore, the need for a cheaper solution came to cheap and affordable application with easy installation and flexible features, nowadays, engineers are using these applications for the industry and educational purposes. The real time simulator commonly used for closed loop testing of protection devices [78].

1. Launch the tool by double clicking the file (SVReceiver.exe).

2. Set the input parameters:

    (a) INPUT General: Here set the (AppID) and the (Network Adapter) fields. The AppID must be in hexadecimal and must match exactly that of the source data stream. Otherwise, no stream will be decoded. To select the right NIC mac address from the (Network Adapter) drop down menu, first, physically connect the source ethernet cable. When you are sure that there's connectivity, then click the (Refresh) button next to the (Network Adapter) input field. At this point, the drop down menu will be populated with the mac addresses of all installed NICs both active and inactive. We can select the MAC which matches the NIC to which the source ethernet cable is connected.

    (b) INPUT − Line Parameters: On this tab, set the values of the respective fields. Apart from (Distribution Line Length, Zone 1, Zone 2), the values of the rest of the fields are obtained from the specifications document of the target power line. (Distribution Line Length) is the target protected line length. (Zone 1 , Zone 2) are protection settings.

    (c) OUTPUT
        i. FAULT DETECTION: When the tool is running and it detects a fault, the indicator(s) light up according to the type of fault detected. The DEA (Differential Equation Algorithm) is the algorithm chosen for this functionality, and it is implemented directly in the c−compiled (svsubscriber.exe) file.
        ii. RMS VALUES (MEASUREMENTS): Here the RMS values of the measured instantaneous voltages and currents are displayed in real time.
        iii. INSTANTANEOUS MEASUREMENTS: The decoded instantaneous voltage and current values are graphically displayed in real time.
        iv. IMPEDANCE CALCULATION PLOTS: The Line to ground and Line to Line impedance, calculated in real time, are displayed graphically.

      v. HARMONICS THD: Here the calculated total harmonic distortion (THD) and harmonic contents of the voltage and current are displayed in real time.

3. Click the (Run) button to start running the tool. As it runs, the post processed source payload is displayed in real time.

4. To end the current running session, just click the (Stop) button.

5. If for any reason the source stream is disconnected from the tool while it in (Run) mode, the tool goes into the (idle) mode where the tool is automatically paused after about 1 minute of idle stream activity. When the stream is restored, you can then click (Run) once more to unpause the tool as shown in figure 7.3 and figure 7.4.
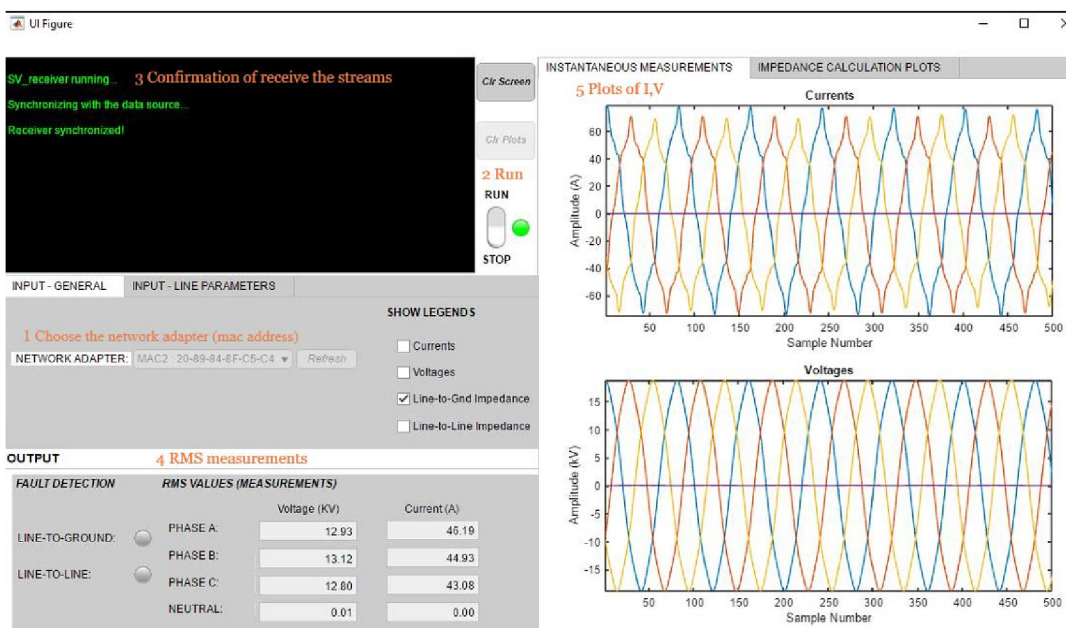
FIGURE 7.3: Instantaneous current and voltage measurements current and voltage harmonics.

In summary: The tool is developed using MATLAB code to read and subscribe the sampled values from a substation near Brno University of Technology according to IEC 61850 9-2 standard. The challenges for developing this tool are the capability to process the sampled values in real time, it has functions (protection characteristics, fault detection, and harmonic components).

7.2.4 DYNAMIC MHO DISTANCE CHARACTERISTIC IMPEDANCE

Mho distance elements continue to be popular for transmission and distribution protection. The technology used in the protection relay is getting developed from coils to microprocessors. The fundamental principles of the mho distance element still exist. Microprocessor relays require an efficient method for determining if a measured impedance is inside the mho operating characteristic. We used equation 7.6 in order to calculate measured impedance to the line angle and corresponding number line for (a) fault within reach point (b) an external fault as shown in figure 7.5.
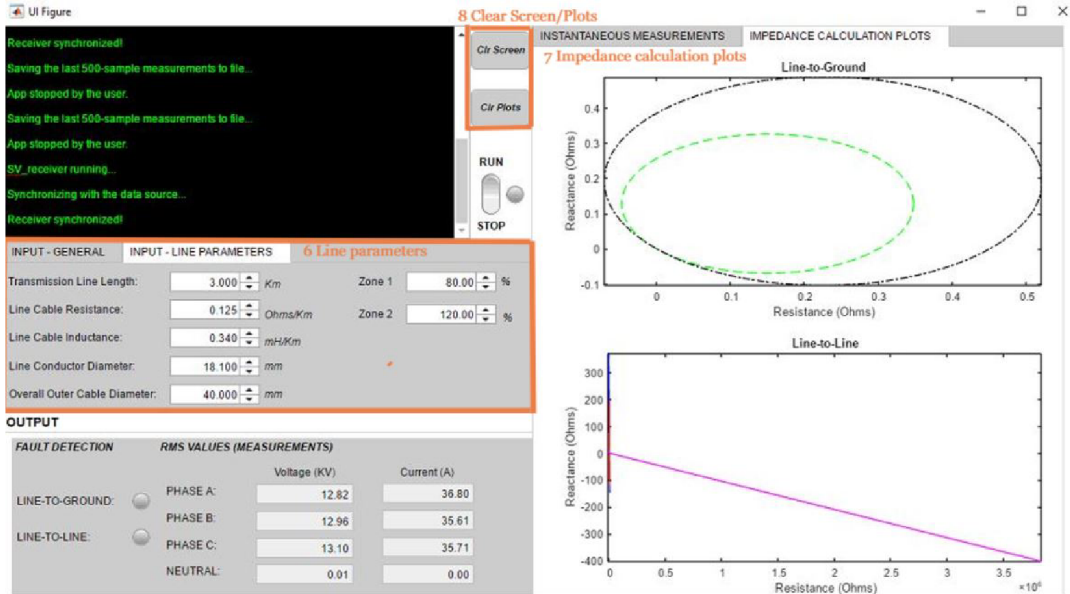
FIGURE 7.4: Instantaneous current and voltage measurements- Current and voltage harmonics
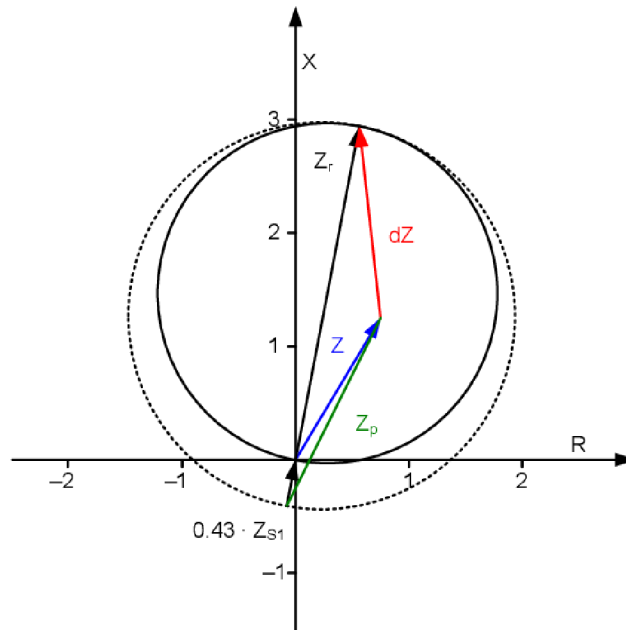
FIGURE 7.5: Impedance mapped to line angle

$$Z_m = \frac{Re[Z \cdot \overline{Z}]}{Re[1\angle Q_Z \cdot \overline{Z}]} \tag{7.6}$$

Z: The relay calculates the impedance Z by using the measured voltage and current phasors at each processing interval

$\overline{Z}$: Calculated Impedance according to Euler's formula [79]

$1\angle Q_Z$: Line impedance angle.

Variety parameters can influence the dynamic mho behavior for example: system parameters, load flow, fault type, and the relay algorithm. Real time transient simulations are recommended for series compensated lines applications.

7.2.5 IMPEDANCE CALCULATION ALGORITHM FOR MICROPRO-CESSOR

This part explains the used algorithm to calculate the impedance of a transmission line fault in the tool, the impedance is calculated using the differential equation algorithm (DEA) from sampled data. DEA is an alternative method to Fourier transform that can be used to estimate and calculate the fault location and fault impedance. For a fully transposed line it can be assumed that *Lac = Lbc*. Hence, the last term in the previous expression vanishes, giving:

$$V_a - V_b = xR_a(I_a - I_b\frac{R_b}{R_a}) + x(L_a - L_{ab})[((\frac{dI_a}{dt}) + (\frac{L_{ab} - L_b}{L_a - L_{ab}})\frac{dI_b}{dt}])(7.7)$$

For a symmetric line, *(Lb - Lab)/(La - Lab)* and *(Rb/Ra)* will be equal to 1 and the above equation reduces to:

$$V_a - V_b = xR_a(i_a - i_b) + x(L_a - L_{ab})\frac{d(i_a - i_b)}{dt} \tag{7.8}$$

The advantage of this method that achieves accurate and efficiency at lower voltages, the differential equation algorithm provides flexibility to present the electrical values and simplifies the design of the numerical relay.

7.2.6 FAULT DETECTION AND IMPEDANCE CALCULATIONS

Evaluation of the tool during the fault, the substation's sampled values streams are healthy and faults are limited to occur, the best way to test the tool is simulated streams that create faults. Figure 7.6 shows the generated voltage and current signals, to place a fault and test the tool with a single phase with a ground fault. As shown in the figure, the phase 1 voltage dropped.
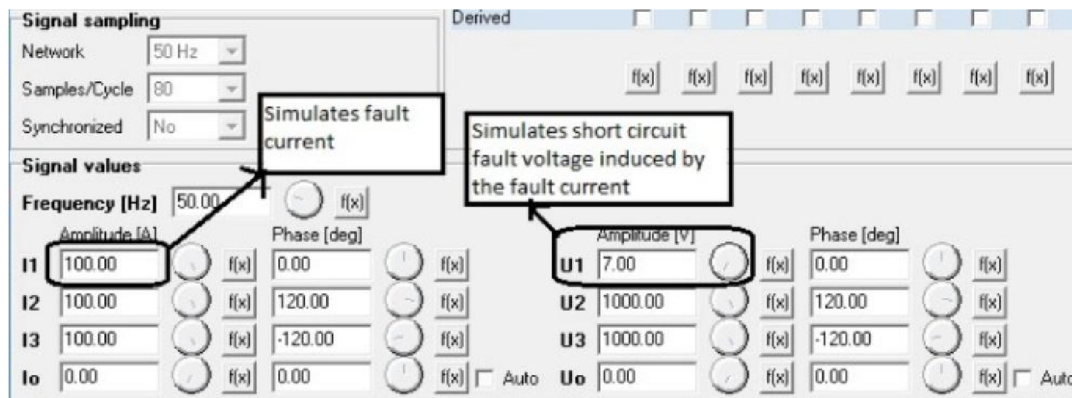
FIGURE 7.6: Sampled values sender

The next step is testing the function of the tool when a fault occurs, due to the fault does not happen frequently in the protected distribution line under study. Therefore, the tool tested during the fault conditions by using streams coming from another source.
In figure 7.7 presents the tool using developed GUI for Mho type distance protection relay. By using GUI, it can study the effect of parameters change on distance relay characteristics such as the effect of fault location and fault resistance. the figure shows fault impedance for phase A to ground, and the line to ground fault detection
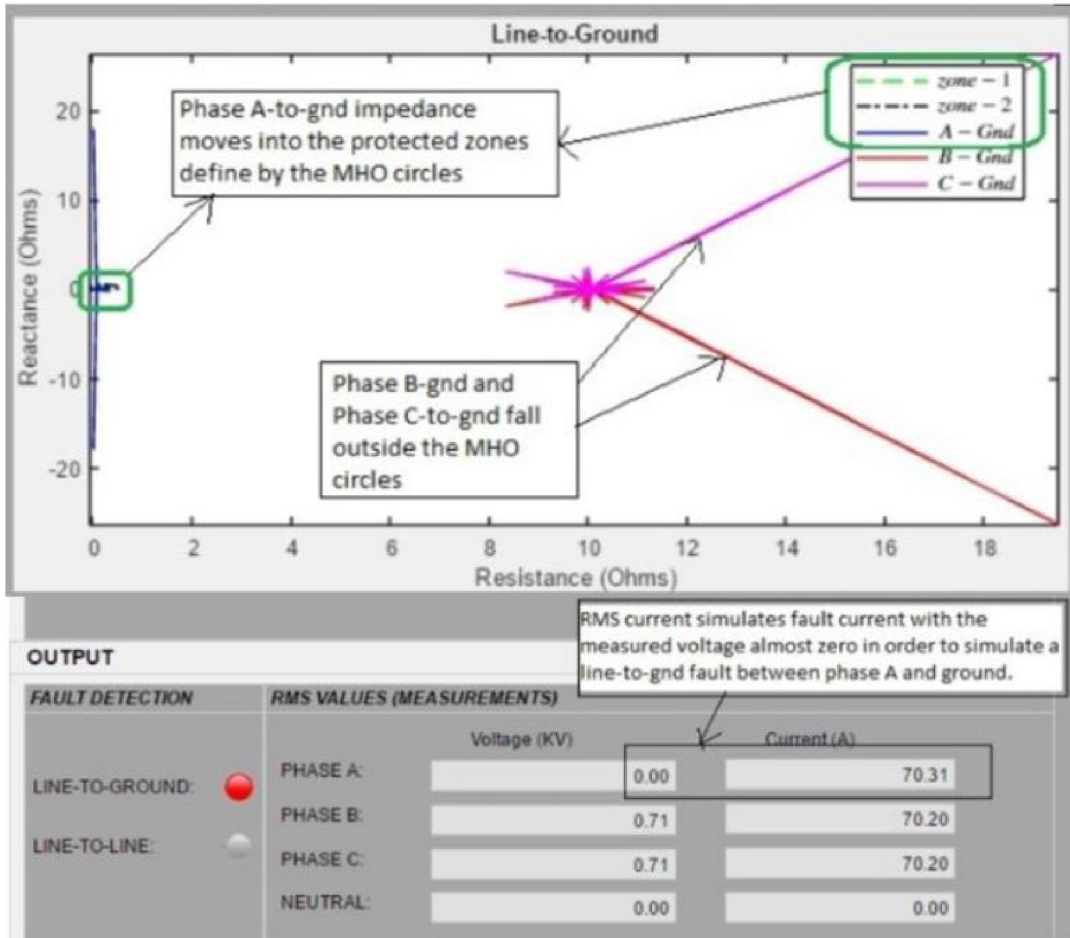
FIGURE 7.7: SLG (phase A) impedance inside outside the zoneV, I
RMS during the fault and fault detection alarm (SLG)

shows a red alarm. The impedance for phases B and C are showing outside the zone; therefore, the distance protection will not send a trip signal. RMS values show the three-phase values for the voltage and current.

In figure 7.8 presents the tool using developed GUI for Mho type distance protection relay. By using GUI, it can study the effect of parameters change on distance relay characteristics such as the effect of fault location and fault resistance. the figure shows fault impedance for line to line (A to B) and the line to ground fault detection shows a red alarm (figure 7.9).
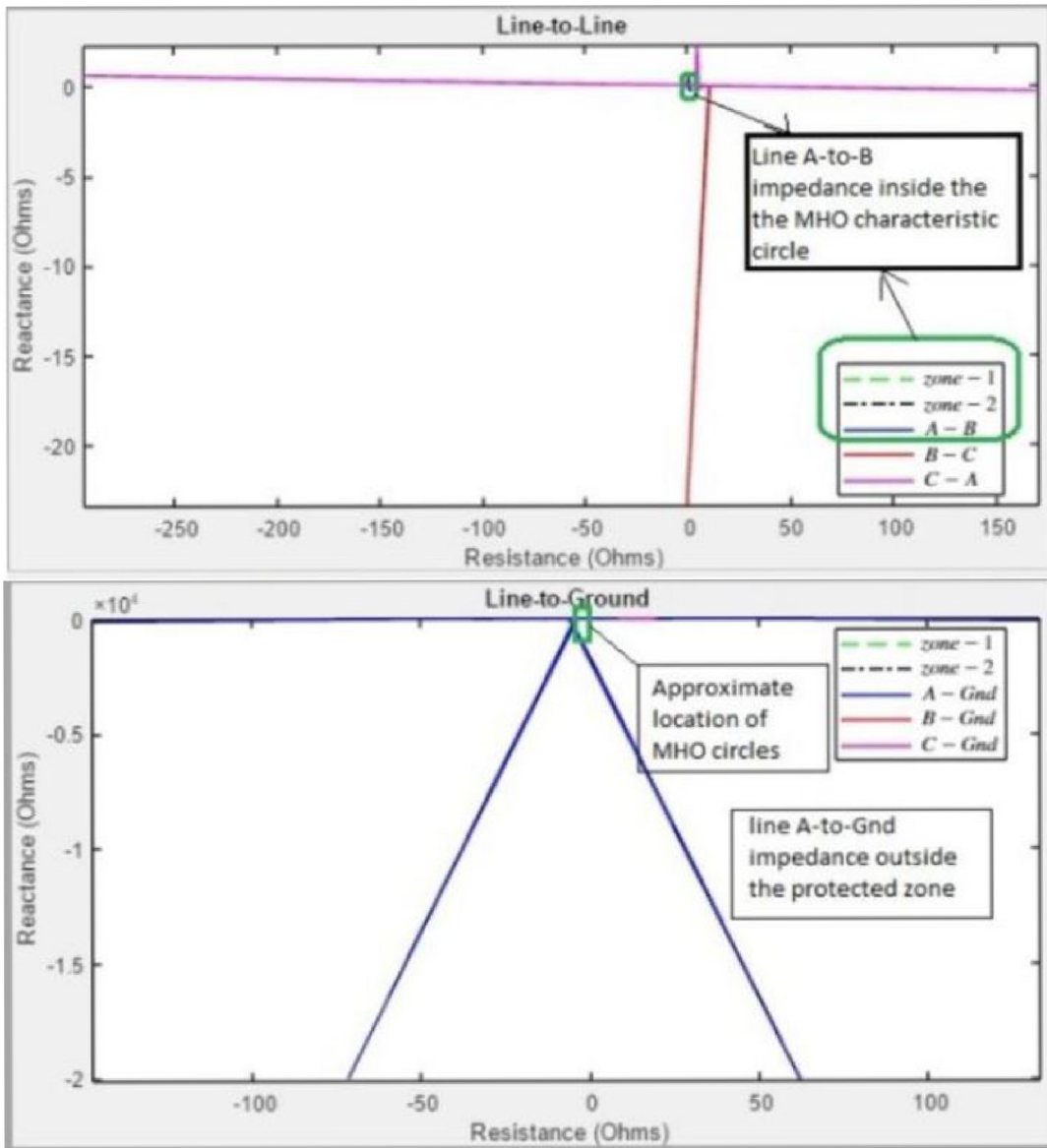
FIGURE 7.8: Line to Line fault

FIGURE 7.9: Fault detection alarm (Line to Line)

7.3   Harmonic Classification Using FFT Spectrum

The wave analyzer measures the amplitude of each harmonic component. It can be either a frequency domain type, using selective filters or a spectrum analyzer, or a time domain type using digital computation to derive the discrete Fourier transform. Harmonic distortion: Harmonics can be understood as different frequency periodic components that are superimposed on the main frequency waveform. In power systems, existing harmonics are a mostly odd integer multiple of the power frequency. The 3rd, 5th, 9th, 7th, 11th, and 13th orders can be identified as the most common harmonics. In addition to these common harmonics, it is possible to face signal components that are not integer multiples of the fundamental. Such components are called "inter-harmonics" and they are usually encountered while dealing with non-periodic signals. through the test, the result shows the harmonic capture ratio from the current and voltage waveform.

FFT is used to convert time-domain waveform into their frequency components. When the waveform is periodical, the Fourier series can be used to calculate the magnitudes and phases of the fundamental and it's Harmonic components. Harmonic distortion is characterized by the harmonic spectrum of the voltage or current signal obtained by applying the Fourier transform. The spectrum of the distorted signal obtained with power system frequency as –Even harmonic component, odd harmonic component, inter harmonic component, and sub-harmonic component and noise.
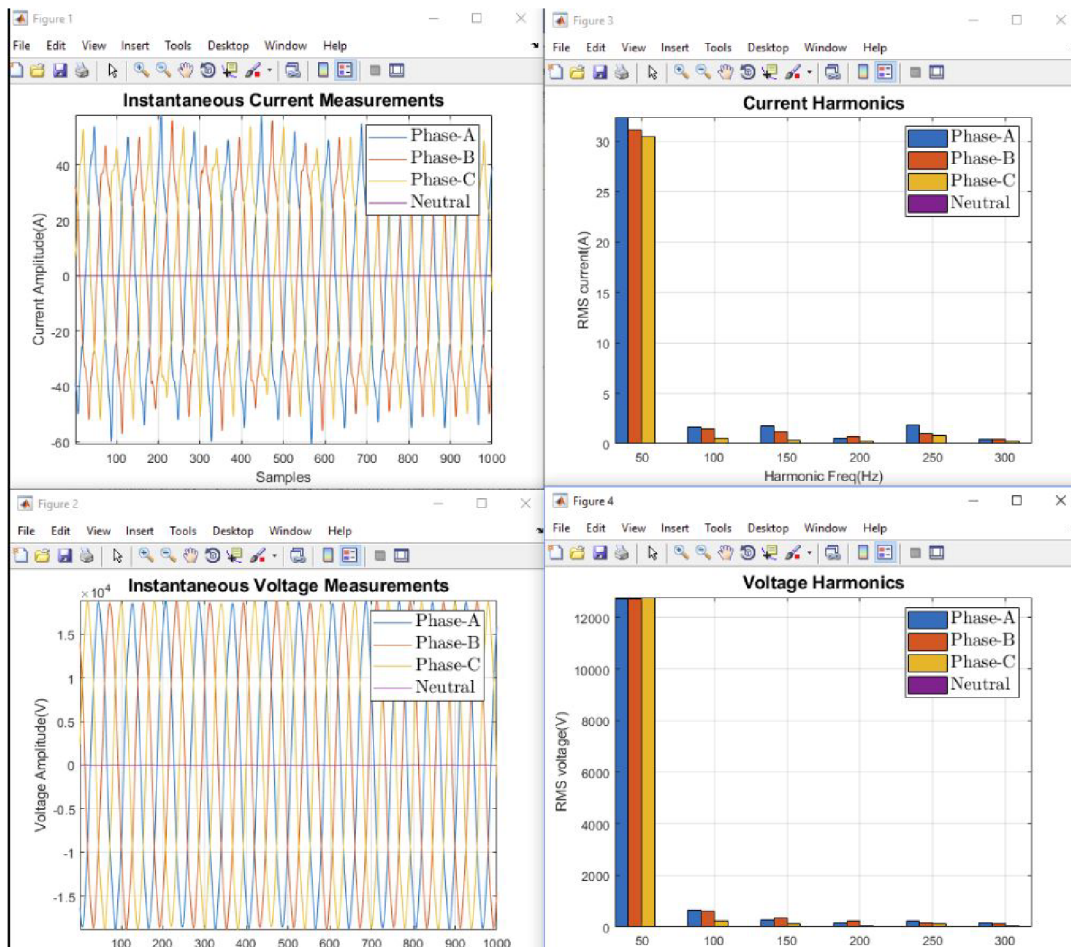
FIGURE 7.10: Instantaneous current and voltage measurements Current and voltage harmonics.

Harmonic detection and mitigation is an important task in the power system. This session presents detailed power quality problems, harmonics, and their types, causes of harmonics, effects, and solutions. It proposes the FFT method of harmonics analysis which is most useful to classify harmonics in odd, even, noise, inter harmonics, sub-harmonics, etc. Figure 7.11 explains the THD calculation using the FFT spectrum.

	PHASE A	PHASE B	PHASE C	NEUTRAL
Current THD (dBc)	-24.52	-33.14	-24.64	-Inf
Voltage THD (dBc)	0.00	0.00	0.00	-14.59

FREQ (Hz)	RMS Current A	RMS Current B	RMS Current C	RMS Current N
50	37.59	36.38	35.73	0.00
100	1.51	0.54	1.44	-Inf
150	1.37	0.42	0.82	-Inf
200	0.68	0.18	0.61	-Inf
250	1.59	0.70	1.50	-Inf
300	0.25	0.18	0.34	-Inf
350	2.56	1.55	2.80	-Inf

FREQ (Hz)	RMS Voltage A	RMS Voltage B	RMS Voltage C	RMS Voltage N
50	12.77	12.85	12.77	0.02
100	0.51	0.19	0.50	0.00
150	0.31	0.13	0.29	0.00
200	0.22	0.06	0.21	0.00
250	0.38	0.14	0.36	0.00
300	0.13	0.04	0.12	0.00
350	0.09	0.04	0.18	0.00

FIGURE 7.11: Current and voltage harmonics

7.4 CONCLUSIONS

This chapter describes the tool of distance relay using Matlab package. Inside the tool, single line to ground (SLG) and double line faults chose to be the fault type and Mho type distance characteristic chose to be the protection scheme. A graphical user interface (GUI) created using a GUI package inside Matlab for the developed tool. Using the sampled values from real substation and analysis in real-time. The tool developed without using any need for additional hardware, the requirements are the ethernet port RJ45 from the substation and pc that is running MATLAB. The benefits and features of the tool, easy to use, ability to implement some the distance protection functions, RMS calculation values of the voltage and current, harmonic distortion, the harmonic components with FTT analysis, distance protection characteristics and fault impedance calculation.

Chapter 8

CONCLUSIONS

- At the beginning of the dissertation, there is an overview of the development of electrical protections from basic electromechanical protections to modern digital protections. The introduction focused on the quadrilateral relay algorithm and improvement of the relay functions. The new measurement method uses sensors to measure current and voltage in the power system and the output signal is a low voltage which transmits through the network over the ethernet cable.

- The main aim of the thesis is to create a model that simulates the distance protection function and algorithm using a digital output from the current and voltage sensors. The dissertation explained the ways to implement IEC 61850 on physical protections with (analog-digital) input data of voltage and current. With the increased interaction between physical devices and communication components, the test proposes a communication analysis for a substation with the conventional method (analog input) and digital method based on the IEC 61850 standard. Moreover, it analyses the merging unit's functions for relays using IEC 61850-9-2LE. The proposed method defines the sampled values source and analysis of the traffic.

- Chapter 5 presents the concept of the impact of harmonic distortion on a digital protection relay. The aim is to verify and determine the reasons of a maltrip or failure to trip the protection relays; the suggested solution of the harmonic distortion is explained by a mathematical model in the MATLAB Simulink programming environment. The digital relays have been tested under harmonic distortions in order to verify the function of the relay's algorithm under abnormal conditions. The comparison between the protection relay algorithm under abnormal conditions and a mathematical model in the MATLAB Simulink programming environment based on injected harmonics of high values is provided.

- In chapter 6, by using neural net pattern recognition that solves the pattern recognition problem, a relation between the inputs (number of samples/interval time between the packets) and the source of the data is found. The benefit of this approach is to reduce the time to test the merging unit by getting the feedback from the merging unit and using the neural network to get the data structure of the publisher IED. Tests examine the GOOSE message and performance using the IEC standard based on a network traffic perspective.

- In chapter 7 has a theoretical description of protection algorithms and their programming in the MATLAB environment.The tool and practice tests provide a new approach to applying digital current and voltage inputs on distance protection. The result of the dissertation shows new possibilities of protection

of distribution devices using the IEC 61850 standard. It demonstrates the possibility of the designed model for real use, whether for the whole substation or groups of panels. The tool provides the quadrilateral relay characteristics, determines the fault type, calculates the fault impedance and total harmonic distortion. In this chapter, we developed a tool that can read the currents and voltages traffic stream in real time according to IEC 61850 sampled values (80 samples/second), this tool can get the current and voltage values from the live stream and run it in MATLAB for additional analysis. The tool is divided to 3 stages:

First stage, devising a means of capturing the Ethernet packets from the connected LAN network adapter of the host computer. After some researches, we preferred to use t-shark (which is a commandline equivalent of Wireshark).

The second stage develops a MATLAB interface or code to import the captured data into the MATLAB environment.

The third stage develops a MATLAB GUI to house the display and processing features for the captured data packets. It can capture live packets directly from the specified ethernet port. In the other mode, it can record the captured packets to Pcap file.

This tool gives the possibility to advanced analysis of the digital processing signals, such as FFT, harmonic distortion, fault type, and fault location calculation. It designed to implement for the distance protection getting the signal of the current and voltage signal from the station near the university (Medlanky station), where merging units installed for the currents and voltages and transmit the signals to the protection lab, the tool provides the possibilities for additional analysis of the signals using MATLAB libraries.

THE CONTRIBUTIONS OF THIS DISSERTATION

The dissertation contains theoretical description of algorithms and their programming in the Matlab development environment. The result of the dissertation shows new possibilities of distribution protection devices using the IEC61850 standard. In the tool, the programmed distance protection functions can determine the RMS values of the voltage and current, decode and the streams in real-time and analyze the streams according to IEC61850 standard, It verifies the distribution line under the test (line length, voltage level, and other parameters).

The machine learning used for the optimization of testing procedures in substations where IEC 61850-9-2LE is implemented. This method can be used for shorter test preparation to lower the cost and help support research projects since it allows one to implement better platform and services as well as to integrate different communication protocols when it's necessary.

The proposed tool already deployed in real high-voltage substation and the digitalized data from IEC6185-9-2 SV transmitted via ethernet to protection laboratory.

We explore the applicability of our method to evaluate real-time streams in real-time transmitted over packet-based networks. We selected seven important parameters that have the most impact on the distribution line. These parameters are line length, line resistance, line conductor, overall outer, and zone1,2.

SUMMARY OF RECOMMENDATIONS AND PROPOSAL FOR FURTHER ACTION

We can identify the following steps that should be taken to develop the tool usage and implement the functions presented in this dissertation:

- Analyzing the captured data and compare the measured values during the abnormal conditions.

- The routine test should be carried out to ensure the integrity of the relay scheme as faulty protective devices may also constitute fault and thus affect the integrity of the protection scheme and may lead to loss of supply of electrical energy.

- Identify reliable sources of inputs data and create easy access to inputs.

- In this approach, it is possible to further improve the protection algorithms and work on the principle of distance protection functions.

Bibliography

[1] Sidhu, T.S.; Pradeep, K. Gangadharan. Control and automation of power system substation using IEC61850 communication. In Proceedings of the 2005 IEEE Conference on Control Applications (IEEE CCA 2005), Toronto, ON, Canada, 28–31 August 2005.

[2] Kriger, C.; Shaheen, B.; John-Charly, R.-M. A detailed analysis of the GOOSE message structure in an IEC 61850 standard-based substation automation system. Int. J. Comput. Commun. Control 2013, 8, 708–721

[3] Štefanka, M. Application of sensors and digitalization based on IEC 61850 in medium voltage networks and switchgears. Ph.D. Thesis, Brno University of Technology, Faculty of Electrical Engineering and Communication, Brno, Czech Republic, 2016.

[4] Andersson, L.; Brand, K.P.; Brunner, C.; Wimmer, W. Reliability investigations for SA communication architectures based on IEC 61850. In Proceedings of the IEEE Power Tech, St. Petersburg, Russia, 27–30 June 2005.

[5] Sheng, C.H.E.N. Application of system networking for substation automation. Power Syst. Technol. Beijing2003, 27, 72–75.

[6] Popova, S.; Iliev, S.; Trifonov, M. Neural Network Prediction of the Electricity Consumption of Trolleybus and Tram Transport in Sofia City. In Proceedings of the Latest Trends in Energy, Environment and Development, Proc. of the Int. Conf. on Urban Planning and Transportation (UPT'14), Salerno, Italy, 3–5 June 2014; pp. 116–120.

[7] Dolezilek, D. IEC 61850: What you need to know about functionality and practical implementation. In Proceedings of the 2006 IEEE Power Systems Conference: Advanced Metering, Protection, Control, Communication, and Distributed Resources (PS'06), Clemson, SC, USA, 14–17 March 2006; pp. 1–17.

[8] Ingram, D.M.E.; Schaub, P.; Richard, R.T.; Duncan, A.C. Performance analysis of IEC 61850 sampled value process bus networks. IEEE Trans. Ind. Inform. 2003, 9, 1445–1454.

[9] Jiang, W.; Henning, S. Modeling of packet loss and delay and their effect on real-time multimedia service quality. In Proceedings of the Nossdav'2000, Chapel Hill, NC, USA, 26–28 June 2000.

[10] Xiang, G.; Pei-Chao, Z. Main features and key technologies of digital substation. Power Syst. Technol. 2006.

[11] Mekkanen, M. On reliability and performance analyses of iec 61850 for digital sas. Ph.D. Thesis, University of Vaasa Faculty of Technology Department of Computer Science, Vaasa, Finland, 2015.

[12] Goran, J.; Havelka, J.; Capuder, T.; Sučić, S. Laboratory Test Bed for Analyzing Fault-Detection Reaction Times of Protection Relays in Different Substation Topologies. Energies 2018, 11, 2482.

[13] Silos, A.; Señís, A.; De Pozuelo, R.M.; Zaballos, A. Using IEC 61850 GOOSE Service for Adaptive ANSI 67/67N Protection in Ring Main Systems with Distributed Energy Resources. Energies 2017, 10, 1685.

[14] Cai, Y.; Chen, Y.; Li, Y.; Cao, Y.; Zeng, X. Reliability Analysis of Cyber–Physical Systems: Case of the Substation Based on the IEC 61850 Standard in China. Energies 2018, 11, 2589.

[15] O'Reilly, R.; Beng, T.C.; Dogger, G. Hidden challenges in the implementation of 61850 in larger substation automation projects. 2016.

[16] Wannous, K.; Toman, P. Sharing sampled values between two protection relays according to standard IEC 61850-9-2LE. In Proceedings of the 19th IEEE International Scientific Conference on Electric Power Engineering (EPE), Brno, Czech Republic, 16–18 May 2018.

[17] Mlynek, P.; Misurec, J.; Toman, P.; Silhavy, P.; Fujdiak, R.; Slacik, J.; Samouylov, K. Performance Testing and Methodology for Evaluation of Power Line Communication. Elektron. Elektrotechnika 2018, 24, 88–96.

[18] Patel, N. IEC 61850: Horizontal Goose Communication and Overview: IEC 61850 Horizontal Communication, Goose Messaging and Documentation: IEC 61850 Standard Overview and Understanding; Lambert Academic Publishing: Saarbrücken, Germany, 2011.

[19] Stefanka, M.; Prokop, V.; Salge, G. Application of IEC 61850-9-2 in MV Switchgear with Sensors Use; IET: London, UK, 2013.

[20] Raussi, P. Real-Time Laboratory Interconnection for Smart Grid Testing; LUT University: Petra, Jordan, 2017.

[21] Al-Musawi, L.; Waye, A.; Yu, W.; Al-Mutawaly, N. The effects of waveform distortion on power protection relays. In Proceedings of the International Protection Testing Symposium, Feldkirch, Austria, 13–14 October 2015.

[22] Wang, F.; Bollen, M. Classification of Component Switching Transients in the Viewpoint of Protective Relays. Ph.D. Thesis, Chalmers University of Technology, Göteborg, Sweden, 2003.

[23] Paithankar, Y.G. Line protection with distance relays. In Book Transmission Network Protection: Theory and Practice, 6th ed.; Dekker, M., Ed.; Dekker: New York, NY, USA; Basel, Switzerland; Hong Kong, China, 1998; pp. 296–321.

[24] Zocholl, S.E.; Benmouyal, G. How microprocessor relays respond to harmonics, saturation, and other wave distortions. In Proceedings of the 24th Annual Western Protective Relay Conference, Spokane, WA, USA, 21 October 1997.

[25] Achleitner, G.; Fickert, L.; Obkircher, C.; Sakulin, M.; IFEA, T.; AG, Ö.I.B. Earth fault distance protection. In Proceedings of the 20th International Conference and Exhibition on Electricity Distribution, Prague, Czech Republic, 8–11 June 2009; pp. 1–4.

[26] Cease, T.W.; Kunsman, S.A.; Apostolov, A.; Boyle, J.R.; Carroll, P.; Hart, D.; Johnson, G.; Kobet, G.; Nagpal, M.; Narendra, K.; et al. Protective Relaying and Power Quality; IEEE PSRC Working Group Report; IEEE: Piscataway, NJ, USA, 2003; pp. 1–65.

[27] Pietkiewicz, A.; Melly, S. Harmonic Filter White Paper; White Paper; In Electric Power Quality; Springer: Dordrecht, The Netherlands, 2008.

[28] Schweitzer, E.O.; Hou, D. Filtering for protective relays. In Proceedings of the IEEE WESCANEX 93 Communications, Computers and Power in the Modern Environment, Saskatoon, SK, Canada, 17–18 May 1993; pp. 15–23.

[29] Kumar, B. Design of Harmonic Filters for Renewable Energy Applications. Master's Thesis, Gotland University, Visby, Sweden, 2011.

[30] Durdhavale, S.R.; Ahire, D.D. A review of harmonics detection and measurement in power system. Int. J. Comput. Appl. 2016, 143, 42–45.

[31] Hodder, S.; Kasztenny, B.; Fischer, N.; Xia, Y. Low second-harmonic content in transformer inrush currents—Analysis and practical solutions for protection security. In Proceedings of the 67th Annual Conference for Protective Relay Engineers, College Station, TX, USA, 31 March–3 April 2014; pp. 1–20.

[32] Kim, G.; Lee, H. A study on IEC 61850 based communication for intelligent electronic devices. In Proceedings of the 9th Russian-Korean International Symposium on Science and Technology, Novosibirsk, Russia, 26 June–2 July 2005.

[33] Leao, P.S.; Barroso, G.C.; Melo, N.X.; Sampaio, R.F.; Barbosa, J.A.; Antunes, F.L. Numerical relay: Influencedby and accessing the power quality. In Book Power Quality, 1st ed.; Eberhard, A., Ed.; InTech: Rijeka, Croatia, 2011; pp. 213–236. ISBN 978-953-307-180-0.

[34] Elphick, S.; Ciufo, P.; Smith, V.; Perera, S. Summary of the economic impacts of power quality on consumers. In Proceedings of the Australasian Universities Power Engineering Conference (AUPEC), Wollongong, Australia, 27–30 September 2015; pp. 1–6.

[35] Daut, I.; Hasan, S.; Taib, S. Magnetizing current, harmonic content and power factor as the indicators of transformer core saturation. J. Clean Energy Technol. 2013, 1, 304–307.

[36] Ho, J.M.; Liu, C.C. The effects of harmonics on differential relay for a transformer. In IEE Conference Publication; Institution of Electrical Engineers: London, UK, 2001; pp. 2–34.

[37] Rafajdus, P.; Bracinik, P.; Hrabovcova, P.; Saitz, J.; Altus, J.; Höger, M.; Pyrhönen, J. Examination of Instrument Transformers for Their Employment in New Fault Location Method; ADE: Bologna, Italy, 2012; pp. 4585–4595.

[38] Cintula, B.; Eleschova, Z.; Belan, A.; Volcko, V.; Konicek, M.; Kovac, M. Impact of fault location on transient stability of synchronous generator. In Proceedings of the 2014 15th International Scientific Conference on Electric Power Engineering (EPE), Brno, Czech Republic, 12–14 May 2014; pp. 17–21.

[39] Alkandari, A.; Soliman, S. Measurement of a power system nominal voltage, frequency and voltage flicker parameters. Int. J. Electr. Power Energy Syst. 2009, 31, 295–301.

[40] Apostolov, A.; Vandiver, B. Maintenance testing of multifunctional distance protection IEDs. In Proceedings of the Transmission and Distribution Conference and Exposition, New Orleans, LA, USA, 19–22 April 2010; pp. 1–6.

[41] Kaspirek, M.; Mikulas, L.; Mezera, D. Analysis of voltage quality parameters in LV distribution grids with connected distributed energy sources. CIRED-Open Access Proc. J. 2017, 2017, 513–516.

[42] Kaspirek, M.; Mikulas, L.; Mezera, D.; Prochazka, K.; Santarius, P.; Krejci, P. Analysis of voltage quality parameters in MV distribution grid. CIRED-Open Access Proc. J. 2017, 2017, 517–521.

[43] Wannous, K.; Toman, P. IEC 61850 communication based distance protection, Electric Power Engineering (EPE), Proceedings of the 2014 15th International Scientific Conference on. IEEE, 2014.

[44] Benabes, P.; Tugui, C. A. Effective modeling of CT functions for fast simulations using MATLAB-Simulink and VHDLAMS applied to Sigma-Delta architectures, Circuits and Systems (ISCAS), 2011 IEEE International Symposium on. IEEE, 2011.

[45] POPESCU, M. C.; MASTORAKIS, N. Modelling and Simulation of Step-Up and Step-Down Transformers,2008.

[46] Wiszniewski; Andrzej; W. Rebizant; and L. Schiel. Correction of current transformer transient performance, Power Delivery, IEEE Transactions on 23.2 (2008): 624-632.

[47] Mooney, J. Distance element performance under conditions of ct saturation, Protective Relay Engineers, 2008 61st Annual Conference for. IEEE, 2008.

[48] Kasztenny, B.; Mazereeuw, J.; DoCarmo, H. CT saturation in industrial applications-Analysis and application guidelines, Protective Relay Engineers, 2007. 60th Annual Conference for. IEEE, 2007.

[49] Ganesan, S. Selection of current transformers and wire sizing in substations, Protective Relay Engineers, 2006. 59th Annual Conference for. IEEE, 2006.

[50] El-Amin, I. M.; Al-Abbas, N. H. Saturation of current transformers and its impact on digital overcurrent relays, Transmission and Distribution Conference and Exposition: Latin America, 2006. TDC'06. IEEE/PES. IEEE, 2006.

[51] McLyman, C.; Wm T, Current Transformer Design, 2004.

[52] Zocholl, S. E.; Roberts, J.; Benmouyal, G. Selecting CTs to Optimize Relay Performance, proceedings of the 23rd Annual Western Protective Relay Conference, Spokane, WA. 1996.

[53] Gers, J.M. ; Holmes, E.J. Protection of Electricity Distribution Networks, 2nd Edition, The IET, 2004, ISBN 978-0-86341-537-1.

[54] Siemens, TechTopics No. 91 Current transformer relaying accuracies IEEE compared to IEC, 2013 Siemens Industry, Inc.

[55] Zocholl, S. E.; Smaha, D. W. Current Transformer Concepts, Electric Council of New England Protective Relaying Committee Meeting No. 60, Rutland, Vermont, April 22, 1993.

[56] Blánquez, F. R.; Revuelta, P.; Rebollo, E.; Platero, C. A. Validation study of the use of MATLAB/Simulink synchronous-machine block for accurate power-plant stability studies, 2014 14th International Conference on Environment and Electrical Engineering (EEEIC). IEEE, pp. 122-126, May 2014, ISBN 978-1-4799-4661-7.

[57] Parasuraman, P.; Sudheendra, K.; Karthik, V. V.; Kumar, V. S. Performance Analysis of Power Swing In Distance Relay (Quadrilateral Relay) Characteristics for Series-Compensated Transmission Line, International Journal of Advanced Research in Electrical, Electronics and Instrumentation Engineering, Vol. 3, Special Issue 2, April 2014, pp 272-281, ISSN 2278 – 8875.

[58] Wannous, K.; Toman, P. IEC 61850 Communication Based Distance Protection, Proccedings of the 2014 15th International Scientific Conference on Electric Power Engineering (EPE), pp. 107-112,May 2014

[59] Yesansure, T. M.; Arora, T. G. Numerical Quadrilateral Distance relay, International Journal of Innovative Research, Engineering and Technology,Vol. 2, Issue 7, July 2013, pp.2920-2927, ISSN 2319-8753

[60] Mrehel, O. G.; Elfetori, H. B.; Hawal, A. O. Implementation and Evaluation a SIMULINK Model of a Distance Relay in MATLAB/SIMULINK. SDIWC, 2013, pp.132-137, ISBN 978-0- 9891305-3-0

[61] Yaghobi, H.; Mortazavi, H.; Ansari, K.;Rajabi Mashhadi, H.; Khorashadi zadeh, H.; Borzoe, H. Study on application of flux linkage of synchronous generator for loss of excitation detection, International Transactions on Electrical Energy Systems, Vol. 23, Issue 6, pp. 802–817, September 2013, ISSN 2050-7038

[62] Jaganathan, S.; Palaniswami, S.; Adithya, R.; Kumaar, M. N. Synchronous Generator Modelling and Analysis for a Microgrid in Autonomous and Grid Connected Mode, International Journal of Computer Applications, Vol. 13, No.5, January 2011, ISSN 0975 - 8887

[63] Mgaya, E.; Müller, Z.; Švec, J.; Tlustý, J. Dynamic Behavior of the Distributed Generation Sources in Island Mode, Proceedings of the 8th International Scientific Conference Electric Power Engineering 2007. Ostrava: VŠB – Technical University of Ostrava, 2007, pp. 179-185, ISBN 978-80-248-1391-2.

[64] Shewarega, F.; Erlich, I.; Rueda, J. L. Impact of large offshore wind farms on power system transient stability, 2009 IEEE/PES Power Systems Conference. IEEE, 2009, pp. 1-8, ISBN 978-1-4244-3810-5

[65] The Math Works, Inc.,SimPowerSystems users guide,Version 4.6,2008.

[66] Ziegler, G. Numerical Distance Protection Principles and Applications,Wiley and Sons, 2006, ISBN 3-89578-266-1.

[67] Sorrentino, E.; Rojas, E.; Hernández, J. Method for Setting the Resistive Reach of Quadrilateral Characteristics of Distance Relays, 2009 Proceedings of the 44th International Universities Power Engineering Conference (UPEC), pp 1-5, September 2009, ISBN 978-1-4244-6823-2

[68] Skendzic, V.; Ender, I.; Zweigle, G. IEC 61850-9-2 process bus and its impact on power system protection and control reliability, In Proceedings of the 9th Annual Western Power Delivery Automation Conference, Spokane, WA. 2007.

[69] Baigent, D.; Adamiak, M.; Mackiewicz, R.; Sisco, G. M. G. M. IEC 61850 Communication Networks and Systems In Substations, 2010, pp 61- 68.

[70] REG, ABB Generator Protection. PCM600, Protection and Control IED Manager, Brochure.

[71] Almas, M. S.; Vanfretti, L. Performance evaluation of protection functions for IEC 61850-9-2 process bus using real-time hardware-inthe-loop simulation approach. 2013,pp 0479-0479.

[72] Valdes, A.; Hang, C.; Panumpabi, P.;Vaidya, N.; Drew, C.; Ischenko, D. Design and simulation of fast substation protection in IEC 61850 environments, In Modeling and Simulation of Cyber-Physical Energy Systems (MSCPES), 2015 Workshop, pp. 1-6.

[73] Altaher, A.; Mocanu, S.; Thiriet, J. M. Experimental Evaluation of an IEC 61850-Station Bus Communication Reliability, In Journées Nationales des Communications Terrestres, 2015.

[74] Yang, L., Crossley, P. A.; Wen, A.; Chatfield, R.; Wright, J. Design and performance testing of a multivendor IEC61850–9-2 process bus based protection scheme, IEEE Transactions on Smart Grid, 5(3), 2014, pp.1159-1164.

[75] UniGear Digital , Engineering and testing IEC 61850-9-2, Process bus.

[76] Jirickova, J. IEC61850: Implementation in new Generation of Electrical Protection, Proceedings of The IVth International Scientific Symposium on electric Power Engineering – Elektroenergetika 2007, pp 471-473, 2007.

[77] Rafajdus, P.; Bracinik, P.; Hrabovcova, V.; Saitz, J.; Altus, J.; Hoger, M.; Pyrhonen, J. Examination of Instrument Transformers for Their Employment in New Fault Location Method, International Review of Electrical Engineering (IREE), Vol. 7, No. 3, Italy, 2012, ADE, pp. 4585 - 4595, ISSN 1827-6660.

[78] Kezunovic, M.; Ren, J.; Lotfifard, S. Design, modeling and evaluation of protective relays for power systems, Springer International Publishing, 2016, ISBN 978-3-319-20919-7.

[79] Fentie, D. D. Understanding the dynamic mho distance characteristic, 69th Annual Conference for Protective Relay Engineers (CPRE). IEEE, 2016.

AUTHOR'S PUBLICATIONS

[80] Bukvisova, Z.; Wannous, K.; Toman, P.; De Paula Alves; P.H.; Topolanek, D. The influence of ripple control signal on protection relay operation.Proceedings of the 10th International Scientific Symposium on Electrical Power Engineering, ELEKTROENERGETIKA 2019.

[81] Wannous, K.; Toman, P.; Jurák, V.; Wasserbauer, V. Analysis of IEC 61850-9-2LE Measured Values Using a Neural Network. ENERGIES, 2019, vol. 12, no. 9, p. 841-861. ISSN: 1996-1073.

[82] Wannous, K.; Toman, P. Evaluation of Harmonics Impact on Digital Relays. ENERGIES, 2018, vol. 11, no. 4, p. 893-893. ISSN: 1996-1073.

[83] Wannous, K.; Toman, P. Sharing Sampled Values Between Two Protection Relays According To Standard IEC 61850-9-2LE. In Proccedings of the 2018 19th International Scientific Conference on Electric Power Engineering (EPE). 2018. p. 185-190. ISBN: 978-1-5386-4611-3.

[84] Wannous, K.; Toman, P. Evaluation of Harmonics Impact on Digital Relays. In Proceedings of the 2017 18th International Scientific Conference on Electric Power Engineering (EPE). Ostrava: VŠB - Technická univerzita Ostrava, 2017. p. 515-520. ISBN: 978-1-5090-6405-2.

[85] Wannous, K.; Toman, P.; Brito Pozzobon, P. Effect of total harmonics distortion on distance and overcurrent relays. In Proceedings of the 9th International Scientific Symposium on Electrical Power Engineering. Stara Lesna: Technical University of Kosice, 2017. p. 670-674. ISBN: 978-80-553-3195-9.

[86] Wannous, K.; Toman, P. The Effects of Harmonics On Overcurrent Relays. In Proceedings of the 2016 17th International Scientific Conference on Electric Power Engineering (EPE). 2016. p. 239-244. ISBN: 978-1-5090-0908-4.

[87] Wannous, K.; Toman, P. The Impact of Current Transformer Saturation on the Distance Protection. In Proceedings of the 2016 17th International Scientific Conference on Electric Power Engineering (EPE). 2016. p. 257-261. ISBN: 978-1-5090-0908-4.

[88] Wannous, K. THE DEVELOPMENT OF THE IMPEDANCE MEASURED BY DISTANCE RELAY. In Proceedings of the 21st Conference STUDENT EEICT 2015. doc. Ing. Vítězslav Novák, Ph.D. Brno: Vysoké učení technické v Brně, Fakulta elektrotechniky a komunikačních, 2015. p. 434-438. ISBN: 978-80-214-5148- 3.

[89] Wannous, K.; Toman, P. The Development of The Impedance Measured by Distance Relay During Near-to- Generator Short Circuit. In Proceedings of the 2015 16th International Scientific Conference on Electric Power Engineering (EPE). 2015. p. 105-110. ISBN: 978-1-4673-6787- 5.

[90] Wannous, K.; Toman, P. IEC 61850 Communication Based Distance Protection. In Procceding of 2014 15th International Scientific Conference on Elektrical Power Engineering. 1. 2014. p. 1-6. ISBN: 978-1-4799-3806-3.